

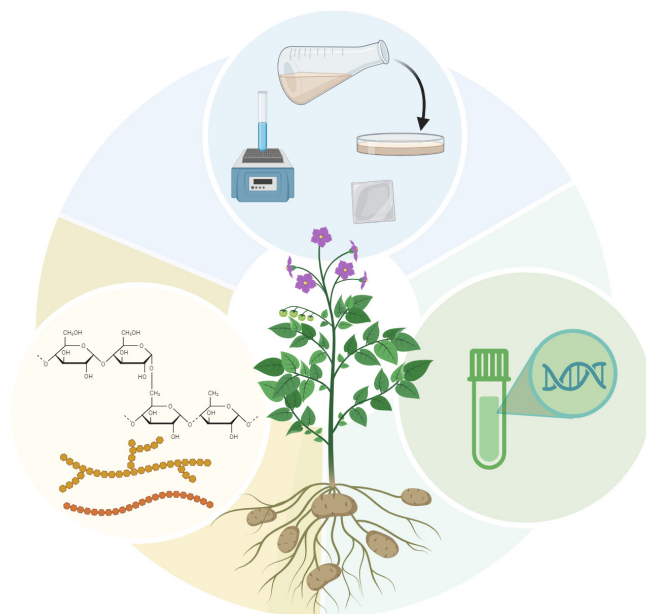


DOCTORAL THESIS NO. 2024:42
FACULTY OF NATURAL RESOURCES AND AGRICULTURAL SCIENCES (NJ)

Novel starch types

Molecular diversity for future applications

SHISHANTHI JAYARATHNA



Novel starch types

Molecular diversity for future applications

Shishanthi Jayarathna

Faculty of Natural Resources and Agricultural Sciences (NJ)

Department of Molecular Sciences

Uppsala



SWEDISH UNIVERSITY
OF AGRICULTURAL
SCIENCES

DOCTORAL THESIS

Uppsala 2024

Acta Universitatis Agriculturae Sueciae
2024:42

Cover: Link between genetic background, molecular and functional properties of starch
(created using BioRender.com)

ISSN 1652-6880

ISBN (print version) 978-91-8046-256-3

ISBN (electronic version) 978-91-8046-257-0

<https://doi.org/10.54612/a.1plo631v25>

© 2024 Shishanthi Jayarathna, <https://orcid.org/0000-0002-7395-314X>

Swedish University of Agricultural Sciences, Department of Molecular Sciences, Uppsala, Sweden

The summary chapter of this thesis is licensed under CC BY 4.0. To view a copy of this license, visit <https://creativecommons.org/licenses/by/4.0/>. Other licences or copyright may apply to illustrations and attached articles.

Print: SLU Grafisk service, Uppsala 2024

Novel starch types. Molecular diversity for future applications

Abstract

This thesis investigated molecular changes in potato starch achieved through targeted mutations in the starch synthesis pathway. CRISPR/Cas9 was used to induce mutations in starch branching enzyme genes (*SBE*), with or without mutations in granule bound starch synthase gene (*GBSS*). The resulting starch was characterised for molecular and functional attributes. Barley starch obtained through conventional cross-breeding was also characterised, to explore potential impacts of fructan synthesis changes on starch synthesis at composition and molecular structure level. Inducing mutations in all alleles of the *SBEI* and some alleles of the *SBEII* produced high-amylose starch, while inducing mutations in all alleles of both *SBEs* resulted in amylose-only starch. *GBSS* mutations alone yielded a waxy starch phenotype, while introducing *GBSS* mutations in *SBEs* mutated background led to non-waxy, low-amylose lines. Mutations in *SBEI* produced starch with unit chain distributions close to the native variety. Mutations in the *GBSS* produced starch with building blocks (BB) distribution resembling the native variety. Significant deviations to unit chain and BB distribution were observed when both *SBEI* and *SBEII* were mutated. Presence of high proportions of large BB elevated gelatinisation and retrogradation temperatures, while high proportions of short amylopectin chains lowered gelatinisation temperature. Potato lines with diverse genetic backgrounds exhibited variations in pasting profiles, influencing film-forming behaviour. Natural genetic variation-based conventional cross-breeding of barley produced starch with modified structures, as upregulated fructan synthesis resulted in starch with a high proportion of large BB. These novel insights into how alterations in starch synthesis pathway affect starch properties pave the way for tailored starch development.

Keywords: Starch branching enzyme gene, granule-bound starch synthase gene, amylose, gelatinisation, retrogradation, building blocks, pasting properties

Nya stärkelsevarianter. Molekylär mångfald för framtida tillämpningar

Sammanfattning

Denna avhandling undersökte molekylära förändringar i potatisstärkelse som åstadkommits genom riktade mutationer i stärkelsebiosyntesen. CRISPR/Cas9 användes för att inducera mutationer i förgreningsenzymernas gener (*SBE*), det granulbundna stärkelsesyntasets gen (*GBSS*), och i kombination. Den resulterande stärkelsen karakteriserades för molekylära och funktionella egenskaper. Kornstärkelse från konventionell korsningsavel karakteriserades också för att utforska potentiella effekter av förändringar i fruktansyntesen på stärkelsesyntesen på kompositions- och molekylär strukturnivå. Att inducera mutationer i alla alleler av *SBEI* och vissa alleler av *SBEII* resulterade i högamylosstärkelse, medan inducering av mutationer i alla alleler av båda *SBE* generna resulterade i amylosstärkelse. Endast *GBSS*-mutationer gav en vaxy stärkelsefenotyp, medan kombinationer av *GBSS*-mutationer med *SBE*-mutationer ledde till icke-vaxy, låg-amylos linjer. Mutationer i *SBEI* producerade stärkelse med kedjelängdsfördelningar liknande ickemodifierade sortens. Mutationer i *GBSS* å andra sidan producerade stärkelse med storleksfördelningar av byggstenar (BB) som liknade ickemodifierade sorten. Signifikanta avvikelser i kedjelängd- och BB-fördelning observerades när både *SBEI* och *SBEII* var muterade. Förekomsten av höga andelar av stora BB höjde gelatiniserings- och retrograderingstemperaturer, medan höga andelar av korta amylopektinkedjor sänkte gelatiniseringstemperaturen. Potatislinjer med olika genetiska bakgrunder uppvisade variationer i viskositet under gelatinisering, vilket påverkade egenskaperna under filmbildning. Konventionell korsningsförädling av korn baserad på naturlig genetisk variation producerade stärkelse med modifierade strukturer, eftersom en uppreglerad fruktansyntes resulterade i stärkelse med en hög andel stora BB. Dessa nya insikter i hur förändringar i stärkelsesyntesvägen påverkar stärkelseegenskaper banar vägen för riktad växtförädling.

Nyckelord: Stärkelseförgreningsenzym gen, granulbundet stärkelsesyntas gen, amylos, gelatinisering, retrogradering, byggstenar (BB), gelatiniseringsegenskaper

Dedication

To the family I was born into and the family I have built

Contents

List of publications.....	9
Abbreviations	13
1. Introduction.....	15
2. Background.....	17
2.1 Starch.....	17
2.1.1 Biosynthesis of storage starch.....	18
2.1.2 Molecular structure of major starch components.....	19
2.1.3 Minor components of starch	21
2.1.4 <i>In-planta</i> modification of starch to suit packaging applications	22
3. Aims.....	23
4. Materials and methods.....	25
4.1 Materials	25
4.1.1 Mutated potato lines	26
4.1.2 Cross-bred barley lines.....	27
4.2 Methods	28
4.2.1 Starch granule size and morphology	28
4.2.2 Starch granule composition	28
4.2.3 Analysis of starch molecular structure	30
4.2.4 Analysis of starch molecular order and crystallinity.....	31
4.2.5 Analysis of starch functional properties	31
4.2.6 Statistical analysis	34
5. Results and discussion	35
5.1 How do alterations in starch biosynthesis enzymes affect the size and morphology of potato starch granules?	35
5.2 How do alterations in starch biosynthesis enzymes affect starch composition?.....	36

5.2.1	Amylose content	36
5.2.2	Total phosphorus and phosphorus forms	38
5.3	How do alterations in starch biosynthesis enzymes affect starch granular order?	40
5.4	How do alterations in starch biosynthesis enzymes affect starch molecular structure?	43
5.4.1	Mutations in <i>SBEs</i> on de-branched chain length distribution pattern	43
5.4.2	Mutations in <i>GBSS</i> in an <i>SBE</i> -mutated background on de-branched chain length distribution pattern	46
5.4.3	Mutations in <i>GBSS</i> in an <i>SBE</i> -mutated background on building block (BB) distribution pattern	48
5.4.4	Mutations in <i>SBEs</i> with/without <i>GBSS</i> on internal chain length distribution pattern.....	49
5.5	What influence do mutations in starch biosynthesis enzymes have on potato starch functionality?	51
5.5.1	Influence of molecular structural and compositional properties on starch thermal properties	51
5.5.2	Influence of molecular structural and compositional properties on starch pasting properties.....	54
5.5.3	Influence of molecular structural and compositional properties on starch film formulation and properties.....	56
5.6	Can alterations in carbon allocation between different carbohydrates achieved by cross-breeding produce starch with tailored molecular properties?	59
6.	Conclusions	61
7.	Future research	63
	References.....	65
	Popular science summary	75
	Populärvetenskaplig sammanfattning	77
	Acknowledgements	79

List of publications

This thesis is based on the work contained in the following papers, referred to by Roman numerals in the text:

- I. Zhao, X.#, **Jayarathna, S.#**, Turesson, H., Fält, A-S., Nestor, G., González, M.N., Olsson, N., Beganovic, M., Hofvander, P., Andersson, R. & Andersson, M.* (2021). Amylose starch with no detectable branching developed through DNA-free CRISPR-Cas9 mediated mutagenesis of two starch branching enzymes in potato. *Scientific Reports* 11 (1), 4311.
- II. **Jayarathna, S.***, Hofvander, P., Péter-Szabó, Z., Andersson, M. & Andersson, R. (2024). *GBSS* mutations in an *SBE* mutated background restore the potato starch granule morphology and produce ordered granules despite differences to native molecular structure. *Carbohydrate Polymers* 331, 121860.
- III. **Jayarathna, S.***, Péter-Szabó, Z., Nestor, G., Andersson, M., Vilaplana, F. & Andersson, R. Impact of mutations in starch synthesis genes on morphological, compositional, molecular structure, and functional properties of potato starch (Submitted).
- IV. **Jayarathna, S.***, Jin, Y., Dotsenko, G., Fei, M., Andersson, M., Andersson, A.A.M., Sun, C. & Andersson, R. (2023). High fructan barley lines produced by selective breeding may alter β -glucan and amylopectin molecular structure. *Carbohydrate Polymers* 316, 121030.

Papers I, II and IV are reproduced with the permission of the publishers. Published in open access.*Corresponding author.

#Shared first authorship.

The contribution of Shishanthi Jayarathna to the papers included in this thesis was as follows:

- I. Participated in designing and planning the experiments, conducted the experiments, analysed and interpreted the data, had co-responsibility for writing and revising the manuscript.
- II. Participated in designing and planning the experiments, conducted the experiments, analysed and interpreted the data, had main responsibility for writing and revising the manuscript, handled correspondence with the journal.
- III. Participated in designing and planning the experiments, conducted the experiments, analysed and interpreted the data, had main responsibility for writing the manuscript, handling correspondence with the journal.
- IV. Participated in designing and planning the experiments, conducted the experiments, analysed and interpreted the data, had main responsibility for writing and revising the manuscript, handled correspondence with the journal.

The following review paper was published during the timeframe of the doctoral project, but is not part of this thesis.

- I. **Jayarathna, S.***, Andersson, M. & Andersson, R. (2022). Recent Advances in Starch-Based Blends and Composites for Bioplastics Applications. *Polymers*, 14 (21), 4557.

Abbreviations

ADP-Glc	ADP glucose
ANOVA	Analysis of variance
BB	Building blocks
daf	Days after flowering
DBE	Starch de-branching enzymes
DP	Degree of polymerisation
DSC	Differential scanning calorimetry
GBSS	Granule-bound starch synthase enzyme
<i>GBSS</i>	Granule-bound starch synthase gene
HPAEC	High-performance anion-exchange chromatography
HPSEC	High-performance size-exclusion chromatography
NMR	Nuclear magnetic resonance
OP	Oxygen permeability
OTR	Oxygen transmission rate
SBE	Starch branching enzyme
<i>SBE</i>	Starch branching enzyme genes
SS	Starch synthases enzyme
SEM	Scanning electron microscopy
TGA	Thermogravimetric analysis
UDMSO	0.6 M urea in 90% dimethyl sulphoxide
α -LDs	α -Limit dextrins
β -LDs	β -Limit dextrins

1. Introduction

Starch, the most abundant storage carbohydrate on earth, plays a vital role as a major energy source in human diets. Apart from starch-based food applications, it is also used in non-food applications such as paper production, cosmetics, textiles, adhesives, pharmaceuticals and packaging (Lawton, 2004).

Industrial starch is derived from various sources, including maize, cassava, potato, wheat, rice and arrowroot. It is predicted that by 2025, 59% of total global starch revenue will derive from the food and feed industry and the remaining 41% will come from other industrial applications. Given the surging demand for starch in non-food applications, use of starch in next-generation applications such as packaging, energy and regenerative medicine is anticipated to grow (Adewale *et al.* 2022).

Starch is a widely available, cheap and renewable natural polymer and has been identified as a promising substitute for petroleum-based materials in different applications (Baek & Song, 2019; Ojogbo *et al.* 2020). However, hydrophilicity, poor thermal and mechanical properties, rapid degradability and limited processability limit the widespread commercial applications of native starch (Ojogbo *et al.* 2020; Agarwal *et al.* 2021). To address these limitations, treatment of starch by physical, chemical, enzymatic or genetic methods, or combinations of these is widely used to produce “modified starch” that has better physicochemical properties for industrial applications (Sagnelli *et al.* 2016; Ojogbo *et al.* 2020; Agarwal *et al.* 2021; Amaraweera *et al.* 2021) (Figure 1).

Among emerging starch modification treatments, *in-planta* modification using genetic methods has received significant attention as an environmentally and economically sustainable approach. *In-planta* modification of starch opens up new opportunities to overcome the

drawbacks of natural starch and could impart beneficial qualities to starch and starch-derived products. In a previous publication (not included in this thesis compilation), I provided a comprehensive review of the potential and advances in production of *in-planta* tailored starch to better suit bioplastics applications (Jayarathna *et al.* 2022).

It is crucial to unlock the significant potential of tailoring starch *in-planta* for diverse applications. A better understanding of the functions of starch synthesis enzymes, methods for altering starch synthesis pathway, and the molecular and functional characteristics of the resulting starch is necessary to establish the links between genetics, molecular structure and functional properties. Inducing targeted mutations in starch synthesis genes followed by characterisation of the resulting starch, represents a promising approach to understand links between genetic composition and starch properties. Thus, the main goal of this thesis was to characterise different starch types produced by targeted gene mutations and conventional cross-breeding, to better understand how these breeding approaches can be employed to customise starch *in-planta* for specific end-uses (Figure 1).

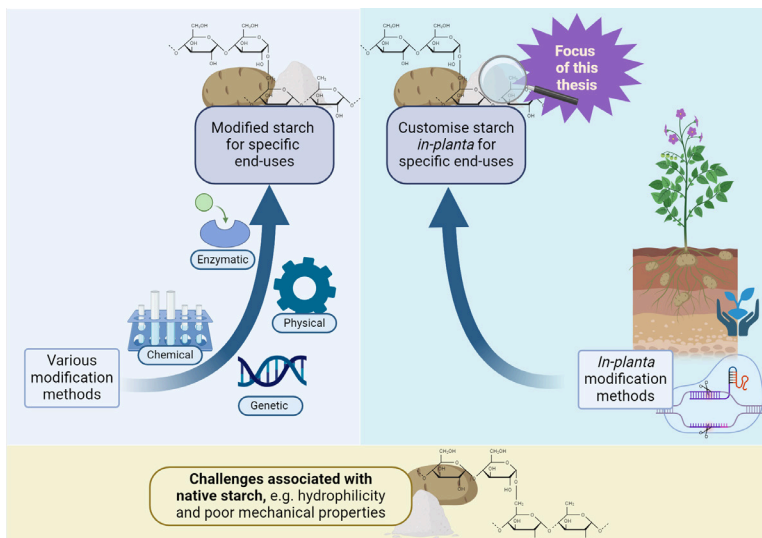


Figure 1. Starch modification for specific end-uses and focus of this thesis

2. Background

2.1 Starch

Starch is produced by green plants in various tissues and organs such as leaves, seeds, stems, roots, fruits and tubers. Starch produced in photosynthetic tissues during the daylight period (transitory starch) is degraded at night to glucose and maltose, which is then transported to the cytoplasm, where it can either be used to make sucrose or serves as an energy source. Sucrose is transported to sink organs to synthesise storage starch (Grennan, 2006).

Starch is a homopolysaccharide made from D-glucose units that are organised to form two different macromolecules, named amylose and amylopectin. Amylose is mostly a linear molecule made from α -1,4 linked D-glucose units, while amylopectin also has α -1,6 branch points that connect α -1,4 linked D-glucose chains. Therefore, amylopectin is a highly branched and larger molecule, with average molecular weight of 10^7 - 10^9 Da, compared with amylose, with molecular weight of 10^5 - 10^6 Da (Buléon *et al.* 1998). In native starch, amylopectin is the major component, comprising 70-80% of total starch by weight. Starch granules have an inner architecture of alternating semi-crystalline and amorphous growth rings (Figure 2). Within the growth rings, there is another level of organisation known as 'blocklets'. Blocklet structure is predominantly formed by crystalline and amorphous lamellae of amylopectin molecules (Gallant *et al.* 1997; Pérez & Bertoft 2010). The amylopectin chains form double helices that can be found in the crystalline lamellae and the amylopectin branch points together with amylose, form amorphous lamellae (Bertoft 2017) (Figure 2). Starch granules vary in size from 1 to 110 μm and exist in various shapes, such as

oval, round, spherical, polygonal and irregular. Starch granular size and shape depend on the botanical origin (Hoover 2001).

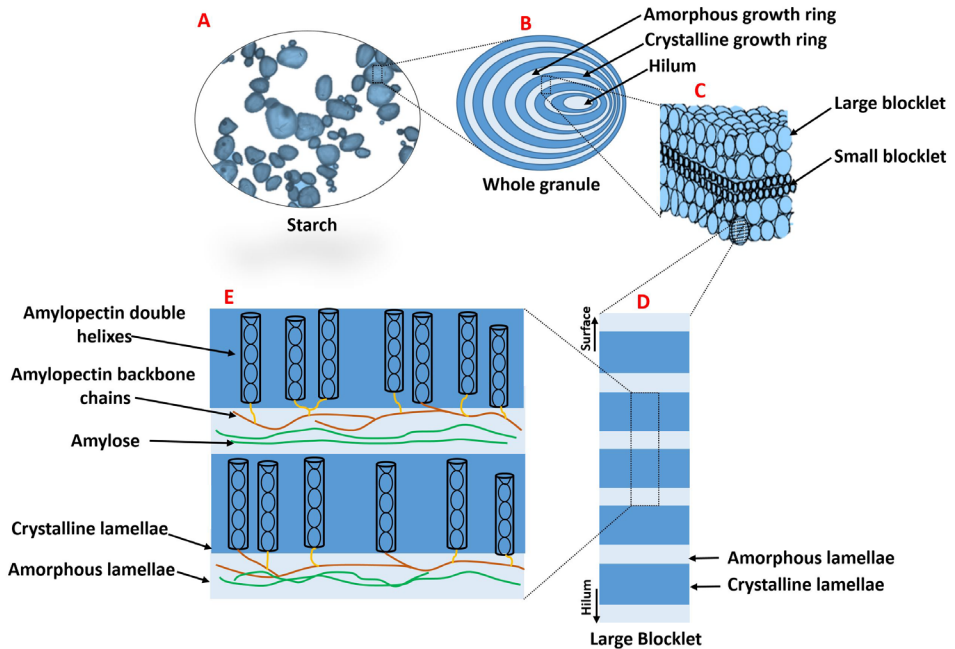


Figure 2. Different levels of structural organisation within the starch granule.

2.1.1 Biosynthesis of storage starch

Biosynthesis of storage starch occurs in specialist amyloplasts located in starch storage tissues. Individual starch granules are generally synthesised separately in separate amyloplasts. An exception is compound starch granules, *e.g.*, rice, waxy rice, oats and wrinkled peas, of which more than one granule is synthesised in the same amyloplast (Pérez & Bertoft 2010). Starch biosynthesis is a complex and highly regulated process that involves many enzymes, such as ADP-glucose pyrophosphorylase, starch synthases (SS), starch branching enzymes (SBE), starch de-branching enzymes (DBE), α -glucan water dikinase (GWD) and phosphoglucan water dikinase (PWD). ADP-glucose (ADP-Glc) is the immediate soluble precursor for starch synthesis and is formed by ADP-glucose pyrophosphorylase from glucose 1-phosphate and ATP. Starch granule formation is believed to start from the central core of the granule, which is known as the hilum (Tetlow & Bertoft

2020). The enzyme responsible for amylose synthesis in plants is granule-bound starch synthase (GBSS), which is an isoform of SS enzymes (Ball *et al.* 1998). There are two tissue-specific isoforms of GBSS (GBSSI, GBSSII), where GBSSI is the form expressed in storage tissues (Vrinten & Nakamura 2000; Tetlow & Bertoft 2020). It is believed that a pre-existing amylopectin scaffold is needed to initiate amylose synthesis. The coordinated activity of three major classes of starch biosynthesis enzymes, *i.e.* SS, SBE and DBE, is needed for amylopectin synthesis. The isoforms of different biosynthesis enzymes involved in amylopectin synthesis differ depending on the plant species. Three SS isoforms (SSI, SSII and SSIII) are involved in elongating linear chains of amylopectin. These isoforms catalyse the introduction of α -1,4 linked glucosyl residues at the non-reducing end of the pre-existing glucan chain, using ADP-Glc as the glucosyl donor (Tetlow & Bertoft 2020). The branched structure of amylopectin molecules arises from the activity of SBE. In plants, there are two major isoforms of SBE (SBEI and SBEII). The general function of SBE is to cleave α -1,4 linked glucan chains of a certain length and transfer the released reducing end to a C6 hydroxyl of the same or different glucan chain. DBE then hydrolyses branch linkages formed by branching enzymes to avoid excessive branching of the amylopectin molecule, which gives rise to the water insoluble properties and the final molecular structure of the amylopectin molecule. There are two DBE types in plants, isoamylase-type and pullulanase-type (Tetlow & Bertoft 2020).

2.1.2 Molecular structure of major starch components

Amylose

Amylose is a linear molecule of α -1,4 linked D-glucose chains (Figure 3). Even though amylose is considered to be a linear molecule, a small proportion of the molecule has a few long-chain branches connected via α -1,6 glycosidic bonds (Hizukuri *et al.* 1981; Shibanuma *et al.* 1994; Vilaplana *et al.* 2012). The average number of chains in a branched molecule depends on the botanical origin (Shibanuma *et al.* 1994).

Amylopectin

The amylopectin molecule consists of many α -1,4 linked glucan chains connected via α -1,6 linkages (Figure 3). Therefore, amylopectin is the highly branched component of starch and is a comparatively larger molecule than

amylose. A nomenclature for the different chains in amylopectin was developed by Peat, Whelan, & Thomas (1952). According to their definition, the outer chains without substitutions are designated A chains, B chains are those carrying other chains as branches, and C chain holds the sole reducing end in addition to A and B chains. Chain length distribution is one of the key parameters used to describe structural characteristics of amylopectin molecules. Techniques such as size-exclusion chromatography, high-performance anion-exchange chromatography (HPAEC) and fluorophore-assisted carbohydrate electrophoresis are currently used to study the chain length distribution of de-branched starch (Bertoft 2017). A model regarding the arrangement of different chains in amylopectin molecules that has gained recent attention is the building block backbone model (Bertoft 2004). This is a two-directional model in which the building blocks (BB) are the basic structural unit and the backbone of the molecule is formed by the long amylopectin chains. The BB which spread out the backbone, form an integrated part of the backbone. The chain segments from the non-reducing end to the outermost branch point (external chains) form double helices that are approximately perpendicular to the backbone (Bertoft 2013). There are different size categories of BB in amylopectin and these increase in size and density as the number of chains increases (Bertoft *et al.* 2012b). Differences in these properties of BB contribute to determining the thermal properties of starch (Källman *et al.* 2015; Zhao *et al.* 2023).

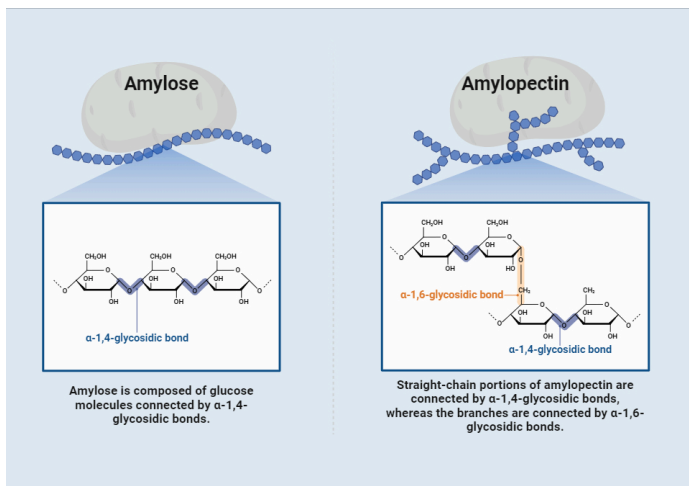


Figure 3. Molecular arrangement of glucose residues in amylose and amylopectin molecules

2.1.3 Minor components of starch

Other than the carbohydrate components, starch also contains proteins, lipids and minerals as minor components. The granule-bound proteins are located either at the granule surface or inside the granules and are present in very low amounts, *i.e.* 0.1-0.7 % by weight (Pérez & Bertoft 2010). Lipids are generally present in cereal starches in the form of free fatty acids or lysophospholipids, while legume starches are lipid-free (Pérez & Bertoft 2010). Among the minute amount of minerals found in starch (calcium, magnesium, phosphorus, potassium, and sodium), phosphorus has been identified as the mineral with most functional significance (Tester *et al.* 2004). Almost all starches contain phosphorus, but in different forms such as phosphate monoesters, phospholipids and inorganic phosphate. Cereal starch typically contains 0.02-0.06% phosphorus on a dry basis, predominantly in the form of phospholipids (Lim *et al.* 1994). In contrast, potato starch has significantly higher levels of phosphate monoesters (0.089% on a dry basis) attached to amylopectin molecules in the C-6 or C-3 position of anhydrous glucose units (Lim *et al.* 1994).

2.1.4 *In-planta* modification of starch to suit packaging applications

In the context of *in-planta* starch modification for packaging applications, significant emphasis has been placed on altering starch composition and/or the molecular structure of glucans, mostly using gene modification techniques. Efforts have been made to create high-amylose or amylose-only starch phenotypes, which exhibit remarkable film-forming and barrier properties and are marked by stable molecular orientation (Rindlav-Westling *et al.* 1998; Myllärinen *et al.* 2002; Menzel *et al.* 2015; Sagnelli *et al.* 2016, 2017). Furthermore, *in-planta* modification of starch granule size has yielded a novel type of potato starch characterised by smaller granules, making it particularly good for generating biodegradable plastic films (Ji *et al.* 2004). Additionally, modifications of starch phosphorylation have led to development of potato starch with reduced phosphate content and favourable film properties, even under wet conditions (Gillgren *et al.* 2011).

3. Aims

There's substantial potential for altering starch within plants to suit particular purposes. Targeted gene editing and cross-breeding offer promising methods to customize starch, particularly in light of changing regulatory standards. Regulatory frameworks, such as the European Union's consideration of different handling of gene-edited crops compared with conventionally genetically modified (transgenic) crops, and existing distinctions in the USA, reflect a global trend towards adopting innovative genetic approaches in agriculture. Therefore, the principal aim of this thesis was to systematically investigate and compare various starches produced by applying targeted mutations using the CRISPR/Cas9 technique and using conventional cross-breeding, focusing on their molecular and functional properties.

Specific objectives of the thesis were to answer the following research questions:

- How do alterations in starch biosynthesis enzymes affect the size and morphology of potato starch granules? (Papers I, II, III)
- How do alterations in starch biosynthesis enzymes affect potato starch composition? (Papers I, II, III)
- How do alterations in starch biosynthesis enzymes affect the granular order of starch? (Papers I, II)
- How do alterations in starch biosynthesis enzymes affect the molecular structure of starch? (Papers I, II, III)
- What influence do the mutations in starch biosynthesis enzymes have on potato starch functionality? (Papers II, III)
- Can alterations in carbon allocation between different carbohydrates achieved by cross-breeding produce starch with tailored properties? (Paper IV)

4. Materials and methods

4.1 Materials

Starch from CRISPR/Cas9-edited potato (Papers I-III), and cross-bred high-fructan barley (Paper IV) were used in this work (Figure 4). Potato starch was isolated according to Larsson *et al.* (1996), with slight modifications. Barley starch was isolated from barley flour obtained by milling the grains in an ultra-centrifugal mill and following the method described by Källman *et al.* (2015) with slight modifications.

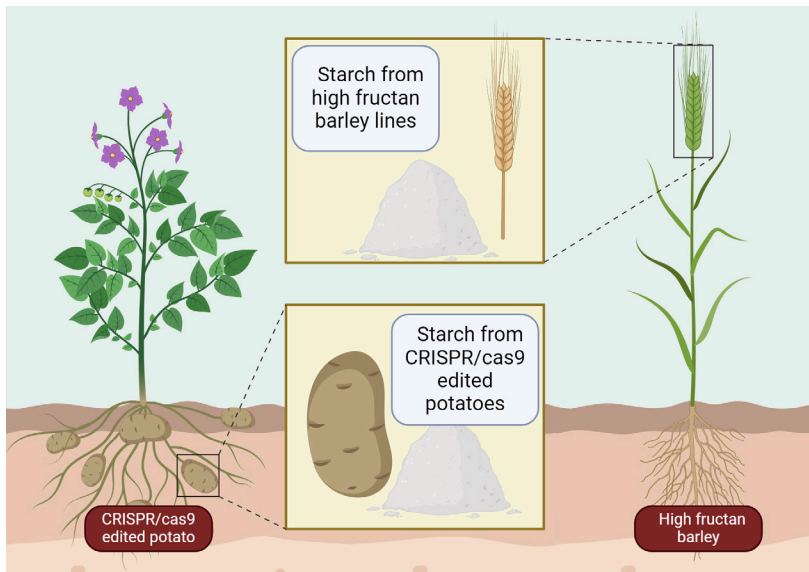


Figure 4. Types of starch analysed in this thesis

4.1.1 Mutated potato lines

All mutated potato lines studied were developed by the Department of Plant Breeding, Swedish University of Agricultural Sciences (SLU), Alnarp, Sweden, using CRISPR/Cas9 technology. The induced mutations in *SBEI*, *SBEII* and *GBSS* genes and the parental variety/line are presented in Table 1. Lines exclusively mutated in *SBEs* were designated high-amylose lines, while those with mutations in *GBSS* were designated high-amylopectin lines. In Paper I, high-amylose lines were divided into three groups based on the mutation: Group 1 (lines with all *SBEI* alleles mutated), Group 2 (lines with additional 2, 3 alleles also mutated in *SBEII*) and Group 3 (all alleles of both *SBEI* and *SBEII* mutated).

Table 1. Types of mutations in potato lines studied in Papers I-III in this thesis.

Group	Potato line	Relevant paper	Parent	Type of mutation		
				<i>SBEI</i>	<i>SBEII</i>	<i>GBSS</i>
High-amylose lines	82007	Paper I	Desiree	✓✓✓✓	-	-
	82050	Paper I	Desiree	✓✓✓✓	-	-
	82079	Paper I	Desiree	✓✓✓✓	-	-
	104011	Paper I	Desiree	✓✓✓✓	-	-
	104032	Paper I	Desiree	✓✓✓✓	-	-
	104001	Paper I	Desiree	✓✓✓✓	✓✓✓	-
	104005	Paper I	Desiree	✓✓✓✓	✓✓✓	-
	104006	Papers I, III	Desiree	✓✓✓✓	✓✓✓	-
	104016	Papers I, III	Desiree	✓✓✓✓	✓✓✓	-
	104018	Papers I, II, III	Desiree	✓✓✓✓	✓✓✓	-
	104034	Papers I, III	Desiree	✓✓✓✓	✓✓✓	-
	104010	Paper I	Desiree	✓✓✓✓	✓✓✓✓	-
	104023	Paper I	Desiree	✓✓✓✓	✓✓✓✓	-
High-amylopectin lines	150172	Papers II, III	104018	✓✓✓✓	✓✓✓	✓✓✓✓
	150183	Papers II, III	104018	✓✓✓✓	✓✓✓	✓✓✓✓
	150154	Paper II	104018	✓✓✓✓	✓✓✓	✓✓✓✓
	150068	Papers II, III	104018	✓✓✓✓	✓✓✓	✓✓✓✓
	150207	Paper II	104018	✓✓✓✓	✓✓✓	✓✓✓
	149108	Paper II	Desiree	-	-	✓✓✓✓

Group: Based on the mutations, e.g., high-amylose lines (*SBE* mutations only) and high-amylopectin lines (with *GBSS* mutations). “✓✓✓✓” indicates all four allele mutations and “✓✓✓” indicates the presence of at least one unmutated allele. “-” indicates no mutations to the respective genes. Desiree (native variety) was included in all three

studies as reference. *SBE*: Starch branching enzyme genes. *GBSS*: Granule-bound starch synthase gene

4.1.2 Cross-bred barley lines

The development of cross-bred barley lines was carried out at the Department of Plant Biology, SLU, Uppsala, Sweden. Four parental lines selected based on high fructan accumulation and low fructan reduction during the development stages were cross-bred in various combinations, to yield six barley lines (Table 2). The resulting barley lines were classified into two groups, Group A and Group B, based on their fructan content at nine days after flowering (daf). Lines in Group A exhibited significantly higher fructan levels ($p < 0.05$) compared with the reference barley variety (Gustav) and, were characterised as having high fructan synthesis activity. All other experimental lines (Group B) and Gustav were classified as having low fructan synthesis activity.

Table 2. Origin of the 10 experimental barley lines (samples 1-10) and reference barley variety Gustav (sample 11) analysed and compared in Paper IV.

Sample	Genealogy	Variety and (developer)	Group
1	#155	SLU 7 (Swedish University of Agricultural Sciences, Sweden)	A
2	#199	KVL 1113 (Royal Veterinary and Agricultural University, Denmark)	A
3	#224	SW 28708 (Lantmännen, Sweden)	B
4	#235	SW 49368 (Lantmännen, Sweden)	B
5	♀#224x♂#155, flat	N/A	A
6	♀#224x♂#199	N/A	A
7	♀#199x♂#155	N/A	A
8	♀#155x♂#199	N/A	A
9	♀#224x♂#155, round	N/A	B
10	♀#199x♂#235	N/A	A
11	#249	Gustav (Lantmännen, Sweden)	B

The samples were grouped into two categories based on fructan synthesis activity: Group A (high activity) and Group B (low activity). N/A: Not Applicable.

4.2 Methods

This thesis utilized various characterisation techniques to analyse starch and films, as depicted in Figure 5 and outlined in sections 4.2.1 to 4.2.5. For more comprehensive descriptions, please refer to Papers I-IV.

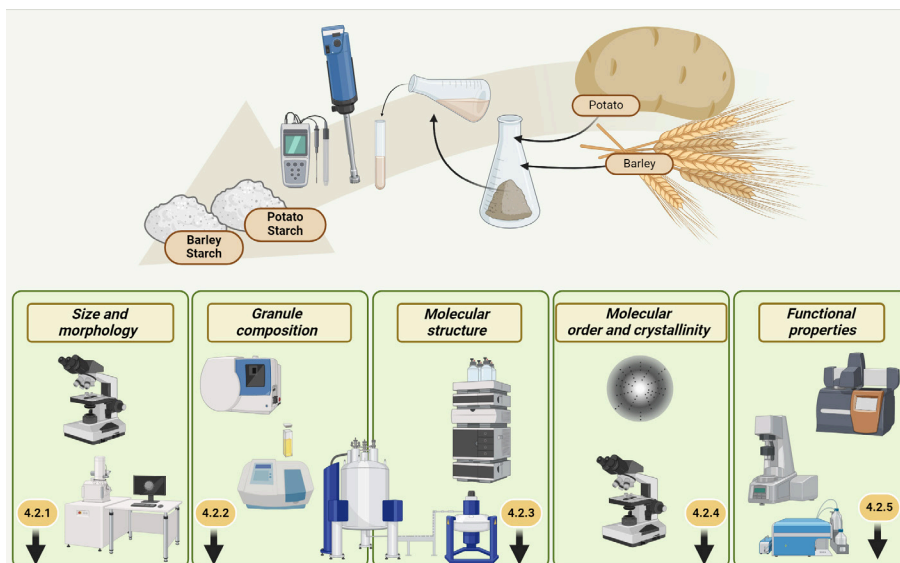


Figure 5. Overview of methods applied in this thesis detailed in sections 4.2.1 to 4.2.5

4.2.1 Starch granule size and morphology

Starch granule size distribution was studied using a SALD-2300 laser diffraction particle size analyser with SALD-BC23 batch cell system configuration (Shimadzu, Japan), using ethanol as the starch dispersion medium (Paper II). The morphology of starch granules stained with Lugo's solution was investigated using a light microscope (LeicaDMLB, Leica Microsystems, Wetzlar, Germany) (Papers I and II).

4.2.2 Starch granule composition

Amylose: amylopectin ratio

Amylose content was studied based on complex formation of amylose component with iodine and stabilised with trichloroacetic acid according to Chrastil (1987). Isolated starch was first solubilised with 0.6 M urea in 90%

aqueous DMSO (UDMSO), before incubating with 0.01 N KI-I₂ solution. UV-visible spectroscopy was used to measure absorbance and amylose content in unknown starch samples were determined by comparison with a standard curve of known amylose contents (Paper I). Due to limitations such as potential overestimation caused by iodine binding to the long external chains of amylopectin (Hoover & Ratnayake 2001), amylose content determination after Concanavalin A precipitation of amylopectin was supplemented in Paper I and, used in Papers II and III. This amylose determination method, which is based on the principle described by Yun & Matheson (1990), involves precipitating amylopectin with Concanavalin A, enzymatically hydrolysing the supernatant to D-glucose, and analysing it with glucose oxidase/oxidase reagent. Concanavalin A forms complexes less frequently with amylose, due to its fewer non-reducing ends compared with amylopectin, as explained by Matheson & Welsh (1988).

Total phosphorus content and amounts of different forms of phosphorus

The phosphorus content in starch was determined using a Spectro Blue inductively coupled plasma instrument (Spectro Analytical Instruments, Germany) with a modified SS 028311 method. Starch samples were weighed and treated with a mixture of 50% concentrated nitric acid and 50% deionised distilled water in glass vials, and simmered on a heat block for about an hour. After cooling, the contents were diluted with deionised distilled water, mixed thoroughly and analysed using the Spectro Blue instrument.

In Paper III, amounts of different forms of phosphorus were determined by ³¹P-NMR analysis. Starch suspension in water (0.1 g/10 mL) was first degraded with α -amylase to ensure proper dissolution, and freeze-dried twice before re-dissolving in 600 μ L D₂O. EDTA (0.5 M in D₂O, pH 8.0) was added to obtain an EDTA sample concentration of 25 mM for enhancement of spectral quality and resolution. Sample pH was adjusted to 8.0 (equivalent to pD 8.5) with sodium hydroxide (0.1 M in D₂O). ³¹P NMR spectra were recorded at 25 °C on a Bruker Avance III 600 MHz spectrometer with a 5 mm broadband observe detection SmartProbe. Spectra were acquired with inverse gated ¹H decoupling and 256 scans, using a spectral width of 8 ppm, an acquisition time of 2.1 s and a relaxation delay of 5 s, and processed with TopSpin 4.1.4. Calculation of the relative amounts of various phosphorus forms was conducted by integration of the corresponding NMR signals. The absolute amounts were then determined, considering the total phosphorus

content analysed by the inductively coupled plasma technique. The ^{31}P chemical shifts were indirectly referenced to external phosphoric acid (85%).

4.2.3 Analysis of starch molecular structure

Chain length and building block distribution of whole starch

Chain length distribution of de-branched whole potato starch was analysed in Papers I-III and BB distribution was analysed in Paper II for potato starch and Paper IV for barley starch. For de-branched chain length distribution analysis, whole starch was solubilised in UDMSO and de-branched by isoamylase and pullulanase enzymes prior to analysis using high-performance size-exclusion chromatography (HPSEC) and HPAEC. Building block distribution was analysed in whole starch by treating starch with α -amylase and β -amylase as described by Zhao *et al.* (2021). β -Amylase was employed to hydrolyse the linear external chains of amylose and amylopectin, generating β -limit dextrins (β -LDs). The β -LDs were hydrolysed with α -amylase to generate α -limit dextrins (α -LDs). These α -LDs were then subjected to β -amylase treatment to eliminate any residual external chains, resulting in formation of BB.

HPSEC analysis was performed according to Andersson *et al.* (2009). The HPSEC system featured a serially connected guard column and two OHPak SB-802.5 HQ columns (Shodex, Showa Denko KK, Miniato, Japan) maintained at a temperature of 35 °C and equipped with a refractive index detector (Wyatt Technology Corp., Santa Barbara, CA in Paper I; Shodex RI-501, Showa Denko KK, Miniato, Japan in Paper II) and a multiple-angle laser light scattering detector (Wyatt Technology Corp., Santa Barbara, CA). ASTRA software (Wyatt Technology Corp., Santa Barbara, CA) was employed for data analysis.

The HPAEC 4500i system (Papers I, II) or the ICS-6000 series (Paper III) from Dionex Corp. (Sunnyvale, CA, USA) was employed alongside a pulsed amperometric detector (PAD) and a BioLC gradient pump for HPAEC analysis. At a temperature of 25 °C, elution was conducted with a flow rate of 1 mL/min and an injection volume of 25 μL , using 0.15 M NaOH (A) and 0.50 M NaOAc + 0.15 M NaOH (B) in an CarboPac PA100 (4 \times 250 mm) analytical column (Dionex, Sunnyvale, USA) coupled with a guard column. The following gradient was applied for de-branched chain length distribution analysis: 0-15 min, 15-28% eluent B; 15-45 min, 28-55% B; 45-75 min, 55-

70% B; and 75-80 min 70-15% B (Papers I-III). The PAD response in de-branched chain length distribution analysis (Papers I- III) was converted to molar percentage (M%).

4.2.4 Analysis of starch molecular order and crystallinity

Polarised light microscopy

Polarised light microscopy was conducted on starch dispersed in distilled water (Papers I & II). A light microscope (Leica DMLB, Wetzlar, Germany) was used to identify the presence and characteristics of Maltese crosses within starch granules. The Maltese cross birefringence pattern of starch is indicative of highly organised granules with crystallites arranged radially.

Wide-angle X-ray diffraction analysis

Crystalline pattern (Papers I & II) and degree of crystallinity (Paper II) of starch were determined by wide-angle X-ray diffraction analysis. Diffraction patterns of powder starch samples were recorded between 5° and 40° 2 θ . A PANalytical X'Pert alpha1 X-ray diffractometer was employed in Paper I, while a Panalytical X'pert Pro diffractometer was employed in Paper II. Degree of crystallinity in Paper II was determined using X-ray diffraction diagrams, following Liu *et al.* (2009) and Dome *et al.* (2020). A fitted smooth line connecting the minimum diffraction intensities of the X-ray diffractogram represented the crystalline region, and degree of crystallinity was calculated as the ratio of this area to the total area above a straight line connecting the entire 5-40° 2 θ range, including both crystalline and amorphous regions.

4.2.5 Analysis of starch functional properties

Thermal properties

The gelatinisation and retrogradation characteristics of starch were examined by modulated differential scanning calorimetry (DSC), using a DSC250 device (TA Instruments, New Castle, DE, USA). For gelatinisation analysis, 20 mg of starch were weighed into high-pressure aluminium pans, equilibrated with 60 μ L water and heated from 20 to 120 °C at a rate of 4 °C/min within the DSC (Papers II & III). The same samples were stored at 5 °C for three days before retrogradation analysis (Paper III). In Paper II, 25 mg of starch were cooked with 50 μ L of water at 121 °C for 15 minutes in

an autoclave-steam steriliser to ensure complete gelatinisation before storage at 5 °C.

Rheological properties

Rheological data on starch dispersions (2.08 g starch in 26 mL distilled water) were acquired using a Discovery HR-3 hybrid rheometer (TA Instruments, New Castle, DE, USA), following the method outlined by Nilsson *et al.* (2022) with modifications. A rheometer was chosen over a conventional rapid visco-analyser in order to achieve high temperatures and pressure, which are required by mutated starch types to complete gelatinisation. A Peltier pressure cell and steel paddle were used. A heating-cooling cycle of 30-130-38 °C was applied to the samples, with a heating rate of 5°C and a cooling rate of 4.2 °C. The samples were held at 130 °C for 5 minutes before the cooling cycle. The rotational speed was set to the device maximum (50 rad/s) for the initial 20 seconds, and then in the actual experiment at 16.75 rad/s, maintained throughout (Paper III).

Starch film formulation and characterisation

Starch films were prepared using high amylose and amylopectin starch and their properties were characterised and compared as indicated in Figure 6. Starch films were prepared by a modified method as explained by Menzel *et al.* (2015) and characterised using the techniques listed in Table 3. Starch dispersions (180 mg dry weight in 6 mL water) were maintained at 128 °C in a sealed tube for 45 minutes with continuous stirring in a Pierce Reacti-Therm heating/stirring module. Heating in sealed tubes was required to ensure gelatinisation of all mutated starch types. The solutions were then cooled to approximately 95 °C and mixed with 40 µL glycerol for 5 minutes before casting 8.4 mL solution to 8.5 cm diameter Petri dishes. The solvent was allowed to evaporate overnight at 23 °C, and the dishes were left to dry for 48 hours.

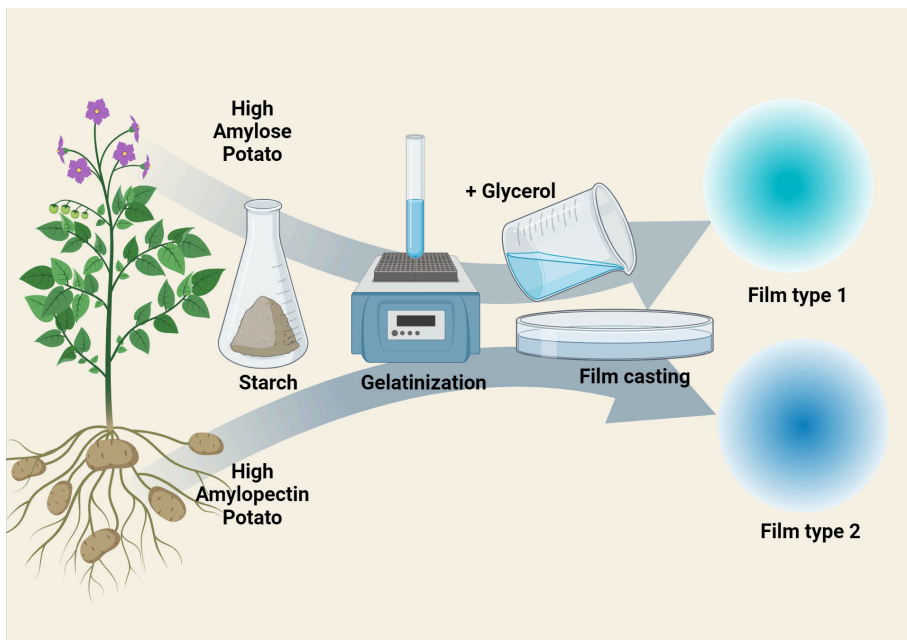


Figure 6. Schematic representation of film formulation from high-amylose and high-amylopectin potato starches.

Table 3. Methods used to characterise potato starch films in Paper III.

Property	Approach	Instruments and Method
Optical properties	Scanning electron microscopy (SEM)	Film samples attached by double-sided tape to an holder were examined using environmental electron microscopy Flex SEM 1000 II (HITACHI, Japan). Micrographs were captured at magnification of 100 \times .
Thermal properties	Thermogravimetric analysis (TGA)	Thermal stability of the starch films was evaluated by TGA, by monitoring their thermal degradation using a Mettler-Toledo TGA/DSC 1 instrument. Films were heated from 30 to 600 $^{\circ}$ C at 10 $^{\circ}$ C/min under nitrogen flow of 50 mL/min.
Tensile properties	Examining Young's modulus, and strain at break	A modified protocol based on ASTM D882-12 and ISO 527-1:2019 was applied to pre-conditioned films (7 days at 23 \pm 2 $^{\circ}$ C and 50 \pm 10 % relative humidity). Tensile testing were conducted on five specimens (10 mm \times 80 mm) from each of two distinct film preparations (batches), using an initial gauge length 25 mm and strain rate 0.1 min $^{-1}$.

Gas barrier properties	Testing oxygen transmittance rate (OTR) and oxygen permeability (OP)	The ASTM-F1927 standard procedure was employed. Gas barrier properties were measured in a 5 cm ² exposure area of films after pre conditioning at 23 °C, 50% relative humidity for 10 hours using an Ox-Tran 2/21 SH instrument (AMETEK–MOCON, Minneapolis. MN. USA)
-------------------------------	--	---

4.2.6 Statistical analysis

In Papers I, II, & III, one-way analysis of variance (ANOVA) was used to check for statistically significant differences between the mean values of the measured parameters. Tukey pairwise comparisons were carried out in Paper II and III, and Dunnett’s test in Paper II, using Minitab 21 (State College, PA, USA) to compare each mean with every other mean of the studied variables and each mean with the control mean. Additionally, in Paper II and III, Pearson correlation coefficient analyses were performed at confidence level 95% ($p < 0.05$) using Minitab 21, to assess the strength of the association between variables.

In Paper IV, Tukey pairwise comparisons and Dunnett’s test were conducted using the Minitab 18 software. The correlations between BB size and other studied parameters were checked by principal component analysis (PCA) using Simca 14.0 software from Umetrics (Umeå, Sweden). Spearman’s rank correlation coefficient analysis was performed using Minitab 18 software to further explore the correlations between BB size and other parameters.

5. Results and discussion

In this chapter, the six research questions defined in Chapter 3 of this thesis are addressed in sequence.

5.1 How do alterations in starch biosynthesis enzymes affect the size and morphology of potato starch granules?

In Papers I and II, the morphology of potato starch granules was studied in relation to type/s of mutation. Clear alterations to starch granule morphology brought about by different mutation types were observed (Figure 7). As explored in Paper I, mutations solely in *SBEI* (Group 1 starch) did not modify the morphology of potato starch granules. However, inducing mutations in one or two alleles of *SBEII* along with *SBEI* (Group 2 starch) resulted in potato starch granules with irregular shapes and rough surfaces compared with the native starch granules, which exhibited oval shape and smooth surface morphology. Granule morphology was most significantly affected when all alleles of both *SBEI* and *SBEII* were mutated (Group 3 starch), producing small irregular granules with a spherical multi-lobed phenotype. These changes observed in the morphology of potato starch granules resulting from the editing of *SBE* genes using CRISPR/Cas9 technology align with findings by Tuncel *et al.* (2019). In Paper II, the altered granule morphology of starch from the *SBE*-mutated Group 2 lines was somewhat restored when *GBSS* was simultaneously mutated with *SBEs* (Figure 7).

In addition to the alterations in granule phenotype, mutations in starch synthesis genes also impacted starch granule size, as reported in Paper III. Four high-amylose lines and three high-amylopectin lines (Table 1) were included in Paper III to investigate the effects of different mutations in starch

synthesis genes on starch granule size. The mean granule size of the native variety was 33 μm , whereas two high-amylose lines, 104006 and 104018, exhibited lower mean granule size of around 23 μm . In contrast, all other high-amylose and high-amylopectin lines demonstrated granule size closer to that of Desiree.

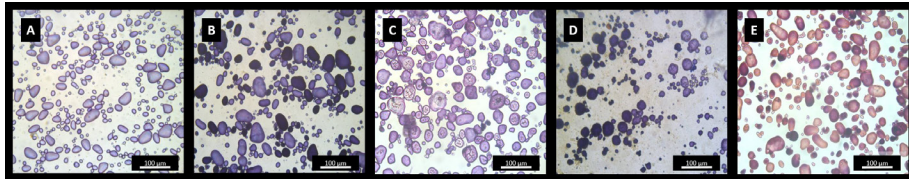


Figure 7. Morphology of potato starch granules. (A) Desiree (B) Group 1 starch (C) Group 2 starch (D) Group 3 starch (E) *GBSS+SBEs* mutated starch. Adopted from Papers I and II with permission.

5.2 How do alterations in starch biosynthesis enzymes affect starch composition?

Effects of mutations in *SBEs* and *GBSS* in relation to the amylose content, total phosphorus content, and amounts of different forms of phosphorus of potato starch are discussed in this section.

5.2.1 Amylose content

Investigation of amylose content as influenced by mutations in *SBE* and *GBSS* was carried out in Papers I-III. Using the enzymatic method after Concanavalin precipitation of amylopectin component, it was found that Group 3 starch with all mutated alleles in both *SBEs* had almost 100% amylose content (Paper I). Therefore, CRISPR/Cas9 mutagenesis in all alleles of both *SBE* genes was able to produce amylose-only potato starch. The amylose content of starch from *SBEs* mutated lines 104006 (34% in Paper III) and 104018 (38% in Paper II and 45% in Paper III) showed significantly higher levels ($p < 0.05$) compared to the amylose content of starch from native Desiree variety (27%). This observation of high amylose content in *SBE*-mutated crops agrees with findings in several previous studies (e.g. Matheson & Welsh 1988; Carciofi *et al.*, 2012; Huang *et al.* 2015; Zhao *et al.* 2018; Li *et al.* 2019). The high amylose feature of *SBE*-mutated crops could be due to several reasons. First, inhibiting *SBE* activity

can decrease amylopectin levels, leading to a higher proportion of amylose. Second, SBE suppression may decrease amylopectin branching, hindering α -1,6-linkages in starch and promoting the formation of elongated amylose-like chains within the amylopectin (Seung 2020; Zhong *et al.* 2022, 2023).

GBSS is the enzyme responsible for plant amylose synthesis, and any mutations in the gene controlling this enzyme should principally produce waxy phenotypes (amylose content <5 %). This was confirmed in Paper II, where inducing mutations only in *GBSS* yielded waxy lines, in agreement to findings by Toinga-Villafuerte *et al.* (2022). However, inducing mutations in *GBSS* in an *SBE*-mutated background did not result in waxy lines (Papers II & III). A particularly intriguing observation was that, despite the complete knockout of *GBSS* in an *SBE*-mutated background, plants exhibited the capability to produce amylose at levels approaching normality. Findings obtained for line 150068 (Papers II & III) exemplified this phenomenon. This suggests potential compensation for the role of GBSS by other active enzymes in starch synthesis when *GBSS* is concurrently mutated in an *SBE*-suppressed context, or synergistic effects of different starch biosynthetic enzyme isoforms. Moreover, isoform SSIII in an *SBE*-suppressed context could generate lengthy amylopectin chains, potentially detected as amylose in an *SBE*-mutated background, due to reduced branching frequency. Additional experimental investigations are required to verify this. Another interesting observation was the very high amylose feature of line 150207, which might result from the remaining wild-type allele in *GBSS*, allowing near-normal amylose production despite probable reduced GBSS enzyme activity. Besides *GBSS*, mutations in *SBEs* may also have contributed to the total amylose content of 150207 line. Notably, line 150207 exhibited a higher amylose content (49%) than the parental line 104018 (38%), despite 104018 lacking a *GBSS* mutation (Paper II).

However, during different greenhouse periods, the starch from some mutated potato lines displayed a difference in amylose content. This observation suggests that starch synthesis in the mutant crops is highly susceptible to variations in environmental conditions.

5.2.2 Total phosphorus and phosphorus forms

Total phosphorus content and the amounts of different forms of phosphorus in starch from high-amylose lines and high-amylopectin lines were investigated in Paper III (Table 4). The major proportion of potato starch phosphorus is present as phosphate monoesters (Kasemsuwan & Jane, 1996) and it plays a vital role in determining starch functional properties (Karim *et al.* 2007). Other forms of phosphorus in starch include free phosphates and phospholipids.

Starch from high-amylose lines with *SBE* mutations exhibited an average two-fold increase in total phosphorus compared with the native variety, Desiree (0.6 g/kg). High phosphorus content of *SBE*-mutated potato starch has been reported previously (Schwall *et al.* 2000; Hofvander *et al.* 2004). Starch from high-amylopectin lines with in-frame mutations in the *GBSS* (have insertion or deletion of nucleotides (base pairs) that are multiples of three, only deleting or adding one or a few amino acids. Hence the protein is not knocked out or truncated, but still present in minor edited form) in an *SBE*-mutated background (lines 150172 and 150183) showed an average four-fold increase in total phosphorus content compared with the native variety. However, starch from the high-amylopectin line with *GBSS* knockout genes together with *SBE* mutations (line 150068) showed only a 0.8-fold increase in total phosphorus content compared with Desiree.

High phosphorylation of all the mutated starches compared with the native variety is an interesting feature from an industrial point of view, since high phosphorylation prevents crystallisation and affects the final viscosity of the product (Ellis *et al.* 1998). The inherent high degree of phosphorylation of these starches can help eliminate or decrease the need for costly and environmentally harmful industrial chemical phosphorylation processes.

The high total phosphorus content of amylopectin starch observed in Paper III might be linked to the fact that most phosphate monoesters are covalently bound to the amylopectin fraction (Blennow *et al.* 2002), and elevated amylopectin content might therefore increase the total content of phosphate monoesters. According to Blennow *et al.* (1998), starch phosphate groups tend to be associated with longer glucan chains. *SBE* mutations generally form long glucan chains with less branching frequency, which might become highly phosphorylated. A negative correlation between the

branching frequency of glucan chains and phosphate content has been reported previously (Wang *et al.* 2021).

As determined by ³¹P NMR analysis (Table 4), in the majority of the mutated potato lines, 80% of phosphorus existed as starch-bound phosphates, while Desiree contained 69% of its phosphorus as starch-bound phosphates. Considering the starch-bound phosphates, all the lines exhibited higher content of phosphates attached at the C6 position compared with C3-attached phosphate groups, in agreement with findings in several previous studies (*e.g.* Lim *et al.* 1994; Blennow *et al.* 2000). The ratio of C3-attached phosphate to C6-attached phosphate was 0.2 in most of the mutated lines, compared with 0.3 in Desiree. Regarding the inorganic phosphate content, the mutated starch samples showed increased levels of inorganic phosphate, ranging from 1.2- to 4.9-fold higher than in Desiree, while the phospholipid content was almost constant irrespective of mutation (Table 4).

Table 4. Total phosphorus (P) content and amounts of different forms of phosphorus in mutated potato lines and Desiree.

Potato line	Total P content (g/kg)	C3 ¹ (g/kg)	C6 ² (g/kg)	C3/C6 ratio	Proportion of total starch-attached phosphates	Free Phosphate (g/ kg)	Phospholipids (g/ kg)
150172	3.0	0.46	1.96	0.23	0.80	0.48	0.10
150183	2.8	0.49	1.77	0.28	0.81	0.42	0.12
150068	1.1	0.15	0.67	0.22	0.75	0.18	0.09
104006	2.2	0.33	1.42	0.23	0.79	0.34	0.12
104016	1.6	0.24	1.01	0.24	0.78	0.24	0.11
104034	1.7	0.24	1.12	0.21	0.79	0.24	0.11
104018	2.0	0.25	1.20	0.21	0.73	0.41	0.14
Desiree	0.6	0.10	0.31	0.33	0.69	0.08	0.10

¹C-3 attached phosphate monoester

²C-6 attached phosphate monoester

5.3 How do alterations in starch biosynthesis enzymes affect starch granular order?

Starch granules, by their inherent nature, possess densely packed crystallites, facilitating their role in performing vital plant physiological functions. This characteristic structure enables efficient energy storage in plants over extended periods. In Papers I and II, two techniques, namely X-ray diffraction analysis and polarised light microscopy, were used to determine the order or crystallinity of starch granules.

X-ray diffraction analysis was used to determine the crystalline pattern of the different starch types (Papers I & II). Tuber starch in general possesses a B-type crystalline arrangement with diffraction peaks at 15° (broad), 17° (strong) and a doublet at $22\text{-}24^\circ$ 2θ (Hizukuri *et al.* 1996). All the high-amylose and high-amylopectin lines studied in this thesis showed a B-type crystalline arrangement (Papers I & II). However, as observed in Paper I, the diffraction intensity of the main peaks was affected in Group 3 starch having mutations in all alleles in both *SBE* genes (Figure 8a). This was the only mutational scenario studied in this thesis that significantly affected the appearance of X-ray diffractograms. The crystallinity of granular starch is predominantly associated with the amylopectin fraction (Bertoft 2017). Consequently, the marked reduction in X-ray diffraction intensity observed in Group 3 starches may be attributable to the considerable loss of the amylopectin fraction in these starch samples, given that the external chains of amylopectin primarily form the crystallites.

When examined under a polarised light microscope, starch granules typically exhibit a distinctive Maltese cross birefringence pattern that indicates a radial arrangement of crystallites within the granules (Pérez *et al.* 2009). In Paper I, starch from Group 3 did not show Maltese cross birefringence, whereas starch from Desiree and high-amylose Group 2 showed the typical pattern (Figure 8b). In Paper II, all the high-amylopectin lines showed Maltese crosses, but starch from 150207 line and the *SBE*s mutated parental line 104018 did not show clear Maltese crosses at the centre of the granules (Figure 8c). As elucidated by French (1984), the intensity of birefringence depends upon factors such as granule thickness, crystallinity and the orientation of crystallites. Therefore, the reduced intensity of Maltese crosses noted in the starch from 150207 and 104018 in Paper II could be attributable to changes in some of these factors.

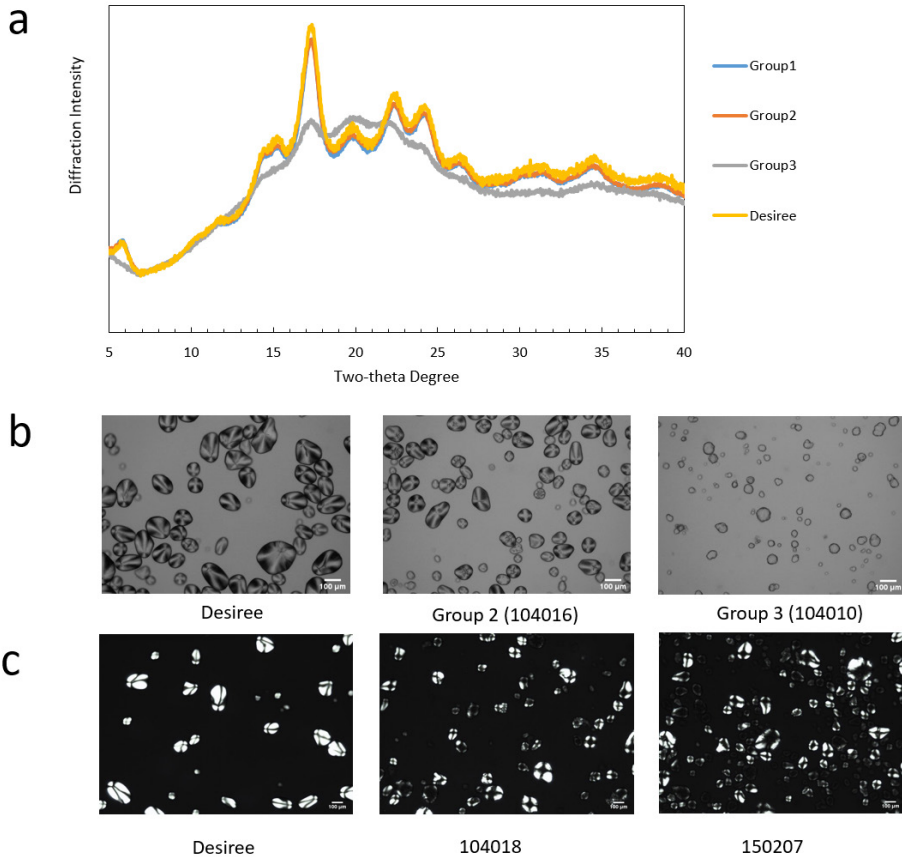


Figure 8. (a) Wide angle X-ray diffractograms and (b) polarised light microscopy images of starches analysed in Paper I and (c) polarised light microscopy images of starches analysed in Paper II, adopted with permission.

In Paper II, the X-ray diffractograms were used to calculate the degree of crystallinity of different starch types (Figure 9). The values obtained were close to previously reported values for native potato starch (20-25%) (dos Santos *et al.* 2016) and waxy potato starch (30%) (Jiranuntakul *et al.* 2011). Analysis by Dunnett's multiple comparison, taking native variety Desiree as the control sample, revealed that potato starches from lines 150183, 150207 and 149108 clustered with Desiree, displaying lower degree of crystallinity than starches from the remaining lines. Particularly, among the lines containing starch with a lower degree of crystallinity, starch from line

150207 demonstrated the lowest value (24.6%). This could be linked to the significant increase in amylose content of starch from that line, resulting in a decrease in the relative content of amylopectin fraction, which is responsible for the crystallinity of starch granules. However, despite the waxy line (149108) having the highest amylopectin content, starch from lines 150172, 150154 and 150068 exhibited higher crystallinity values. This discrepancy suggests that other features of these starches (such as variation in the molecular structure of amylopectin) may contribute to the development of crystalline regions, promoting the packing of double helices and establishing a more organised crystalline lattice. Further experiments are needed to uncover the specific factors influencing starch crystallinity.

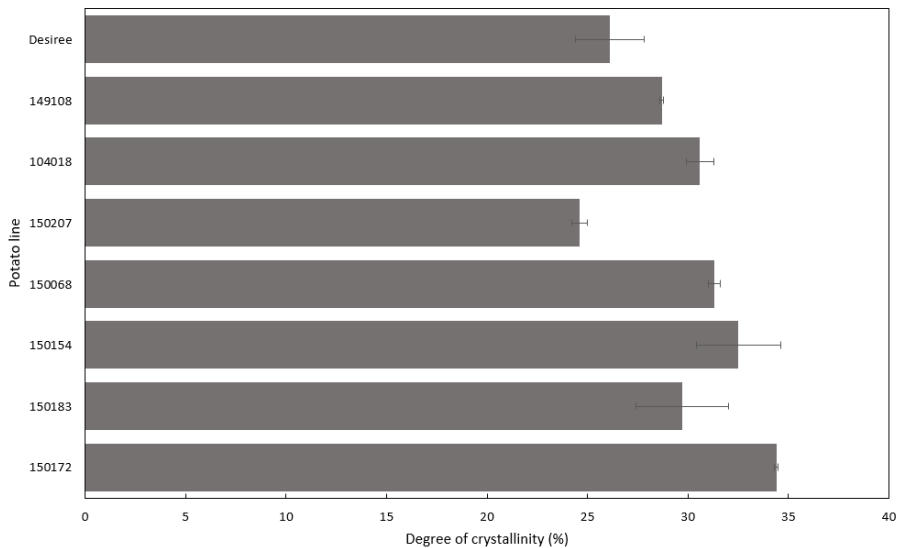


Figure 9. Degree of crystallinity (%) of potato lines analysed in Paper II.

5.4 How do alterations in starch biosynthesis enzymes affect starch molecular structure?

The effects of mutations in genes controlling starch synthesis enzymes on starch molecular structure were investigated from various perspectives. These included an examination of their impact on unit chain distribution patterns (Papers I-III), internal chain length distribution patterns (Paper III), and building block distribution pattern (Paper II).

5.4.1 Mutations in *SBEs* on de-branched chain length distribution pattern

The impact of various mutations in *SBEs* on the de-branched chain length distribution pattern of whole potato starch was extensively examined in Paper I. The investigation involved inducing mutations in three distinct groups: (i) *SBEI* only (Group 1 starches); (ii) *SBEI* and the 2, 3 alleles in *SBEII* (Group 2 starches); and (iii) all alleles of both *SBEI* and *SBEII* (Group 3 starches).

In HPSEC analysis, alterations in chain length distribution pattern were noted in both the amylose and amylopectin fractions, correlating with the specific mutation type (Figure 10a). The fraction eluting before 13 mL in the chromatogram represented the amylose fraction, whereas the fraction eluting after 13 mL constituted the amylopectin fraction. The amylose fraction exhibited three populations, characterised by short, intermediate and long chains, as discerned in the chromatogram (Figure 10a). Notably, mutations in *SBEI* alone (Group 1 starches) did not induce significant changes in the amylopectin chain length distribution pattern, aligning well with the amylopectin chain length distribution of Desiree in the HPSEC chromatogram (Figure 10a). According to Schwall *et al.* (2000), this could stem from the fact that the presence of the *SBEII* isoform alone is adequate for synthesis of amylopectin with a normal branching structure and *SBEII* can compensate for decreased activity of *SBEI*, while the reverse scenario is only partially effective, suggesting differences in enzyme specificities.

Upon closer examination of the amylopectin fraction using HPAEC analysis, slight differences in the chain length distribution pattern were observed in Group 1 starches compared with Desiree. These differences included a lower abundance of chains with DP 7-11 and DP 22-33, and a higher abundance of chains with DP 12-21 (Figure 10b).

Inducing mutations to *SBEII* together with *SBEI* caused drastic alterations to the chain distribution pattern of mutated starch of Groups 2 and 3, as shown by the HPSEC and HPAEC chromatograms (Figure 10). This observation aligns with literature reports of altered chain length distribution in potato starch with mutations in both *SBEI* and *SBEII* induced using techniques such as CRISPR/Cas 9 (Tuncel *et al.* 2019) and other gene modification methods (Schwall *et al.* 2000; Hofvander *et al.* 2004). Group 2 starches exhibited a modified amylose chain length distribution in comparison with Desiree, notably featuring a smaller peak for intermediate amylose chains (Figure 10a). HPAEC analysis revealed that Group 2 starches displayed a reduced proportion of short amylopectin chains $DP \leq 13$ and an increased proportion of chains with DP 14-33 compared with Desiree.

Among all induced mutations, the most profound impact on the chain length distribution pattern was associated with Group 3 starches. As depicted in the HPSEC chromatogram (Figure 10a), the amylopectin fraction entirely disappeared, compensated for by elevated amounts of the amylose fraction. This finding aligns with the results of the amylose content analysis (see section 5.2.1). In addition, the amylose fraction of Group 3 starches lacked the peak corresponding to short-chain amylose chains observed in Desiree. The chain lengths of Group 3 starches were beyond the separation capacity of the HPAEC instrumentation, and therefore no chromatogram was obtained for Group 3 starches.

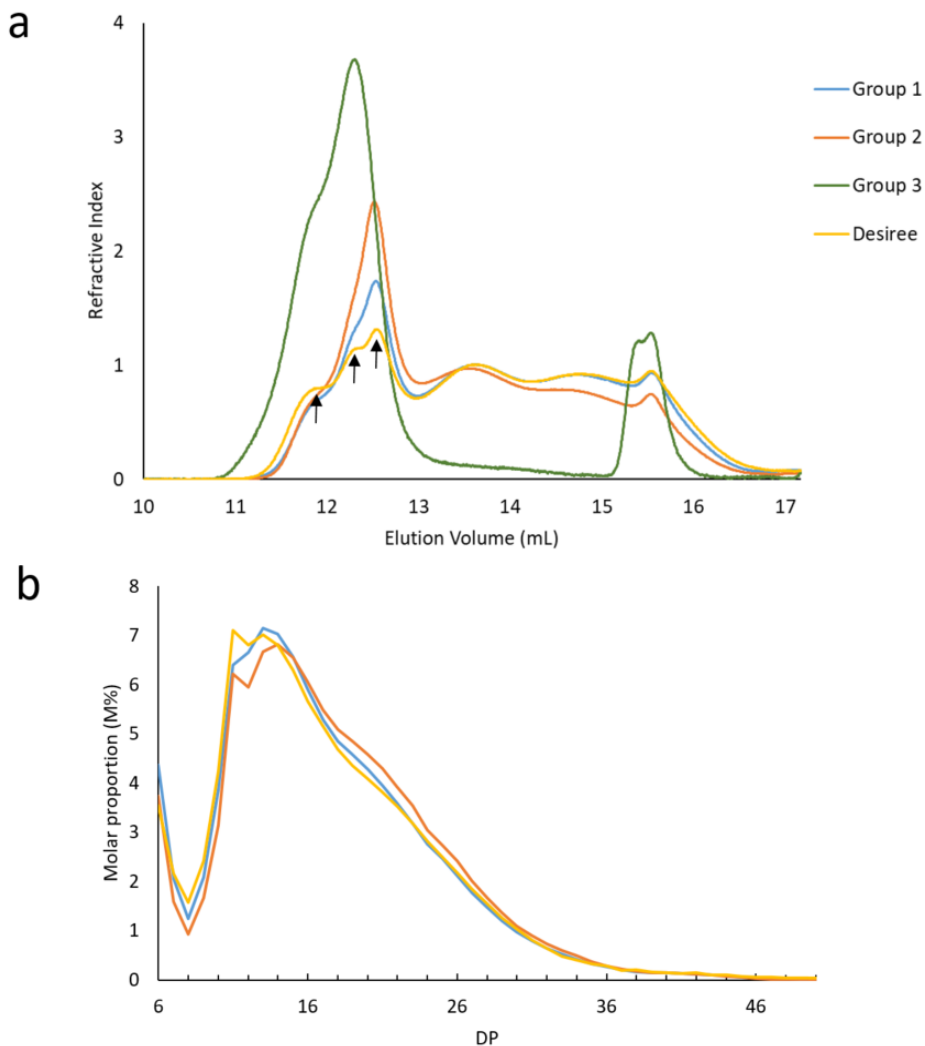


Figure 10. (a) Chain length distribution of de-branched starches of potato lines from Groups 1, 2 and 3 after normalisation for peak area, analysed with HPSEC. The arrows from left to right indicate the long, intermediate and short-chain amylose fraction, respectively. (b) Chain length distribution of de-branched starch on a relative molar basis (M%) with degree of polymerisation (DP) 6-50, based on HPAEC analysis. Adopted from Paper I with permission.

5.4.2 Mutations in *GBSS* in an *SBE*-mutated background on de-branched chain length distribution pattern

The impact of inducing mutations in *GBSS* in an *SBE*-mutated background on the de-branched chain length distribution pattern of whole potato starch was investigated in Papers II and III. In Paper II, the unit chain distribution was analysed by HPSEC (Figure 11a) and HPAEC (Figure 11b).

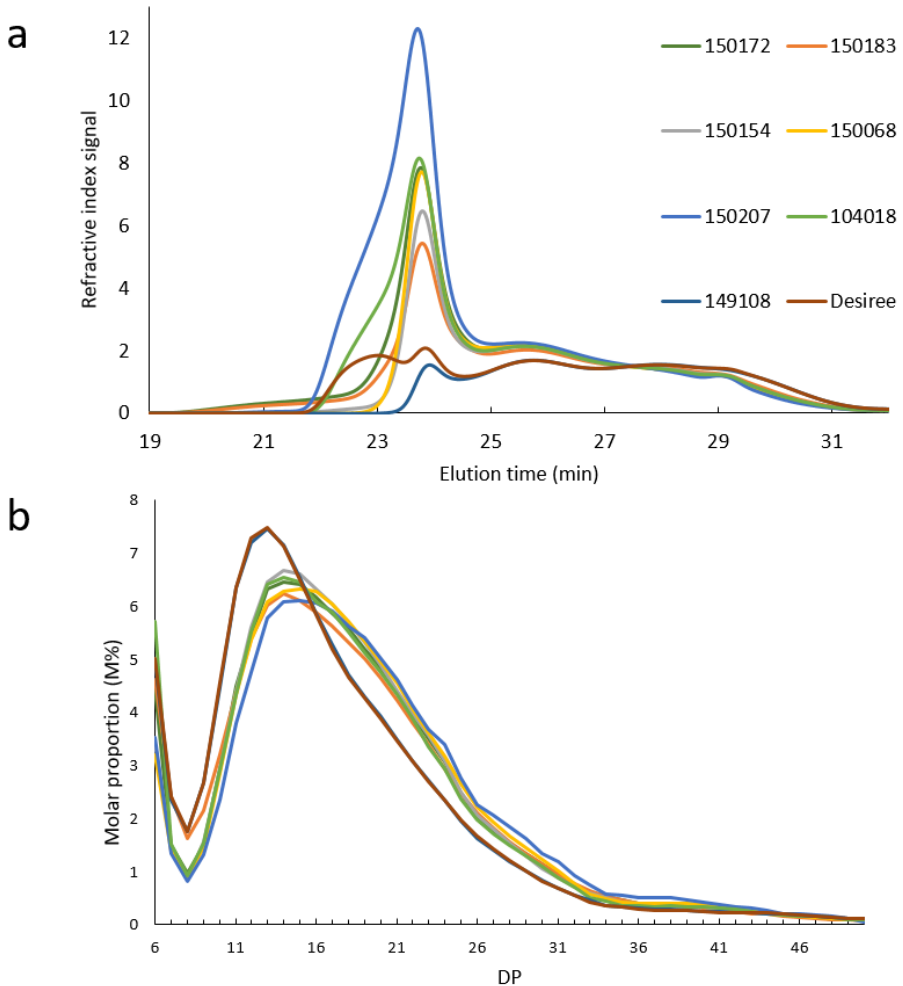


Figure 11. (a) Chain length distribution of de-branched starches of potato lines normalised for the amylopectin peak area (25-32 min), analysed with HPSEC. (b) Chain length distribution of de-branched starch on a relative molar basis (M%) with degree of polymerisation (DP) 6-50, based on HPAEC analysis. Reproduced from Paper II with permission.

In the HPSEC chromatogram (Figure 11a), the peaks that appeared before 25 minutes were linked to chains arising from amylose molecules, while peaks appearing after 25 minutes originated from the amylopectin molecules. As deduced from the HPSEC outcomes, starch from the mutated potato lines exhibited markedly distinct patterns in the distribution of unit chain lengths compared with Desiree, as evident in both amylose and amylopectin fractions. However, the amylopectin fraction in starch from the *GBSS*-knockout line 149108 closely resembled that observed in Desiree. This aligns with the results obtained in HPAEC analysis (Figure 11b). It indicates that knocking out only the *GBSS* gene did not influence the amylopectin unit chain distribution pattern.

The distribution pattern of amylose peaks exhibited a strong correlation with the specific mutations. For example, starch from all potato lines with mutations in *SBE* displayed a higher abundance of amylopectin chains eluting around 24 minutes (Figure 11a). This distinctive feature was consistently observed in potato starch with *SBE* mutations throughout all experiments and could be a characteristic of high-amylose starch formed due to restricted activity of SBE. Starch with this characteristic was designated “amylose-like material” by Zhong *et al.* (2022).

Starch from line 150207 displayed a distinctive unit chain distribution characterised by high abundance ($p < 0.05$) of the longest amylopectin fractions (fractions eluting between 25-27 min in HPSEC analysis, $DP \geq 25$ in HPAEC analysis). Consequently, line 150207 exhibited a unique starch profile, featuring elevated amylose content and long amylopectin chains, suggesting good potential as a healthy carbohydrate. Thus the functional wild-type *GBSS* allele in 150207 not only increased the amylose proportion in starch (see section 5.2.1), but also exerted a minor influence on the molecular structure of amylose and amylopectin polyglucans in a background with mutated *SBEs*. The role of *GBSS* enzyme activity in determining the molecular structure of amylopectin, as evident in Figure 11, has been documented previously (Brummell *et al.* 2015). The modified chain length distribution of starch observed in *SBE+GBSS*-mutated lines compared with the parental *SBE*-mutated 104018 line indicates the influence of *GBSS* mutations within an *SBE*-mutated context on the chain length distribution of starch. Thus, the investigation into the role of *GBSS* in shaping the chain

length distribution of starch in the presence of an *SBE*-mutated background produced particularly intriguing results.

5.4.3 Mutations in *GBSS* in an *SBE*-mutated background on building block (BB) distribution pattern

The impact of inducing mutations in *GBSS* in an *SBE*-mutated background on the BB distribution pattern of potato starch was investigated in Paper II. The distribution of BB exhibited two distinct patterns, correlating with samples possessing or lacking mutations in the *SBE* genes (Figure 12). Table 5 lists individual variations in the abundance of different BB groups, which were likely attributable to the specific mutations present. Mutations exclusively in *GBSS*, observed in starch from potato line 149108, did not impact the size distribution of BB, aligning closely with Desiree. Mutations exclusively in *SBEs* (line 104018) led to modifications in the size distribution of BB compared with Desiree, highlighting the substantial role of *SBE* mutations in shaping starch fine structure at BB level. In addition, there were differences in specific BB group categories between starches from lines with different *GBSS* mutations in an *SBE*-mutated background and the parental line 104018 (Table 5). This finding highlights the influential role of the *GBSS* in determining the abundance of various size categories of BB in an *SBE*-mutated background.

Table 5. Variation in normalised peak area of different size groups (G6-G2) of building block distributions in potato lines

Potato line	Building block group				
	G6	G5	G4	G3	G2
150172	17.3 ^{ab}	85.6 ^b	356.7 ^b	121.3 ^c	419.1 ^d
150183	12.1 ^c	70.6 ^d	320.1 ^d	141.6 ^b	455.6 ^b
150154	14.4 ^{bc}	79.3 ^c	345.8 ^c	128.5 ^c	432.1 ^c
150068	19.4 ^a	90.7 ^a	365.7 ^b	120.6 ^d	403.6 ^c
150207	14.9 ^{bc}	88.2 ^{ab}	382.2 ^a	112.2 ^e	402.5 ^e
104018	13.2 ^c	79.1 ^c	347.3 ^c	132.1 ^c	428.3 ^{cd}
149108	2.1 ^d	24.5 ^c	189.3 ^e	199.6 ^a	584.5 ^a
Desiree	2.9 ^d	26.9 ^c	195.5 ^e	197.0 ^a	577.7 ^a

Values within columns with different superscript letters showed significant differences (ANOVA, $\alpha=0.05$). Adopted from Paper II with permission.

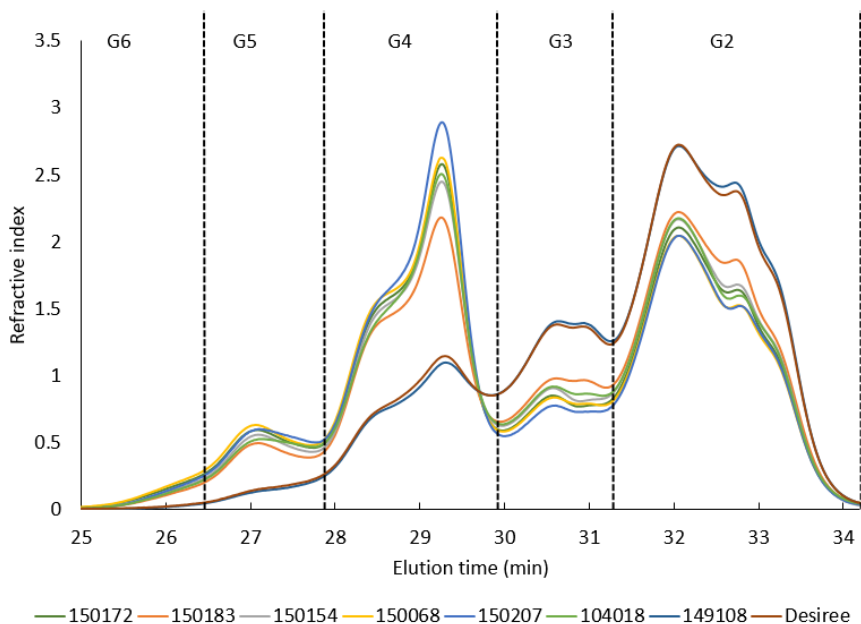


Figure 12. Building block distribution in starch from potato lines after normalisation for peak area, as determined by HPSEC. The distribution was bucketed in groups (G) as G6: elution time 25.0-26.4; G5: 26.4-27.9; G4: 27.9-29.9; G3: 29.9-31.3; G2: 31.3-34.3 min. Reproduced from Paper II with permission.

5.4.4 Mutations in *SBEs* with/without *GBSS* on internal chain length distribution pattern

The segments of the chains that extend from the furthest branching point to the non-reducing end of the amylopectin chain are referred to as external chains (Zhu *et al.* 2011). Removal of these external chains using exo-acting enzymes reveals the internal part of the amylopectin molecule, which can be de-branched to determine the distribution pattern of internal chains (Bertoft *et al.* 2012a). Similarly, the distribution of internal chains of potato starch was analysed by HPSEC in Paper III after beta-amylolysis of starch, followed by de-branching of the resulting β -limit dextrins, which resembled the internal amylopectin chains (Figure 13).

Starch from potato lines 104018 and 104006 exhibited a nearly identical pattern in their distribution of de-branched β -limit dextrins. Similarly, starch from lines 104016, 104034, 150172 and 150183 displayed a comparable

distribution. The internal chain distribution of 150068 closely resembled that of Desiree. In high-amylopectin lines (with *GBSS* mutations; Table 1), absence of very long internal chains originating from the amylose fraction (eluting between 22-23 min) was observed. Instead, a peak around 24 min, corresponding to short internal chains from amylose, was prominent both in high-amylose (with only *SBE* mutations; Table 1) and high-amylopectin lines compared with Desiree (Figure 13). For more detailed analysis of amylopectin internal chains, the chromatogram was divided into three distinct fractions (25.0-26.2, 26.2-28.2 and 28.2-32 min), as outlined in Table 6. These segments were designated short, intermediate and long internal amylopectin chains, respectively. Starch from both high-amylose and high-amylopectin lines exhibited a higher proportion of long internal amylopectin chains and a lower proportion of short amylopectin internal chains compared with Desiree (Table 6).

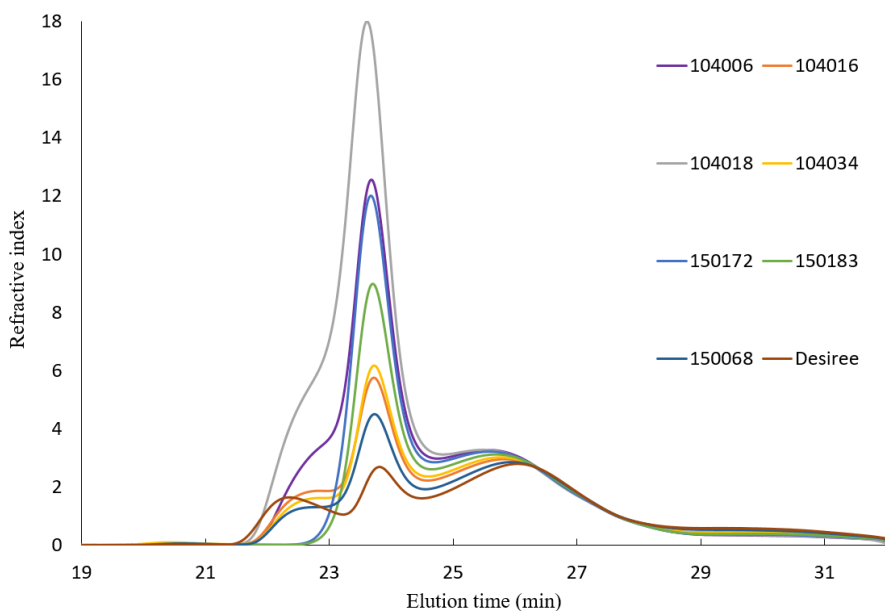


Figure 13. Internal chain length distribution of de branched β -limit dextrins analysed by HPSEC on a relative weight basis after normalising for amylopectin peak area 25-32 min. Reproduced from Paper III.

Table 6. Abundance of different categories of amylopectin internal chains in different potato lines as analysed by HPSEC.

Potato line	Long chains (25-26.2 min)	Intermediate chains 26.2-28.2 min	Short chains 28.2-32 min
104006	468 ^a	383 ^{cd}	150 ^f
104016	415 ^d	390 ^{ab}	195 ^c
104018	468 ^a	378 ^d	154 ^f
104034	427 ^c	390 ^{ab}	183 ^d
150172	459 ^a	380 ^d	160 ^{ef}
150183	444 ^b	387 ^{bc}	168 ^e
150068	391 ^e	392 ^{ab}	216 ^b
Desiree	369 ^f	394 ^a	238 ^a

Values within columns with different superscript letters showed significant differences (ANOVA, $\alpha=0.05$). Adopted from Paper III.

5.5 What influence do mutations in starch biosynthesis enzymes have on potato starch functionality?

5.5.1 Influence of molecular structural and compositional properties on starch thermal properties

The gelatinisation and retrogradation properties of starch in relation to starch molecular structure and composition were studied in Papers II and III (Table 7). Discrepancies in gelatinisation and retrogradation parameters within the same potato starch in the two papers may be attributable to alterations in molecular and compositional features influenced by varying cultivation years. For retrogradation parameters, differences in sample preparation between the two studies could also have been a contributing factor.

Gelatinisation properties

The starch from mutated lines displayed elevated gelatinisation temperatures and a reduced enthalpy change during gelatinisation (ΔH) compared with Desiree starch (Table 7). This trend was seen for all starches analysed in Papers II and III except line 150068 in Paper III.

Table 7. Gelatinisation and retrogradation properties of starches from different potato lines studied in Papers II & III

Potato line	Gelatinisation parameters					Retrogradation parameters	
	T_o	T_p	T_e	T_e-T_o	ΔH	T_p	ΔH
Paper II							
150172	67.5 ^c	75.8 ^b	85.3 ^b	17.7 ^{ab}	16.0 ^{cd}	74.0 ^{ab}	10.6 ^{ab}
150183	68.4 ^b	75.4 ^b	83.4 ^b	15.0 ^e	16.7 ^{cd}	73.0 ^{ab}	11.0 ^a
150154	67.7 ^c	75.3 ^b	84.1 ^b	16.4 ^{bc}	17.8 ^{bc}	74.2 ^{ab}	10.2 ^{abc}
150068	68.4 ^b	76.9 ^a	85.2 ^b	16.8 ^{bc}	16.0 ^{cd}	75.0 ^a	9.8 ^{abc}
150207	68.5 ^{ab}	76.8 ^a	87.8 ^a	19.2 ^a	15.1 ^d	73.2 ^{ab}	9.3 ^{abc}
104018	67.0 ^d	75.3 ^b	84.0 ^b	17.0 ^{bc}	19.5 ^{ab}	70.8 ^{bc}	8.4 ^c
149108	68.8 ^a	72.8 ^c	78.7 ^c	9.9 ^e	17.4 ^{bcd}	67.3 ^d	9.5 ^{abc}
Desiree	64.8 ^e	69.3 ^d	77.4 ^c	12.6 ^d	20.7 ^a	68.3 ^{cd}	8.8 ^{bc}
Paper III							
104006	67.4 ^a	76.4 ^a	86.5 ^a	19.1 ^a	15.5 ^c	73.4 ^{ab}	7.0 ^e
104016	66.2 ^{bc}	72.9 ^{cd}	81.6 ^c	15.4 ^d	19.5 ^b	70.3 ^{bc}	9.0 ^{bcd}
104018	67.3 ^{ab}	75.3 ^b	85.9 ^a	18.6 ^{ab}	11.4 ^d	70.3 ^{bc}	6.7 ^e
104034	65.0 ^d	71.4 ^e	81.5 ^c	16.5 ^c	20.2 ^b	71.0 ^{bc}	9.4 ^{abc}
150172	65.3 ^{cd}	73.3 ^c	83.2 ^b	17.9 ^b	14.3 ^c	75.0 ^a	7.8 ^{de}
150183	65.6 ^{cd}	72.2 ^{de}	81.3 ^c	15.8 ^d	15.7 ^c	73.3 ^{ab}	8.5 ^{cd}
150068	63.1 ^e	68.0 ^f	75.6 ^e	12.4 ^f	19.2 ^b	70.2 ^{bc}	9.8 ^{ab}
Desiree	63.0 ^e	68.7 ^f	76.7 ^d	13.7 ^e	22.4 ^a	67.9 ^c	10.4 ^a

T_o : onset temperature, T_p : peak temperature, T_e : endset temperature ΔH : enthalpy change corrected for amylopectin proportion. Values within columns with different superscript letters showed significant differences within each Paper (ANOVA, $\alpha=0.05$). Adopted from Papers II (with permission) and III.

Pearson correlation analysis revealed strong negative correlations ($p<0.05$) between gelatinisation temperatures (T_o , T_p , T_e) or gelatinisation temperature range (T_e-T_o) and A chains, while positive correlations were observed with B1, B2 and B3 chains of the amylopectin fraction (Paper II). According to Zhong *et al.* (2023), amylopectin with DP 6-12 (referred to as A chains) may introduce defects into the crystals, resulting in the formation of starch granules that gelatinise at lower temperatures. The gelatinisation parameters also demonstrated strong positive correlations ($p<0.05$) with large BB of G4, G5 and G6, and negative correlations with small BB of G2

and G3 (Paper II), aligning with the findings of Zhao *et al.* (2023). In Paper III, gelatinisation temperatures displayed significant positive correlations ($p<0.05$) with the long internal chain category of amylopectin, and negative correlations with intermediate and short internal chain categories. According to Zhu (2018), amylopectin characterised by a longer internal chain length has a tendency to form a more organised arrangement of double helices within the starch granules, which contributes to enhanced thermal stability. This may partly explain the elevated gelatinisation temperatures observed in samples containing a relatively higher proportion of long internal amylopectin chains.

A positive correlation ($p<0.05$) was observed between the enthalpy change during gelatinisation (ΔH) and the amylopectin A-chain category (Paper II). However, a negative correlation ($p<0.05$) was observed between B chains (Papers II & III) and the long internal chain category of amylopectin (Paper III). In Paper III, negative correlations were also identified between ΔH and total phosphorus content, C6-bound phosphate content, phospholipid content and inorganic phosphate content. These findings strongly suggest an adverse impact of phosphorus on the degree of crystallinity, thereby influencing the ΔH of starch during the gelatinisation process.

Retrogradation properties

Gelatinised starch undergoes transformation from a disordered to an ordered state known as retrogradation. In this thesis work, the analysis of retrogradation parameters was particularly pertinent to retrograded amylopectin, since crystal melting of retrograded amylose typically occurs at a higher temperature range (130-160 °C) than crystal melting of amylopectin.

Both studies (Papers II & III) revealed that starch from lines with mutations in the *SBE* genes had elevated peak temperature of retrogradation (T_p) (Table 7). Pearson correlation analysis identified a robust positive correlation ($p<0.05$) between the T_p and large BB categories (G4, G5 and G6), along with a strong negative correlation with small BB categories (G2, G3) in Paper II and with short internal amylopectin chains and A unit chains in Paper III. These findings align with those in previous studies on correlations between BB size categories and retrogradation parameters (Zhao *et al.* 2023). In addition, T_p of crystal melting showed positive correlations with total phosphorus content and with amount of total starch-bound phosphate groups (Paper III).

Moreover, the enthalpy change (ΔH) of retrogradation exhibited a negative correlation ($p < 0.05$) with the proportions of the long internal amylopectin chain category and B2 and B3 unit chains (Paper III). This negative relationship between long internal chains and retrogradation enthalpy concurs with findings by Zhao *et al.* (2023). Essentially, the longer the internal amylopectin chain length, the lower the branching density of amylopectin, reducing the likelihood of molecular rearrangement and the formation of retrograded crystals. Enthalpy change (ΔH) of retrogradation also showed negative correlations with phospholipid content and inorganic phosphate content in Paper III.

5.5.2 Influence of molecular structural and compositional properties on starch pasting properties

Paper III investigated the pasting properties of starch from various potato lines. The pasting curves for the potato starch samples are depicted in Figure 14. Clear variations in pasting behaviour were apparent among samples with different mutations, as evidenced by the distinct pasting curves (Figure 14).

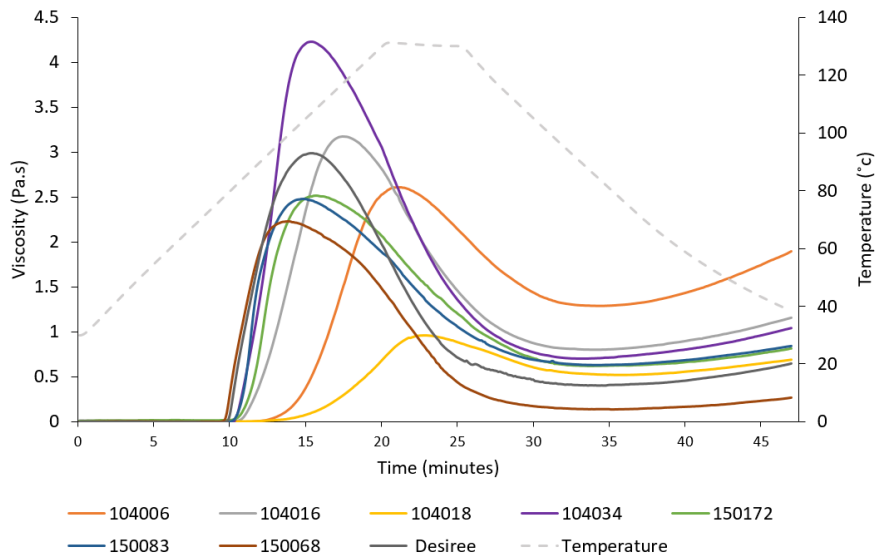


Figure 14. Pasting curves of starch from different potato lines. Reproduced from Paper III.

Pasting temperature indicates the point at which viscosity begins to increase due to water absorption and loss of starch structure. The analyses revealed a distinct connection of pasting temperature to molecular structural and granular features. It demonstrated positive correlations with the unit chains of B2 category and long internal chain category of amylopectin, and negative correlations with intermediate and short internal chain categories, as well as with starch granule size. This agrees well with the knowledge that granule swelling is hindered by long amylopectin chains, which delay the onset of pasting in starch due to their role in maintaining granular integrity (Singh *et al.* 2017).

Peak viscosity represents the maximum viscosity achieved during the continuous temperature rise when granule swelling is at its maximum, just before extensive granule breakdown. The starch that reached peak viscosity at the longest duration and highest temperature was from potato line 104018, which also had the highest amylose content (45%). This observation suggests that granule swelling is constrained by the amylose component, aligning with previous findings (Chen *et al.* 1998; Jane *et al.* 1999).

Shear thinning of starch pastes occurred, leading to a reduction in viscosity to minimum values. Breakdown viscosity, defined as percentage change in viscosity from the peak to the minimum value, showed positive correlations with medium and short chain categories of amylopectin internal chains. A positive correlation was also identified with starch granule size, aligning with earlier findings (Zaidul *et al.* 2007; Singh *et al.* 2017). In contrast, a negative correlation was observed with the amylopectin long internal chain category and B2 unit chain category. This negative correlation between breakdown viscosity and long amylopectin chains is consistent with results reported by Singh *et al.* (2017). The correlations are due to lower swelling of starch with long amylopectin chains, leading to a diminished degree of disintegration and, consequently, lower breakdown viscosities.

Viscosity increases on cooling of the pastes, resulting in the final viscosity. The difference between minimum and final viscosity is referred to as setback viscosity and is caused by amylose forming a gel network matrix (Chen *et al.* 1998). In Paper III, a trend was observed where the *SBE*-mutated lines exhibited the highest final and setback viscosities in comparison with Desiree, followed by the *SBE+GBSS* mutated lines.

5.5.3 Influence of molecular structural and compositional properties on starch film formulation and properties

Starch film formulation and characterisation were performed in Paper III. All the high-amylose and high-amylopectin lines (see Table 1) were able to form starch films. The highest surface roughness (as visualised by SEM) was achieved by starch film of high-amylose potato line 104018, while starch from high-amylopectin line 150068 produced the smoothest and most uniform film surface compared with Desiree (Figure 15). The increased surface roughness observed in starch film from line 104018 may be attributable to its elevated amylose content (45%) and rapid aggregation of amylose during the cooling process. It could also be due to the presence of granule remnants after gelatinisation, as indicated by the high resistance to gelatinisation.

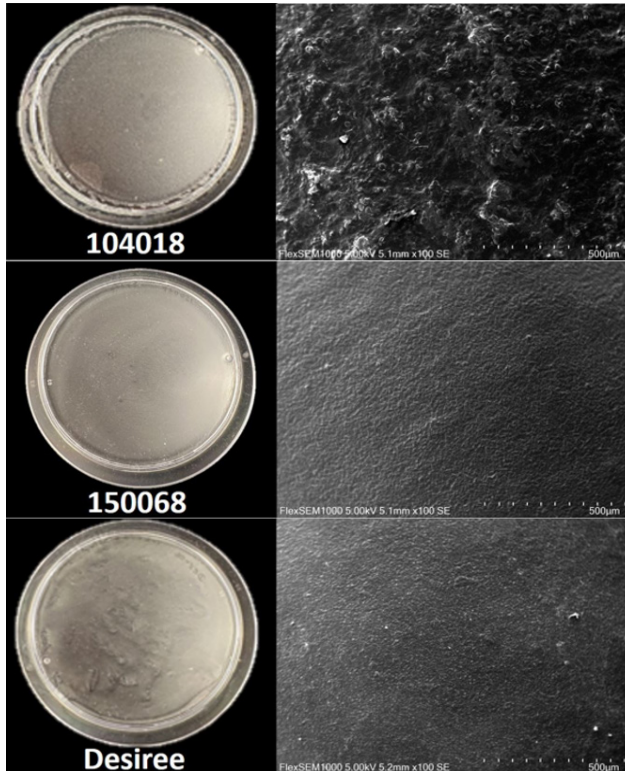


Figure 15. Morphology of starch films from high-amylose potato line 104018, high-amylopectin line 150068 and native variety (Desiree). Left: Digital images of the films; Right: the corresponding SEM images. Adopted from Paper III.

Young's modulus and strain at break were studied for all film samples (Table 8). Great variation in tensile properties for different film formulation replicates was observed, which is likely attributable to the variations in the sensitivity of different starch types to conditions during film formulation. This variability may have resulted in the absence of significant differences between various starch films in terms of studied tensile properties. Starch film from potato line 104016 exhibited a higher modulus value than Desiree, while starch film from line 104018 displayed the lowest modulus value. The starch film from line 150068 demonstrated the lowest standard deviation of modulus among different film replicates, suggesting that film formulation from starch from line 150068 was more reproducible. The film samples from lines 104006, 104018, 150068 and 150172 had lower Young's modulus (<1000 MPa), and could be stretched above 10% strain.

TGA was conducted to evaluate the thermal stability of different films. The peak temperature at which thermal decomposition was observed is presented in Table 8. In Paper III, films derived from mutated potato starch tended to exhibit lower decomposition peak temperatures than Desiree, indicating diminished thermal stability. Starch films from the *GBSS*-mutated high-amylopectin lines displayed lower decomposition temperatures than those from solely *SBE*-mutated high-amylose lines, with the exception of starch film of 104018. The lower peak temperature of decomposition in *GBSS*-mutated high amylopectin lines could be linked to their elevated total phosphorus content. This suggestion is supported by the observed negative correlation between peak temperature of decomposition and both total and free phosphate content (Pearson's correlation, $p < 0.05$). It has been posited that the high phosphorus content in starch may impart greater amorphous characteristics to the films, disrupting the rearrangement of starch chains within the film (Domene-López et al. 2019).

Oxygen barrier properties were investigated for film made with starch from 150068 line and compared with film from Desiree. The reason for this selection was grounded in the intriguing biological aspects (e.g. similar amylose content to Desiree, despite mutations in *GBSS*), functional characteristics (closest starch pasting and thermal properties to Desiree) and film-making attributes (lowest time to paste, very low viscosity at the time of casting, smooth film surface, easiness to handle and replicate) of starch from line 150068 compared with starch from other potato lines. Given the

well-established understanding of the effective oxygen barrier properties of starch films, the objective was to ascertain whether these desirable barrier properties persist in potato starch film from line 150068.

The results indicated that the oxygen transmission rate (8.5 ± 1 cc/m²/24h) and oxygen permeability (0.3 ± 0.05 cc·mm/m²·24h·atm) of 150068 did not exhibit a significant difference ($p>0.05$) to those of Desiree (7.4 ± 0.8 cc/m²/24h and 0.3 ± 0.02 cc·mm/m²·24h·atm, respectively). Consequently, the oxygen barrier properties of the film from 150068 line remained uncompromised compared with the starch film from Desiree.

Table 8. Tensile and thermal properties of starch films investigated in Paper III.

Potato line	Modulus (Mpa)	Strain at break (%)	Peak temperature of decomposition (°C)
104006	724.6±103.5	15.3±3.5	297 ^c
104016	1280.2±190	4.9±2.5	300 ^b
104018	419.3±274	10.6±4.9	289 ^e
104034	1043.1±754	18.1±16.1	297 ^c
150172	560.2±197	21.3±1.5	290 ^e
150183	1060.3±311	4.5±4.0	293 ^d
150068	598.0±7.5	12.0±2.4	294 ^d
Desiree	1213.9±135.7	4.6±2.0	307 ^a

Values within last column with different superscript letters showed significant differences within each film samples (ANOVA, $\alpha=0.05$). Adopted from Paper III.

5.6 Can alterations in carbon allocation between different carbohydrates achieved by cross-breeding produce starch with tailored molecular properties?

A cross-breeding approach was employed to generate barley lines exhibiting high fructan synthesis activity and low fructan hydrolysis activity during the developmental stages. The primary objective of this breeding strategy was to produce barley lines with augmented fructan content at the mature stage. The impact of the strategy on the content and molecular structure of starch was investigated in Paper IV.

Since barley fructan synthesis occurs early in development, fructan synthesis activity was defined based on the fructan content of progeny lines at 9 daf. Barley lines demonstrating significantly higher ($p<0.05$) fructan content at 9 daf compared with a reference variety (Gustav) were designated as having high fructan synthesis activity (Group A; see Table 2). All other lines, including Gustav, were classified as barley lines with low fructan synthesis activity (Group B; see Table 2). The mean fructan content of Group A at 9 daf was $31.5\pm 3.6\%$, while Group B demonstrated a content of $21.2\pm 0.8\%$ at 9 daf. Subsequent analyses were conducted on the mature grain fructan content, starch content and starch molecular structure of both Group A and B barley lines. Group A lines exhibited a significantly higher ($p<0.05$) mature grain fructan content, averaging $4.5\pm 2.6\%$, compared with Group B lines, which had an average content of $1.2\pm 0.6\%$. There was an inverse relationship between mature grain fructan content and starch content, with Group A lines displaying significantly ($p<0.05$) lower starch content ($38.7\pm 3.5\%$) than Group B lines (mean $49.9\pm 3.9\%$). Therefore, the employed cross-breeding strategy not only altered the fructan content, but also affected the starch content.

Upregulation of fructan synthesis downregulated starch synthesis and also influenced alterations in starch molecular structure at the BB level (Figure 16). Starch BB were analysed by HPSEC and the chromatogram was partitioned into different buckets to categorise BB into various size groups: BB from B1, B2, and B3 were categorised as large BB, those from B4 as medium-sized BB, and those from B5 and B6 as smaller-size BB.

Examination of calculated area within the HPSEC chromatogram revealed that Group A lines had a higher proportion of larger BB (B1-B3) and a lower proportion of smaller BB (B5-B6). Conversely, Group B lines

displayed a lower proportion of B1-B3 and a higher proportion of B5 and B6 ($p < 0.05$). Therefore, the cross-breeding strategy aimed at upregulating the mature grain fructan content in barley not only affected starch synthesis in terms of content, but also induced changes in the molecular structure of starch. Given that changes in the molecular structure of starch impact its functionality, these findings offer valuable insights to plant breeders for *in-planta* modification of starch to align with the intended end-uses.

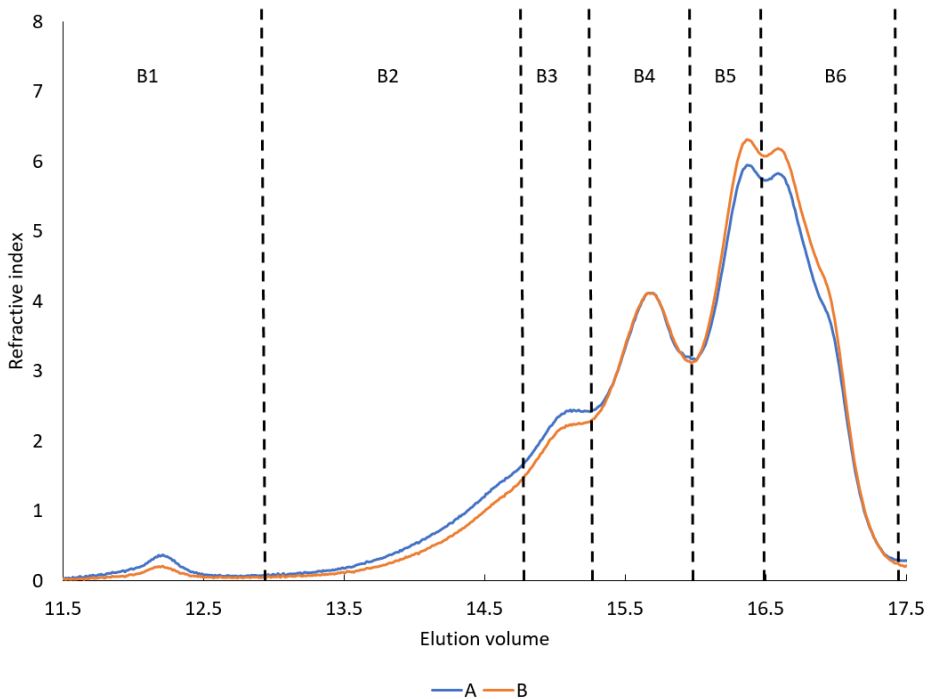


Figure 16. Building block distribution of barley starch Groups A and B, as analysed by HPSEC. The chromatogram was divided into different buckets (B1-B6) for further analysis. Adopted from Paper IV with permission.

6. Conclusions

- CRISPR/Cas9 technology can effectively generate starch with varied molecular features by targeting different enzymes or combinations of enzymes in the starch synthesis pathway.
- Mutations only in *SBEI* or *GBSS* had minor effects on the morphological and molecular structure features of potato starch.
- Mutations in both *SBEs*, with or without mutations in *GBSS*, resulted in potato starch with altered granule morphology and composition, characterised by longer amylopectin unit chains, longer amylopectin internal chains and larger building blocks compared with the native variety.
- Mutations in all the alleles of both *SBEs* resulted in amylose-only potato starch.
- Knocking out only *GBSS* resulted in a waxy potato starch phenotype (amylopectin <5%), while knocking out *GBSS* in an *SBE*-mutated background did not generate waxy phenotypes.
- Mutating *SBEs* resulted in starch with two-fold higher total phosphorus content compared with starch from the native variety. Starch from lines with mutations in *GBSS* within an *SBE*-mutated background showed even greater increases, averaging four-fold.
- The alterations in molecular structure features observed in potato starch from mutated lines led to generation of starch with modified thermal and pasting properties.
- Natural genetic variation-based cross-breeding of barley showed potential in producing starch with altered molecular structure in which upregulated fructan synthesis resulted in starch with a high proportion of large BB.

7. Future research

The primary aim of this thesis was to explore how mutations in starch synthesis enzyme genes affect molecular structure, morphological, and functional characteristics of starch. While addressing the principal objective and formulated sub-goals, the following several additional research questions meriting further investigation emerged.

- In Paper I, a type of starch solely composed of amylose without branching was found and it was intriguing to note that these starches could still form granules. Further investigation into the self-organisation of these granules would be beneficial.
- In Papers II and III, certain potato lines capable of producing amylose relatively normally despite complete knockout of *GBSS* in a background of *SBE* mutation were identified. The precise reason for this phenomenon remains unknown and warrants further study, as it could significantly enhance understanding of the starch synthesis pathway.
- A comprehensive understanding of the roles played by different enzymes in starch synthesis pathways, their intricate interactions and synergistic effects would greatly enhance interpretation of the results obtained in this thesis. Therefore, inducing mutations in various combinations of genes encoding different enzymes and studying the resulting starch would be valuable.
- In Papers I-III, various mutations were observed to affect the molecular structure of the amylose component. In Paper IV, it emerged that there was an effect on the molecular structure of amylose due to *SUSIBA* (sugar signalling in barley)-based cross-breeding of barley. Therefore, comprehensive investigations

focusing on the molecular structure of the amylose component would significantly enhance understanding of the entire starch synthesis process.

- In Paper II, a remarkable starch type characterised by very high amylose content and long amylopectin chains was identified. Future studies exploring the potential health benefits, nutritional benefits and applications of this starch type are recommended.
- Further investigations into the various applications of novel starch types in both food and non-food domains would expand understanding of the structure-function relationship of these innovative starches.
- The amylose: amylopectin ratio of some gene-edited potato lines appeared to vary depending on the growing season. Therefore, conducting a thorough investigation into the impact of environmental conditions on the molecular properties of mutated starch types would be interesting.

References

- Adewale, P., Yancheshmeh, M.S. & Lam, E. (2022). Starch modification for non-food, industrial applications: Market intelligence and critical review. *Carbohydrate Polymers*, 291, 119590. <https://doi.org/10.1016/j.carbpol.2022.119590>
- Agarwal, S., Singhal, S., Godiya, C.B. & Kumar, S. (2021). Prospects and Applications of Starch based Biopolymers. *International Journal of Environmental Analytical Chemistry*, 0 (0), 1–20. <https://doi.org/10.1080/03067319.2021.1963717>
- Amaraweera, S.M., Gunathilake, C., Gunawardene, O.H.P., Fernando, N.M.L., Wanninayaka, D.B., Dassanayake, R.S., Rajapaksha, S.M., Manamperi, A., Fernando, C.A.N., Kulatunga, A.K. & Manipura, A. (2021). Development of Starch-Based Materials Using Current Modification Techniques and Their Applications: A Review. *Molecules*, 26 (22), 6880. <https://doi.org/10.3390/molecules26226880>
- Andersson, R., Fransson, G., Tietjen, M. & Åman, P. (2009). Content and Molecular-Weight Distribution of Dietary Fiber Components in Whole-Grain Rye Flour and Bread. *Journal of Agricultural and Food Chemistry*, 57 (5), 2004–2008. <https://doi.org/10.1021/jf801280f>
- Baek, S.-K. & Song, K.B. (2019). Characterization of Active Biodegradable Films Based on Proso Millet Starch and Curcumin. *Starch - Stärke*, 71 (3–4), 1800174. <https://doi.org/10.1002/star.201800174>
- Ball, S.G., Wal, M.H.B.J. van de & Visser, R.G.F. (1998). Progress in understanding the biosynthesis of amylose. *Trends in Plant Science*, 3 (12), 462–467. [https://doi.org/10.1016/S1360-1385\(98\)01342-9](https://doi.org/10.1016/S1360-1385(98)01342-9)
- Bertoft, E. (2004). On the nature of categories of chains in amylopectin and their connection to the super helix model. *Carbohydrate Polymers*, 57 (2), 211–224. <https://doi.org/10.1016/j.carbpol.2004.04.015>

- Bertoft, E. (2013). On the Building Block and Backbone Concepts of Amylopectin Structure. *Cereal Chemistry*, 90 (4), 294–311. <https://doi.org/10.1094/CCHEM-01-13-0004-FI>
- Bertoft, E. (2017). Understanding Starch Structure: Recent Progress. *Agronomy*, 7 (3), 56. <https://doi.org/10.3390/agronomy7030056>
- Bertoft, E., Koch, K. & Åman, P. (2012a). Building block organisation of clusters in amylopectin from different structural types. *International Journal of Biological Macromolecules*, 50 (5), 1212–1223. <https://doi.org/10.1016/j.ijbiomac.2012.03.004>
- Bertoft, E., Koch, K. & Åman, P. (2012b). Structure of building blocks in amylopectins. *Carbohydrate Research*, 361, 105–113. <https://doi.org/10.1016/j.carres.2012.08.012>
- Blennow, A., Bay-Smidt, A.M., Olsen, C.E. & Møller, B.L. (2000). The distribution of covalently bound phosphate in the starch granule in relation to starch crystallinity. *International Journal of Biological Macromolecules*, 27 (3), 211–218. [https://doi.org/10.1016/S0141-8130\(00\)00121-5](https://doi.org/10.1016/S0141-8130(00)00121-5)
- Blennow, A., Bay-Smidt, A.M., Wischmann, B., Olsen, C.E. & Møller, B.L. (1998). The degree of starch phosphorylation is related to the chain length distribution of the neutral and the phosphorylated chains of amylopectin. *Carbohydrate Research*, 307 (1), 45–54. [https://doi.org/10.1016/S0008-6215\(98\)00015-9](https://doi.org/10.1016/S0008-6215(98)00015-9)
- Blennow, A., Nielsen, T.H., Baunsgaard, L., Mikkelsen, R. & Engelsen, S.B. (2002). Starch phosphorylation: a new front line in starch research. *Trends in Plant Science*, 7 (10), 445–450. [https://doi.org/10.1016/S1360-1385\(02\)02332-4](https://doi.org/10.1016/S1360-1385(02)02332-4)
- Brummell, D.A., Watson, L.M., Zhou, J., McKenzie, M.J., Hallett, I.C., Simmons, L., Carpenter, M. & Timmerman-Vaughan, G.M. (2015). Overexpression of STARCH BRANCHING ENZYME II increases short-chain branching of amylopectin and alters the physicochemical properties of starch from potato tuber. *BMC Biotechnology*, 15 (1), 28. <https://doi.org/10.1186/s12896-015-0143-y>
- Buléon, A., Colonna, P., Planchot, V. & Ball, S. (1998). Starch granules: structure and biosynthesis. *International Journal of Biological Macromolecules*, 23 (2), 85–112. [https://doi.org/10.1016/S0141-8130\(98\)00040-3](https://doi.org/10.1016/S0141-8130(98)00040-3)
- Carciofi, M., Blennow, A., Jensen, S.L., Shaik, S.S., Henriksen, A., Buléon, A., Holm, P.B. & Hebelstrup, K.H. (2012). Concerted suppression of all starch branching enzyme genes in barley produces amylose-only starch granules. *BMC Plant Biology*, 12 (1), 223. <https://doi.org/10.1186/1471-2229-12-223>

- Chen, Y.Y., Mcpherson, A.E., Radosavljević, M., Lee, V., Wong, K. & Jane, J. (1998). Effects of starch chemical structures on gelatinization and pasting properties., 1998. <https://www.semanticscholar.org/paper/Effects-of-starch-chemical-structures-on-and-Chen-Mcpherson/274a37314549c1cc883192a33a5849e1a2d05a12> [2024-01-18]
- Chrastil, J. (1987). Improved colorimetric determination of amylose in starches or flours. *Carbohydrate Research*, 159 (1), 154–158. [https://doi.org/10.1016/S0008-6215\(00\)90013-2](https://doi.org/10.1016/S0008-6215(00)90013-2)
- Dome, K., Podgornbunskikh, E., Bychkov, A. & Lomovsky, O. (2020). Changes in the Crystallinity Degree of Starch Having Different Types of Crystal Structure after Mechanical Pretreatment. *Polymers*, 12 (3), 641. <https://doi.org/10.3390/polym12030641>
- Domene-López, D., Delgado-Marín, J.J., Martín-Gullon, I., García-Quesada, J.C. & Montalbán, M.G. (2019). Comparative study on properties of starch films obtained from potato, corn and wheat using 1-ethyl-3-methylimidazolium acetate as plasticizer. *International Journal of Biological Macromolecules*, 135, 845–854. <https://doi.org/10.1016/j.ijbiomac.2019.06.004>
- Ellis, R.P., Cochrane, M.P., Dale, M.F.B., Duffus, C.M., Lynn, A., Morrison, I.M., Prentice, R.D.M., Swanston, J.S. & Tiller, S.A. (1998). Starch production and industrial use. *Journal of the Science of Food and Agriculture*, 77 (3), 289–311. [https://doi.org/10.1002/\(SICI\)1097-0010\(199807\)77:3<289::AID-JSFA38>3.0.CO;2-D](https://doi.org/10.1002/(SICI)1097-0010(199807)77:3<289::AID-JSFA38>3.0.CO;2-D)
- French, D. (1984). CHAPTER VII - ORGANIZATION OF STARCH GRANULES. In: Whistler, R.L., Bemiller, J.N., & Paschall, E.F. (eds) *Starch: Chemistry and Technology (Second Edition)*. Academic Press. 183–247. <https://doi.org/10.1016/B978-0-12-746270-7.50013-6>
- Gallant, D.J., Bouchet, B. & Baldwin, P.M. (1997). Microscopy of starch: evidence of a new level of granule organization. *Carbohydrate Polymers*, 32 (3), 177–191. [https://doi.org/10.1016/S0144-8617\(97\)00008-8](https://doi.org/10.1016/S0144-8617(97)00008-8)
- Gillgren, T., Blennow, A., Pettersson, A.J. & Stading, M. (2011). Modulating rheo-kinetics of native starch films towards improved wet-strength. *Carbohydrate Polymers*, 83 (2), 383–391. <https://doi.org/10.1016/j.carbpol.2010.07.054>
- Grennan, A.K. (2006). Regulation of Starch Metabolism in Arabidopsis Leaves. *Plant Physiology*, 142 (4), 1343–1345. <https://doi.org/10.1104/pp.104.900209>

- Hizukuri, S., Takeda, Y., Yasuda, M. & Suzuki, A. (1981). Multi-branched nature of amylose and the action of debranching enzymes. *Carbohydrate Research*, 94 (2), 205–213. [https://doi.org/10.1016/S0008-6215\(00\)80718-1](https://doi.org/10.1016/S0008-6215(00)80718-1)
- Hofvander, P., Andersson, M., Larsson, C.-T. & Larsson, H. (2004). Field performance and starch characteristics of high-amylose potatoes obtained by antisense gene targeting of two branching enzymes. *Plant Biotechnology Journal*, 2 (4), 311–320. <https://doi.org/10.1111/j.1467-7652.2004.00073.x>
- Hoover, R. (2001). Composition, molecular structure, and physicochemical properties of tuber and root starches: a review. *Carbohydrate Polymers*, 45 (3), 253–267. [https://doi.org/10.1016/S0144-8617\(00\)00260-5](https://doi.org/10.1016/S0144-8617(00)00260-5)
- Hoover, R. & Ratnayake, W. s. (2001). Determination of Total Amylose Content of Starch. *Current Protocols in Food Analytical Chemistry*, 00 (1), E2.3.1-E2.3.5. <https://doi.org/10.1002/0471142913.fae0203s00>
- Huang, J., Shang, Z., Man, J., Liu, Q., Zhu, C. & Wei, C. (2015). Comparison of molecular structures and functional properties of high-amylose starches from rice transgenic line and commercial maize. *Food Hydrocolloids*, 46, 172–179. <https://doi.org/10.1016/j.foodhyd.2014.12.019>
- Jane, J., Chen, Y.Y., Lee, L.F., McPherson, A.E., Wong, K.S., Radosavljevic, M. & Kasemsuwan, T. (1999). Effects of Amylopectin Branch Chain Length and Amylose Content on the Gelatinization and Pasting Properties of Starch. *Cereal Chemistry*, 76 (5), 629–637. <https://doi.org/10.1094/CCHEM.1999.76.5.629>
- Jayarathna, S., Andersson, M. & Andersson, R. (2022). Recent Advances in Starch-Based Blends and Composites for Bioplastics Applications. *Polymers*, 14 (21), 4557. <https://doi.org/10.3390/polym14214557>
- Ji, Q., Oomen, R.J.F.J., Vincken, J.-P., Bolam, D.N., Gilbert, H.J., Suurs, L.C.J.M. & Visser, R.G.F. (2004). Reduction of starch granule size by expression of an engineered tandem starch-binding domain in potato plants. *Plant Biotechnology Journal*, 2 (3), 251–260. <https://doi.org/10.1111/j.1467-7652.2004.00069.x>
- Jiranuntakul, W., Puttanlek, C., Rungsardthong, V., Pancha-arnon, S. & Uttapap, D. (2011). Microstructural and physicochemical properties of heat-moisture treated waxy and normal starches. *Journal of Food Engineering*, 104 (2), 246–258. <https://doi.org/10.1016/j.jfoodeng.2010.12.016>

- Källman, A., Vamadevan, V., Bertoft, E., Koch, K., Seetharaman, K., Åman, P. & Andersson, R. (2015). Thermal properties of barley starch and its relation to starch characteristics. *International Journal of Biological Macromolecules*, 81, 692–700. <https://doi.org/10.1016/j.ijbiomac.2015.08.068>
- Karim, A. a., Toon, L. c., Lee, V. p. l., Ong, W. y., Fazilah, A. & Noda, T. (2007). Effects of Phosphorus Contents on the Gelatinization and Retrogradation of Potato Starch. *Journal of Food Science*, 72 (2), C132–C138. <https://doi.org/10.1111/j.1750-3841.2006.00251.x>
- Kasemsuwan, T. & Jane, J.-L. (1996). Quantitative method for the survey of starch phosphate derivatives and starch phospholipids by ³¹P nuclear magnetic resonance spectroscopy. *Cereal Chemistry*, 73 (6), 702–707
- Larsson, C.-T., Hofvander, P., Khoshnoodi, J., Ek, B., Rask, L. & Larsson, H. (1996). Three isoforms of starch synthase and two isoforms of branching enzyme are present in potato tuber starch. *Plant Science*, 117 (1), 9–16. [https://doi.org/10.1016/0168-9452\(96\)04408-1](https://doi.org/10.1016/0168-9452(96)04408-1)
- Lawton, J.W. (2004). STARCH | Uses of Native Starch. In: Wrigley, C. (ed.) *Encyclopedia of Grain Science*. Elsevier. 195–202. <https://doi.org/10.1016/B0-12-765490-9/00104-X>
- Li, H., Dhital, S., Slade, A.J., Yu, W., Gilbert, R.G. & Gidley, M.J. (2019). Altering starch branching enzymes in wheat generates high-amylose starch with novel molecular structure and functional properties. *Food Hydrocolloids*, 92, 51–59. <https://doi.org/10.1016/j.foodhyd.2019.01.041>
- Lim, S.-T., kasemsuwan, T. & Jane, J.-L. (1994). Characterization of Phosphorus in Starch by ³¹P-Nuclear Magnetic Resonance Spectroscopy. *Cereal Chemistry*, 71 (5), 488–493
- Liu, Q., Donner, E., Tarn, R., Singh, J. & Chung, H.-J. (2009). Chapter 8 - Advanced Analytical Techniques to Evaluate the Quality of Potato and Potato Starch. In: Singh, J. & Kaur, L. (eds) *Advances in Potato Chemistry and Technology*. Academic Press. 221–248. <https://doi.org/10.1016/B978-0-12-374349-7.00008-8>
- Matheson, N.K. & Welsh, L.A. (1988). Estimation and fractionation of the essentially unbranched (amylose) and branched (amylopectin) components of starches with concanavalin A. *Carbohydrate Research*, 180 (2), 301–313. [https://doi.org/10.1016/0008-6215\(88\)80087-9](https://doi.org/10.1016/0008-6215(88)80087-9)
- Menzel, C., Andersson, M., Andersson, R., Vázquez-Gutiérrez, J.L., Daniel, G., Langton, M., Gällstedt, M. & Koch, K. (2015). Improved material properties of solution-cast starch films: Effect of varying

- amylopectin structure and amylose content of starch from genetically modified potatoes. *Carbohydrate Polymers*, 130, 388–397. <https://doi.org/10.1016/j.carbpol.2015.05.024>
- Myllärinen, P., Partanen, R., Seppälä, J. & Forssell, P. (2002). Effect of glycerol on behaviour of amylose and amylopectin films. *Carbohydrate Polymers*, 50 (4), 355–361. [https://doi.org/10.1016/S0144-8617\(02\)00042-5](https://doi.org/10.1016/S0144-8617(02)00042-5)
- Nilsson, K., Sandström, C., Özeren, H.D., Vilaplana, F., Hedenqvist, M. & Langton, M. (2022). Physiochemical and thermal characterisation of faba bean starch. *Journal of Food Measurement and Characterization*, 16 (6), 4470–4485. <https://doi.org/10.1007/s11694-022-01543-7>
- Ojogbo, E., Ogunsona, E.O. & Mekonnen, T.H. (2020). Chemical and physical modifications of starch for renewable polymeric materials. *Materials Today Sustainability*, 7–8. <https://doi.org/10.1016/j.mtsust.2019.100028>
- Peat, S., Whelan, W. & Thomas, G.J. (1952). Evidence of multiple branching in waxy maize starch. *Journal of The Chemical Society (resumed)*,. <https://www.semanticscholar.org/paper/Evidence-of-multiple-branching-in-waxy-maize-starch-Peat-Whelan/47d3c5d5f521cdcc06a92856fdce6dc1122e59e1> [2023-06-02]
- Pérez, S., Baldwin, P.M. & Gallant, D.J. (2009). Chapter 5 - Structural Features of Starch Granules I. In: BeMiller, J. & Whistler, R. (eds) *Starch (Third Edition)*. Academic Press. 149–192. <https://doi.org/10.1016/B978-0-12-746275-2.00005-7>
- Pérez, S. & Bertoft, E. (2010). The molecular structures of starch components and their contribution to the architecture of starch granules: A comprehensive review. *Starch - Stärke*, 62 (8), 389–420. <https://doi.org/10.1002/star.201000013>
- Rindlav-Westling, A., Stading, M., Hermansson, A.-M. & Gatenholm, P. (1998). Structure, mechanical and barrier properties of amylose and amylopectin films. *Carbohydrate Polymers*, 36 (2), 217–224. [https://doi.org/10.1016/S0144-8617\(98\)00025-3](https://doi.org/10.1016/S0144-8617(98)00025-3)
- S. Hizukuri, J.-I. Abe & I. Hanashiro (1996). Starch: Analytical aspects. In: *Carbohydrates in Food*. CRC Press.
- Sagnelli, D., Hebelstrup, K.H., Leroy, E., Rolland-Sabaté, A., Guilois, S., Kirkensgaard, J.J.K., Mortensen, K., Lourdin, D. & Blennow, A. (2016). Plant-crafted starches for bioplastics production. *Carbohydrate Polymers*, 152, 398–408. <https://doi.org/10.1016/j.carbpol.2016.07.039>

- Sagnelli, D., Hooshmand, K., Kemmer, G.C., Kirkensgaard, J.J.K., Mortensen, K., Giosafatto, C.V.L., Holse, M., Hebelstrup, K.H., Bao, J., Stelte, W., Bjerre, A.-B. & Blennow, A. (2017). Cross-Linked Amylose Bio-Plastic: A Transgenic-Based Compostable Plastic Alternative. *International Journal of Molecular Sciences*, 18 (10). <https://doi.org/10.3390/ijms18102075>
- dos Santos, T.P.R., Leonel, M., Garcia, É.L., do Carmo, E.L. & Franco, C.M.L. (2016). Crystallinity, thermal and pasting properties of starches from different potato cultivars grown in Brazil. *International Journal of Biological Macromolecules*, 82, 144–149. <https://doi.org/10.1016/j.ijbiomac.2015.10.091>
- Schwall, G., Safford, R., Westcott, R., Jeffcoat, R., Tayal, A., Shi, Y., Gidley, M. & Jobling, S. (2000). Production of very-high-amylose potato starch by inhibition of SBE A and B. *Nature biotechnology*, 18, 551–4. <https://doi.org/10.1038/75427>
- Seung, D. (2020). Amylose in starch: towards an understanding of biosynthesis, structure and function. *New Phytologist*, 228 (5), 1490–1504. <https://doi.org/10.1111/nph.16858>
- Shibanuma, K., Takeda, Y., Hizukuri, S. & Shibata, S. (1994). Molecular structures of some wheat starches. *Carbohydrate Polymers*, 25 (2), 111–116. [https://doi.org/10.1016/0144-8617\(94\)90146-5](https://doi.org/10.1016/0144-8617(94)90146-5)
- Singh, N., Kaur, A., Shevkani, K., Ezekiel, R., Kaur, P., Isono, N. & Noda, T. (2017). Structural, Morphological, Thermal, and Pasting Properties of Starches From Diverse Indian Potato Cultivars. *Starch - Stärke*, 70 (3–4), 1700130. <https://doi.org/10.1002/star.201700130>
- Tester, R.F., Karkalas, J. & Qi, X. (2004). Starch—composition, fine structure and architecture. *Journal of Cereal Science*, 39 (2), 151–165. <https://doi.org/10.1016/j.jcs.2003.12.001>
- Tetlow, I.J. & Bertoft, E. (2020). A Review of Starch Biosynthesis in Relation to the Building Block-Backbone Model. *International Journal of Molecular Sciences*, 21 (19), 7011. <https://doi.org/10.3390/ijms21197011>
- Toinga-Villafuerte, S., Vales, M.I., Awika, J.M. & Rathore, K.S. (2022). CRISPR/Cas9-Mediated Mutagenesis of the Granule-Bound Starch Synthase Gene in the Potato Variety Yukon Gold to Obtain Amylose-Free Starch in Tubers. *International Journal of Molecular Sciences*, 23 (9), 4640. <https://doi.org/10.3390/ijms23094640>
- Tuncel, A., Corbin, K.R., Ahn-Jarvis, J., Harris, S., Hawkins, E., Smedley, M.A., Harwood, W., Warren, F.J., Patron, N.J. & Smith, A.M. (2019). Cas9-mediated mutagenesis of potato starch-branching enzymes generates a range of tuber starch phenotypes. *Plant*

- Biotechnology Journal*, 17 (12), 2259–2271.
<https://doi.org/10.1111/pbi.13137>
- Vilaplana, F., Hasjim, J. & Gilbert, R.G. (2012). Amylose content in starches: Toward optimal definition and validating experimental methods. *Carbohydrate Polymers*, 88 (1), 103–111.
<https://doi.org/10.1016/j.carbpol.2011.11.072>
- Vrinten, P.L. & Nakamura, T. (2000). Wheat Granule-Bound Starch Synthase I and II Are Encoded by Separate Genes That Are Expressed in Different Tissues1. *Plant Physiology*, 122 (1), 255–264. <https://doi.org/10.1104/pp.122.1.255>
- Wang, L., Wang, Y., Makhmoudova, A., Nitschke, F., Tetlow, I.J. & Emes, M.J. (2021). CRISPR–Cas9-mediated editing of starch branching enzymes results in altered starch structure in *Brassica napus*. *Plant Physiology*, 188 (4), 1866–1886.
<https://doi.org/10.1093/plphys/kiab535>
- Yun, S.-H. & Matheson, N.K. (1990). Estimation of Amylose Content of Starches after Precipitation of Amylopectin by Concanavalin-A. *Starch - Stärke*, 42 (8), 302–305.
<https://doi.org/10.1002/star.19900420805>
- Zaidul, I.S.M., Yamauchi, H., Takigawa, S., Matsuura-Endo, C., Suzuki, T. & Noda, T. (2007). Correlation between the compositional and pasting properties of various potato starches. *Food Chemistry*, 105 (1), 164–172. <https://doi.org/10.1016/j.foodchem.2007.03.061>
- Zhao, X., Andersson, M. & Andersson, R. (2018). Resistant starch and other dietary fiber components in tubers from a high-amylose potato. *Food Chemistry*, 251, 58–63.
<https://doi.org/10.1016/j.foodchem.2018.01.028>
- Zhao, X., Andersson, M. & Andersson, R. (2021). A simplified method of determining the internal structure of amylopectin from barley starch without amylopectin isolation. *Carbohydrate Polymers*, 255, 117503. <https://doi.org/10.1016/j.carbpol.2020.117503>
- Zhao, X., Hofvander, P., Andersson, M. & Andersson, R. (2023). Internal structure and thermal properties of potato starches varying widely in amylose content. *Food Hydrocolloids*, 135, 108148. <https://doi.org/10.1016/j.foodhyd.2022.108148>
- Zhong, Y., Qu, J.Z., Liu, X., Ding, L., Liu, Y., Bertoft, E., Petersen, B.L., Hamaker, B.R., Hebelstrup, K.H. & Blennow, A. (2022). Different genetic strategies to generate high amylose starch mutants by engineering the starch biosynthetic pathways. *Carbohydrate Polymers*, 287, 119327.
<https://doi.org/10.1016/j.carbpol.2022.119327>

- Zhong, Y., Tai, L., Blennow, A., Ding, L., Herburger, K., Qu, J., Xin, A., Guo, D., Hebelstrup, K.H. & Liu, X. (2023). High-amylose starch: Structure, functionality and applications. *Critical Reviews in Food Science and Nutrition*, 63 (27), 8568–8590. <https://doi.org/10.1080/10408398.2022.2056871>
- Zhu, F. (2018). Relationships between amylopectin internal molecular structure and physicochemical properties of starch. *Trends in Food Science & Technology*, 78, 234–242. <https://doi.org/10.1016/j.tifs.2018.05.024>
- Zhu, F., Corke, H. & Bertoft, E. (2011). Amylopectin internal molecular structure in relation to physical properties of sweetpotato starch. *Carbohydrate Polymers*, 84 (3), 907–918. <https://doi.org/10.1016/j.carbpol.2010.12.039>

Popular science summary

Starch serves as a primary source of energy in the human diet and is a key ingredient in numerous food products. Starch also has diverse non-food applications, including use in the food packaging sector for creating starch films or coatings. It acts as a sizing agent in the textile industry, serves as an adhesive and binder in the paper industry, and is utilised as an excipient in the pharmaceutical industry. However, in both the food and non-food industries, the use of native starch is hindered by characteristics such as poor processability, insufficient post-processing stability, high susceptibility to moisture, inadequate barrier properties and inferior mechanical characteristics. Therefore, before starch is employed in various industries, it typically undergoes physical, chemical or enzymatic modification, or a combination of these, to overcome these drawbacks. However, post-harvest modification of starch is often labour- and energy-intensive, resulting in high costs and high environmental impact. In contrast, *in-planta* starch modification, using biotechnological approaches to customise starch within plants themselves, represents an appealing and environmentally friendly approach. The main aim of the work in this thesis was to characterise different *in-planta* modified starches, to better understand how genetic engineering methods and conventional cross-breeding techniques could be employed to tailor-make starch within plants.

Starch typically contains approximately 25% amylose and 75% amylopectin, with the actual balance between amylose and amylopectin within starch significantly affecting its functional characteristics. This thesis demonstrated that the advanced genetic engineering tool CRISPR/Cas9 can effectively adjust the amylose: amylopectin ratio within plants. Inducing mutations in all alleles of specific genes controlling the synthesis of starch branching enzyme I and II resulted in production of only amylose potato

starch, while targeting the granule-bound starch synthase gene led to amylopectin-rich starch. Various combinations of mutations in alleles of starch synthesis genes produced potato starch with varying amylose: amylopectin ratio.

The total phosphorus content of potato starch was also modifiable by targeting specific genes. For example, mutating starch branching enzyme genes I and II together with the granule-bound starch synthase gene produced starch with very high total phosphorus content, which is beneficial for applications that require unique properties imparted by high phosphorus content in starch.

Other than altering the composition of potato starch, the molecular structure of starches can be effectively modified through targeted mutations in various genes involved in the starch synthesis pathway. Inducing mutations in starch branching enzyme I and II genes, either alone or in combination with granule-bound starch synthase genes, was found to result in starches with modified molecular structures compared with the native variety. These molecular structural changes were shown to have significant effects on the thermal and pasting properties of the starches.

The results obtained in this thesis also demonstrated good potential of cross-breeding methods based on natural variations in barley fructan synthesis activity to produce starch with altered molecular structure.

In essence, these findings improve understanding of how manipulating starch biosynthesis can influence the properties of the resulting starch. This knowledge can be applied within plant breeding to generate crops yielding tailor-made starches aimed for specific applications.

Populärvetenskaplig sammanfattning

Stärkelse fungerar som en primär energikälla i vår kost och är en nyckelingrediens i många livsmedelsprodukter. Stärkelse har också olika icke-livsmedelsapplikationer, inklusive användning inom livsmedelsförpackningssektorn för att skapa stärkelsefilmer eller ytbehandlingar. Den fungerar som ett storleksmedel inom textilindustrin, tjänar som ett klister och bindemedel inom papperstillverkningen och används som en tillsats inom läkemedelsindustrin. Men både inom livsmedels- och icke-livsmedelsindustrier hindras användningen av naturlig stärkelse av egenskaper såsom dålig bearbetbarhet, otillräcklig efterbehandlingsstabilitet, hög känslighet för fukt, otillräckliga barriäregenskaper och bristande mekaniska egenskaper. Därför genomgår stärkelse vanligtvis fysisk, kemisk eller enzymatisk modifiering, eller en kombination av dessa, för att övervinna dessa nackdelar innan den används inom olika branscher. Dock är modifiering av stärkelse efter skörd ofta arbets- och energikrävande, vilket resulterar i höga kostnader och hög miljöpåverkan. I motsats till detta representerar in-planta modifiering av stärkelse, med användning av bioteknologiska metoder så att växterna själva anpassar stärkelsen, ett tilltalande och miljövänligt tillvägagångssätt. Det huvudsakliga syftet med arbetet i denna avhandling var att karakterisera olika in-planta modifierade stärkelser för att bättre förstå hur genetiska manipuleringsmetoder och konventionella korsningsmetoder kan användas för att skräddarsy stärkelse i växter.

Stärkelse innehåller vanligtvis cirka 25 % amylos och 75 % amylopektin, där balansen mellan amylos och amylopektin avsevärt påverkar dess funktionella egenskaper. Denna avhandling visade att det avancerade genetiska verktyget CRISPR/Cas9 effektivt kan justera förhållandet mellan

amylos och amylopektin i växter. Genom att inducera mutationer i alla alleler av båda specifika gener som kontrollerar produktionen av stärkelseförgreningsenzym I och II resulterade i produktion av uteslutande amylos-potatisstärkelse, medan inriktning på genen för granlbundet stärkelsesyntas ledde till stärkelse rik på amylopektin. Olika kombinationer av mutationer i gener som styr stärkelsesyntesen producerade potatisstärkelse med varierande förhållande mellan amylos och amylopektin.

Det totala fosforinnehållet i potatisstärkelse var också möjligt att ändra genom att rikta in sig på specifika gener. Till exempel producerade mutationer i stärkelseförgreningsenzymgenerna I och II tillsammans med genen för granlbundet stärkelsesyntas stärkelse med mycket högt totalt fosforinnehåll, vilket är fördelaktigt för tillämpningar som kräver unika egenskaper som tillskrivs högt fosforinnehåll i stärkelse.

Förutom att ändra sammansättningen av potatisstärkelse kan även den molekylära strukturen hos stärkelser effektivt modifieras genom riktade mutationer i olika gener som är involverade i stärkelsesyntesvägen. Att inducera mutationer i generna för stärkelseförgreningsenzym I och II, antingen enskilt eller i kombination med gener för granlbundet stärkelsesyntas, visade sig resultera i stärkelser med modifierade molekylära strukturer jämfört med föräldrasorten. Dessa molekylära strukturella förändringar visade sig ha betydande effekter på de termiska och förklustringsmässiga egenskaperna hos stärkelsena.

Resultaten som erhöles i denna avhandling visade också på god potential för korsningsmetoder baserade på naturliga variationer i kornens fruktansynteshastighet för att producera stärkelse med ändrad molekylär struktur.

Sammanfattningsvis förbättrar dessa fynd förståelsen för hur manipulation av stärkelsebiosyntesen kan påverka egenskaperna hos den resulterande stärkelsen. Denna kunskap kan tillämpas inom växtförädling för att generera grödor som ger skraddarsydda stärkelser avsedda för specifika tillämpningar.

Acknowledgements

I extend my heartfelt appreciation to my primary supervisor, Professor Roger Andersson, for his outstanding guidance, supervision and faith in my abilities throughout my PhD journey. His invaluable insights, support and words of encouragement significantly influenced the outcome of this thesis. I am deeply grateful for his understanding, flexibility and collaborative spirit, which granted me the freedom and resources needed to explore and pursue my research interests effectively.

I am truly fortunate to have Associate Professor Mariette Andersson as my co-supervisor. I would like to extend my heartfelt appreciation for her guidance, supervision, sharing of knowledge, expertise, encouragement and commitment. Her mentorship enriched both my academic experience and professional growth and I thank her for trusting in my potential and believing in me.

I want to extend my sincere gratitude to all my colleagues who played a role in bringing this thesis to completion. I am grateful to Xue Zhao, Per Hufvander, Gustav Nestor, Gleb Dotsenko, Francisco Vilapana, Zsuzsanna Péter-Szabó, Annica Andersson, Yunkai Jin, and Chuanxin Sun for their support and dedication throughout this journey. I also want to express my appreciation to all other colleagues at the Department of Plant Breeding, SLU, for their contributions to development of exceptional potato lines that yield remarkable starch.

I would like to thank Henrik for his consistent availability whenever I encountered issues related to the DIONEX instrumentation. Gulaim, your gracious assistance with the SEM analysis is greatly appreciated. Vadim, I am grateful for your support as Head of Department and for your efforts in conducting X-ray analysis on my starch samples.

I want to express my heartfelt gratitude to all current and former members of my research group. The collaborative atmosphere you cultivated played an important role in the successful completion of my PhD studies. Janicka, I am immensely grateful for your invaluable assistance in the lab and for your warm and friendly relationship shared with me. Annica, Santanu, Gleb and Per, your insights and discussions were invaluable on my scientific journey. Sunera, Qingxuan, Xue, Laura and Louise, your support as fellow PhD colleagues meant the world to me, and I cherish the moments we shared both professionally and personally.

My journey at SLU began with the dairy group, and I am grateful to Monika and Åse for welcoming me into the team. A heartfelt thank you is extended to Professor Janak Vidanarachchi for facilitating my transition from the University of Peradeniya to SLU through the Erasmus+ scholarship program. I also want to express my gratitude to Bettina for giving me the chance to enter a new arena. During that time, I perfected my lab skills with guidance from Bettina and Simon, and I am truly thankful for their mentorship. Yasha, I appreciate the shared moments we had during that period.

I would like to extend sincere thanks to all my past and current PhD colleagues and to all the members of the Department of Molecular Sciences for the memorable moments we shared together. I gratefully acknowledge the invaluable support from the Department's IT and administration teams.

I am grateful to the LiFT research school, FFB and the other PhD programmes for providing valuable courses. Special thanks to my LiFT industrial mentor, Mathias, for the insightful meetups and discussions we had. Laxmi, I deeply appreciate your supportive discussions on the research topic, which were truly inspiring for me. Ilya Zelikman from Shimadzu, Sweden, is acknowledged for his collaboration regarding the analysis of starch particle size.

My dear Liisa, your nurturing presence made you an additional mother figure for us while we were away from home. Maria, your role in connecting us to Liisa and becoming part of our extended family away from home is deeply appreciated. To all my Sri Lankan friends residing in Sweden, thank you for the countless joyful moments we shared together. Your constant presence and support meant the world to me.

My parents and aunt, your unwavering dedication to nurturing me into the person I am today fills me with gratitude. Your boundless love, care and

support are the pillars of strength in my life. My brother and sister-in-law, thank you for your constant presence and for looking after our parents in my absence. Your support was invaluable to me. Hasi, my dear husband, your love and support have been a source of immense comfort throughout my adult life. To my precious daughter, Samahi, thank you for being who you are, your affectionate hugs have been my solace during difficult times.

I am grateful to have undertaken my doctoral studies and research training at SLU, one of the top-rated universities in the world. This PhD project was (partly) funded by Trees and Crops for the Future (TC4F), a Strategic Research Area at SLU supported by the Swedish Government. Diagrams in the thesis, including the cover image, latter image, and figures 1,3,4,5 and 6 were created using BioRender.com.

Lastly, I wish to express my profound gratitude for the invaluable gift of the free education system in Sri Lanka and for the unwavering dedication of my beloved teachers. The opportunity to receive quality education without financial constraints laid the foundation in shaping my academic journey and in my pursuit of a PhD degree. This education provided me with the necessary knowledge and skills and also fostered in me a deep appreciation for learning and a drive to excel in my academic endeavours.





OPEN Amylose starch with no detectable branching developed through DNA-free CRISPR-Cas9 mediated mutagenesis of two starch branching enzymes in potato

Xue Zhao^{1,5}, Shishanthi Jayarathna^{1,5}, Helle Turesson², Ann-Sofie Fält², Gustav Nestor¹, Matías N. González^{3,4}, Niklas Olsson², Mirela Beganovic², Per Hofvander², Roger Andersson¹ & Mariette Andersson²✉

DNA-free genome editing was used to induce mutations in one or two branching enzyme genes (*Sbe*) in tetraploid potato to develop starch with an increased amylose ratio and elongated amylopectin chains. By using ribonucleoprotein (RNP) transfection of potato protoplasts, a mutation frequency up to 72% was achieved. The large variation of mutations was grouped as follows: Group 1 lines with all alleles of *Sbe1* mutated, Group 2 lines with all alleles of *Sbe1* as well as two to three alleles of *Sbe2* mutated and Group 3 lines having all alleles of both genes mutated. Starch from lines in Group 3 was found to be essentially free of amylopectin with no detectable branching and a chain length (CL) distribution where not only the major amylopectin fraction but also the shortest amylose chains were lost. Surprisingly, the starch still formed granules in a low-ordered crystalline structure. Starch from lines of Group 2 had an increased CL with a higher proportion of intermediate-sized chains, an altered granule phenotype but a crystalline structure in the granules similar to wild-type starch. Minor changes in CL could also be detected for the Group 1 starches when studied at a higher resolution.

Genome editing in plants has opened up new possibilities, both in terms of research and development of crops with novel traits beneficial for human health or the environment. The method can be used to create knockouts of enzymatic functions, which in many cases has been difficult to achieve with traditional genetic engineering methods, e.g. RNAi. Protocols for genome editing through CRISPR-Cas9 have been successfully established for inducing mutations in potato¹. In addition, using transient approaches for genome editing of potato is possible, which is a big advantage when plants free of recombinant DNA are desired. A transient approach has a clear benefit for highly heterozygous clonally propagated crops like potato, since segregation through seed generations is more or less impossible².

Potato is an important, high-yielding, nutritious and starch-rich staple crop³. Starch is composed of glucose units linearly linked by $\alpha(1 \rightarrow 4)$ glycosidic bonds and branched by $\alpha(1 \rightarrow 6)$ bonds. Starch is generally deposited as highly ordered granules directed by the highly branched amylopectin molecule with the addition of the essentially linear molecule amylose to a ratio of approximately 4:1⁴. In food products, the high amylose content and the long chains of amylopectin contribute to formation of resistant starch and relate to a low glycaemic index (GI) after intake^{5,6}. By increasing the average chain length of potato starch, a starch with health benefits can be developed. The increased chain length can yield resistant starch (RS) leading to a low GI and concur health

¹Department of Molecular Sciences, Swedish University of Agricultural Sciences, Box 7015, 750 07 Uppsala, Sweden. ²Department of Plant Breeding, Swedish University of Agricultural Sciences, P.O. Box 101, 23053 Alnarp, Sweden. ³Consejo Nacional de Investigaciones Científicas Y Técnicas, (C1425FQB), Buenos Aires, Argentina. ⁴Laboratorio de Agrobiotecnología, IPADS (INTA - CONICET), Ruta 226, Km 73.5, B7620 Balcarce, Argentina. ⁵These authors contributed equally: Xue Zhao and Shishanthi Jayarathna. ✉email: mariette.andersson@slu.se

benefits by promoting the growth of healthy gut flora, and lowering both the caloric intake and cholesterol levels in the blood⁵. The long-chain quality of starch also creates beneficial properties as a raw material for producing bioplastic films⁷, which in the future might replace some of the fossil-based plastics produced today.

The research and development of potatoes with novel starch qualities has been ongoing for a long time. Potatoes that synthesise solely amylopectin starch have been developed by eliminating granule-bound starch synthase (GBSS) activity through traditional mutagenesis, antisense, RNAi and most recently CRISPR-Cas9^{8–11}. The development of potatoes with a high ratio of amylose starch and/or altered starch chain length distribution has been achieved by targeting two starch branching enzymes (SBEs) using traditional gene silencing technologies and recently genome editing^{12–14}. A very high amylose starch content was found synthesised at the expense of total starch content and plant development¹⁵. Based on those results and the fact that, so far, no potato studies have resulted in pure amylose starch, it could be speculated that the presence of a fraction of amylopectin in potato starch is essential for plant development. In contrast, barley with suppressed activity of three SBEs (SBEI, SBEIIa and SBEIIb) was found to have an amylose-only starch in the endosperm¹⁶. In that study, the high amylose content only had a minor impact on grain yield and starch content.

In a recent study by Tuncel et al.¹⁴, CRISPR-Cas9 was used to target the two SBEs in potato. Lines with mutations in *Sbe1* or *Sbe2* alone or in combination were developed using either traditional *Agrobacterium*-mediated transformation or PEG-mediated protoplast transfection with vector DNA. In that study, lines mutated in *Sbe1* were not found affected in their starch structure, while tuber cells from *Sbe2* mutated lines displayed an increased number of granules. One line had a strong reduction in both SBEs, resulting in starch with an altered granule phenotype, longer amylopectin chains and a degree of branching that was reduced by half.

Other crops have also been targeted for developing high-amylose starch genotypes using genome editing, such as rice and sweet potato. Rice was subjected to mutagenesis in the respective *Sbe* genes through CRISPR-Cas9 and *Agrobacterium*-mediated transformation¹⁷. In that study, mutations in the *Sbe1* gene did not result in any major changes in the starch compared to the parental variety, while mutations in *Sbe2* led to a starch with increased amylose content from ca. 15 to 25% and an amylopectin chain-length distribution which shifted towards longer chains¹⁷. Similar results were obtained on sweet potato mutated in *Sbe2*, with an increase in amylose content from ca. 27 to 40%¹⁸.

In this study, we used a previously established CRISPR-Cas9 RNP-method to induce mutations in *Sbe1* individually and *Sbe1-Sbe2* simultaneously in potato. By using genome editing to induce mutations in all eight *Sbe* alleles, we were able to develop, for the first time, a unique potato starch essentially lacking branching. We further investigated the effects of this starch as well as starches with altered amylopectin structure on plant development and starch granular structure and phenotype.

Results

***Sbe1* and *Sbe2* targeted mutagenesis and genotyping of regenerated potato lines.** *Sbe1* was targeted alone or in combination with *Sbe2* in the potato variety Desiree (Supplementary Fig. S1). Dual sgRNAs named BE1T3, BE1T4 (*Sbe1*) and BE2T3 and BE2T4 (*Sbe2*) (Supplementary Fig. S1c) were preassembled with Cas9 and transfected to potato protoplasts as ribonucleoprotein complexes (RNPs). In the single gene target experiment, 221 regenerated shoots were analysed using high-resolution fragment analysis (HRFA), while in the stacking gene target experiment, 68 regenerated lines were analysed. The experiments had a mutation frequency of 52% and 72% respectively, calculated based on the number of lines where at least one allele was mutated (Supplementary Table S2). Thirteen lines were selected for further study and genotyped using Sanger sequencing to confirm the insertions/deletions (indels) size and to investigate the genomic structure of the mutations (Table 1). Based on the number and combination of alleles mutated, the lines were divided into three groups: five lines had mutations in all four alleles of *Sbe1*, 82007, 82050, 82079, 104011 and 104032 (Group 1), six lines had four-allele mutations in *Sbe1* combined with two to three alleles mutated in *Sbe2*, 104001, 104005, 104006, 104016, 104018 and 104034 (Group 2) and two lines, 104010 and 104023, had all eight alleles mutated (Group 3). Both lines in Group 3 contained in-frame indels in the *Sbe1* and/or *Sbe2* mutated alleles (Table 1, Supplementary Table S3).

Sanger sequencing results were in line with the results from the HRFA except for large indels, where a 1 bp difference could occasionally be noted (Table 1). The majority of the lines had at least one allele with a large deletion in *Sbe1* due to dual sgRNA mediated cuts, but only one of them, 104005, had a large deletion in all four alleles. The frequency of large deletions due to dual cuts was considerably lower in *Sbe2*. In alleles with mutations not corresponding to a predicted large deletion, indels could be found at both target sites of the sgRNA pair (Table 1). No indels could be observed in one of the alleles of the BE2T4 target region, which had a 1 bp mismatch directly adjacent the protospacer adjacent motif (PAM) site (Supplementary Fig. S1c).

Yield, dry matter, tuber phenotype and sprouting of greenhouse-grown tubers. The thirteen selected lines were grown in a greenhouse until senescence. As comparators during the greenhouse trial and subsequent analyses, the parental variety Desiree and a high-amylose RNAi line T-2012 were included.

Tubers from the Group 3 lines were clearly reduced in size and had a significant total tuber yield drag per plant of 60–80% compared to the parental variety (Supplementary Fig. S2b,c and S3d,e). Further conclusions concerning the number of tubers, total tuber yield per plant and average tuber weight cannot be drawn since the results fluctuated considerably between the lines and biological replicates (Supplementary Fig. S2a–c).

Tuber phenotype was unaffected in Group 1 lines compared to the parental variety (Supplementary Fig. S3a,g), while tubers in the Group 2 lines had some additional buddings detected (Supplementary Fig. S3b,c). The most dramatic phenotypical differences compared to parental variety were found in the Group 3 lines, where tubers were small and elongated with numerous additional buddings from the main tuber (Supplementary Fig. S3d,e). Tubers from the Group 3 lines had a significant decrease in dry matter content (Supplementary Fig. S2d), a

Group	Line	Size of indels confirmed by Sanger sequencing (results from HRFA in brackets)	
		Sbe1	Sbe2
Group 1	82007	$-38^{\text{d}}/-3^{\text{a}}/+70^{\text{e}}$ (-38/-3/+70)	0 ^e (0)
	82050	$-22^{\text{d}}/-1^{\text{a}}/+38^{\text{e}}/+165^{\text{a,c}}$ (-22/-1/+38/+166)	0 ^e (0)
	82079	$-1^{\text{a}}/+47^{\text{a,c}}$ (-1/+47)	0 ^e (0)
	104011	$-94^{\text{ab}}/-4^{\text{e}}$ (-95/-4)	0 ^e (0)
	104032	$-55^{\text{ab}}/+26^{\text{ab}}$ (-56/+26)	0 ^e (0)
Group 2	104001	$-94^{\text{ab}}/+3^{\text{a,b}}$ (-95/+3)	$-129^{\text{c,d}}/-3^{\text{e,d}}/-1^{\text{f}}$ 0 ^e (-130/-3/-1/0)
	104005	$-93^{\text{a,b}}/-92^{\text{a,b}}$ (-94/-93)	$-10^{\text{d}}/-4^{\text{c,d}}/0^{\text{e}}$ (-10/-4/0)
	104006	$-92^{\text{ab}}/-5^{\text{ab}}/-1^{\text{e}}$ (-92/-5/-1)	$-11^{\text{d}}/-1^{\text{d}}$ 0 ^e (-11/-1/0)
	104016	$-93^{\text{a,b}}/-4^{\text{a,b}}$ (-94/-4)	$-2^{\text{f}}/0^{\text{f}}/+6^{\text{d}}$ (-2/0/+6)
	104018	$-93^{\text{a,b}}/-23^{\text{ab}}/-17^{\text{f}}/+153^{\text{a,b}}$ (-94/-23/-17/+153)	$-1^{\text{f}}/0^{\text{f}}/+104^{\text{d}}$ (-1/0/+105)
	104034	$-94^{\text{ab}}/-93^{\text{a,b}}/-5^{\text{a,b}}/+60^{\text{a,b}}$ (-95/-94/-5/+60)	$-8^{\text{c,d}}/-6^{\text{c,d}}/0^{\text{e}}$ (-8/-6/0)
Group 3	104010	$-5^{\text{b}}/+92^{\text{ab}}/+123^{\text{a,b}}$ (-5/+93/+122)	$-2^{\text{d}}/-1^{\text{f}}/+48^{\text{c,d}}/+194^{\text{d}}$ (-2/-1/+48/+195)
	104023	$-92^{\text{ab}}/-3^{\text{a,b}}/+13^{\text{a,b}}/+251^{\text{a,b}}$ (-92/-3/+13/+252)	$-127^{\text{c,d}}/-9^{\text{c,d}}/-5^{\text{c,d}}$ (-128/-9/-5)

Table 1. Size of indels in respective line analysed with Sanger sequencing and HRFA (in brackets), where “0” indicates the wild type allele fragment size, “-” represents a deletion and “+” represents an insertion. Less than four different indels indicates that at least two alleles share the same genetic context. Lack of “0” means no wild type allele remaining in the line. Group 1 represents lines mutated in all four alleles of *Sbe1*; Group 2 represents lines mutated in all four alleles of *Sbe1* and two to three alleles in *Sbe2*; Group 3 represents lines mutated in all alleles of both *Sbe1* and *Sbe2*. [†] Wild type alleles. [‡] In-frame indels. [§] Indels at BE1T3 target site, [¶] Indels at BE1T4 target site, ^{||} Indels at BE2T3 target site and [∆] Indels at BE2T4 target site. [∇] Insert origination from vector used for in vitro transcription.

consequence of smaller and decreased number of starch granules in the tuber cells (Fig. 6f) compared to the comparators and lines from Group 1 and 2 (Fig. 6b,d,h,j). The dry matter content of the tubers from Group 1 and 2 was not significantly different from the parental variety (Supplementary Fig. S2d).

Sprouting of harvested tubers was studied after five months in cold storage. Tubers from all lines already had sprouts initiated at the end of the cold storage period, which continued to develop further at room temperature with no major differences among the lines (Supplementary Fig. S4).

Amylose content and chain-length distribution of tuber starch. Starch was isolated from tubers harvested from the thirten mutated lines and their comparators. Starch quality and structure was studied using several methods. Based on an enzymatic method, the amylose content was found to be 98% in both lines in Group 3 (Fig. 1). No significant increase in amylose could be found for lines in Groups 1 and 2 compared to the parental variety (25% amylose), while the RNAi line T-2012 showed an amylose content of 40%. The amylose content was also measured using a colorimetric method, which was found to be more influenced by variations in the chain length distribution of the amylopectin molecule but overestimating the amylose ratios (Fig. 1b). This method yielded an amylose content of 159–168% in the lines of Group 3. An intermediate amylose content between 40 and 48% was measured in the Group 2 lines. The majority of the lines in Group 1 was found to be ranging from 31 to 35%, which was somewhat lower than for the parental variety having an amylose content of 38%. An exception was line 104032 in Group 1, which was determined to have a 45% amylose content. The amylose content of the RNAi line was measured to be 87%, which is close to the originally published results of 89% for T-2012 using the same colorimetric method.

High-performance size exclusion chromatography (HPSEC) and high-performance anion exchange chromatography (HPAEC) were used to investigate the chain-length distribution of debranched starches. In the HPSEC analysis, the debranched starch samples of Group 1 lines showed a similar chain-length distribution pattern as the parental variety (Fig. 2) but with slightly different amounts for different fractions of amylose. An exception was line 104032, whose chain-length distribution pattern was close to the Group 2 starches (Supplementary Fig. S5). Based on calculations using MALLS, it could be seen that the molecular weight at around 13 mL is in the order of 100,000 g/mol (Supplementary Fig. S6). The molecular weight of amylose generally ranges from about 80,000 to about 1,000,000 g/mol¹⁹, which indicates that the fraction eluted before an elution volume of 13 mL is the major amylose fraction and the fraction eluted after an elution volume of 13 mL is the major amylopectin fraction. Three peaks were eluted between 11 and 13 mL in the starch from the parental variety, which may correspond to three different chain lengths of amylose and are referred as long, intermediate and short-chain amylose fractions hereafter.

Substantial changes to the chain-length distribution pattern, both in the amylose and amylopectin fractions, could be observed for the lines of Group 2 and Group 3 compared to the parental variety (Fig. 2). The peak, which may correspond to the intermediate amylose, is smaller for the lines in Group 2. Alterations in the chain-length distribution were most prominent in Group 3 where the amylopectin fraction between the elution volume of 13 mL and 15 mL was absent and compensated by clearly elevated fractions of amylose. However, compared to the parental variety, these lines lacked the population that may correspond to the short-chain amylose fraction.

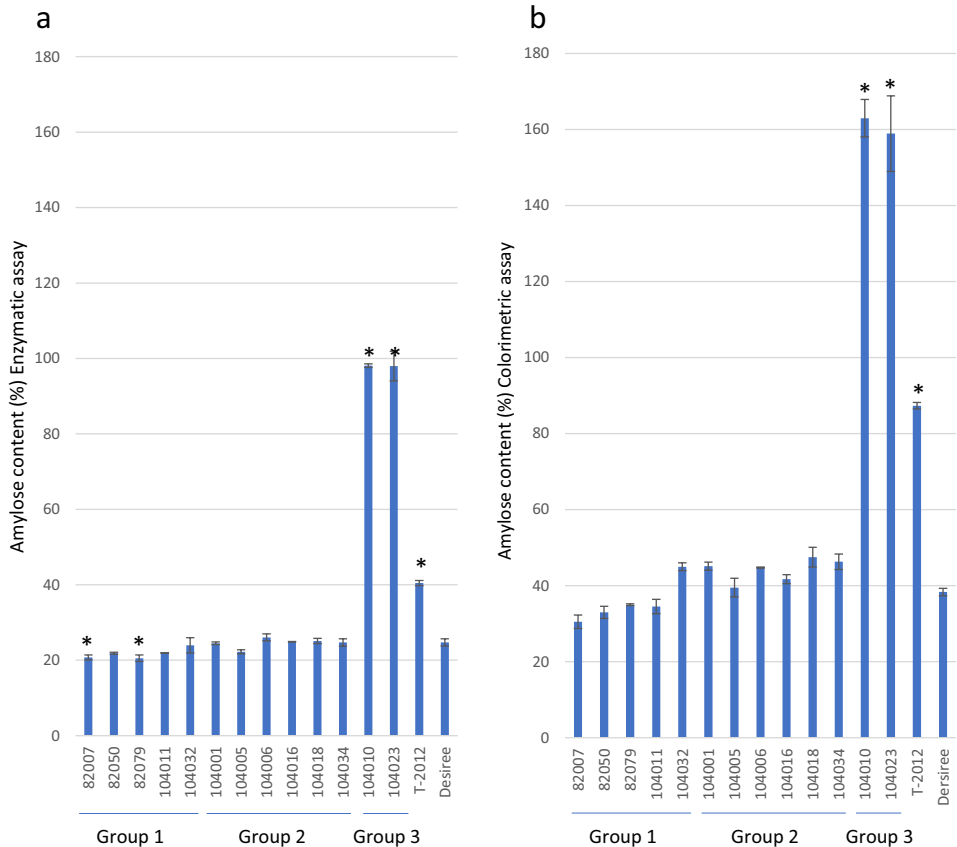


Figure 1. Amylose content of extracted starches measured using a. enzymatic assay and b. colorimetric assay. The results are a mean of two technical replicates, error bar represents standard deviation (s.d.). Values that differ from the parental variety Desiree by Dunnett's test ($P < 0.05$) are marked with *.

Moreover, an extra peak appeared at an elution volume of 15.4 mL, which in theory represents a short-chain amylopectin fraction ($DP > 6$). However, it was not possible to observe any peak for maltodextrins ($DP > 6$) from the HPAEC analysis for the starches from Group 3. This limits the possibility that the extra peak is associated with a short-chain amylopectin fraction. The T-2012 RNAi-line had a chain-length distribution pattern that differs from all other lines with an altered amylopectin chain-length distribution and an elevated fraction of amylose or amylose-like long glucan chains (Fig. 2).

The molar proportion distribution of different chain lengths of starch from the potato lines, analysed by HPAEC, is given in Fig. 3. Starch from Desiree showed a pattern where there is a predominant broad peak of chains spanning the $DP \sim 9-33$ range, with a shoulder at DP11 and a slight increase of chains from DP18 (Fig. 3). Starch from T-2012, however had a very different pattern of the chain length distribution, where there was a large decrease in short chains of DP7–10, a high and sharp peak of chain at DP11, and less chains of DP12–18 and more chains of DP19–42 than the other samples (Fig. 3). The proportion of chain lengths of $DP \geq 43$ was very low for all the potato lines. Starch from Group 1 lines was very similar to the parental variety in the chain length distribution of long chains of $DP > 33$, with increased abundance of moderately sized chains of DP12–21 and reduced number of short chains of DP7–11 and intermediate-sized chains of DP22–33 (Fig. 3, Supplementary Fig. S7a). The biggest effect was observed with an increase in the proportion of chains at DP6 (Supplementary Fig. S7a). In the starch from lines in Group 2, there was a decline in the proportion of short chains of $DP \leq 13$, and an increase in those of the intermediated-sized chains of DP14–33 and, effects on chains of $DP > 33$ were not pronounced compared to the parental variety (Fig. 3, Supplementary Fig. S7b). There was no peak detected for debranched amylopectin chains from the HPAEC analysis for the starches from Group 3. Amylose is essentially

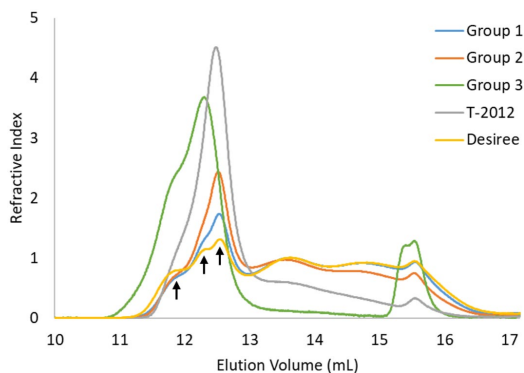


Figure 2. Chain-length distribution of debranched starches from the potato lines after normalisation for the peak area, analysed with HPSEC. The averages of the potato lines from Groups 1, 2 and 3 are shown. The parental variety Desiree and the high-amylose line T-2012 were included for comparison. The arrows from left to right point out the three populations of amylose chains, i.e. long, intermediate, and short chain amylose fraction, respectively. Software used is ASTRA software version 4.70.07 (wyatt.com/products/software/astra.html, Wyatt Technology Corp., Santa Barbara, CA).

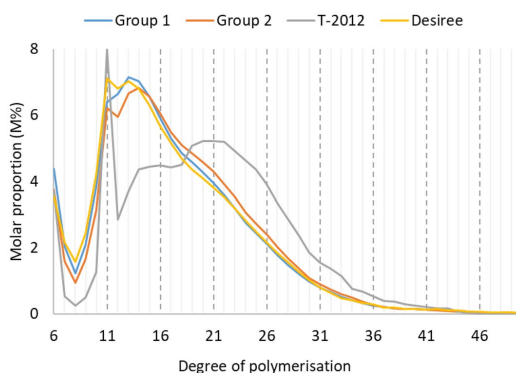


Figure 3. Chain-length distribution of debranched starches on a relative molar basis (M%) with degree of polymerization (DP) 6–50, based on HPAEC analysis with averages of potato lines from Groups 1 and 2. No peak was detected for the starches from Group 3. The parental variety Desiree and the high-amylose line T-2012 were included for comparison.

long linear molecule which was beyond the separation range of HPAEC, and the chain-length distribution from the HPAEC analysis did not account the chains originating from the amylose fraction (Fig. 3).

Degree of branching of Group 3 starches. The degree of branching (DB) was analysed using NMR spectroscopy on starch from lines in Group 3 and the parental variety Desiree. At the branching point, the anomeric proton at the $\alpha(1 \rightarrow 6)$ -linkage has a different chemical shift compared to other anomeric protons and can thus be used for quantification of the DB. Neither starch from line 104010 nor 104023 showed any detectable branching ($< 0.1\%$), whereas the starch from Desiree showed a DB of 3.0% (Fig. 4). Similarly, the amount of terminal residues was markedly different, with the non-reducing end H4 yielding a clear signal from the Desiree starch but a very weak signal from the Group 3 starches (Fig. 4).

Crystalline type and molecular order of the starch granules. As displayed in Fig. 5, most of the potato lines showed the B-type X-ray diffraction pattern²⁰ with diffraction peaks at 15° (broad), 17° (strong) and a doublet at $22\text{--}24^\circ$ 2θ , which is the common pattern for the tuber starches. However, the X-ray diffraction pat-

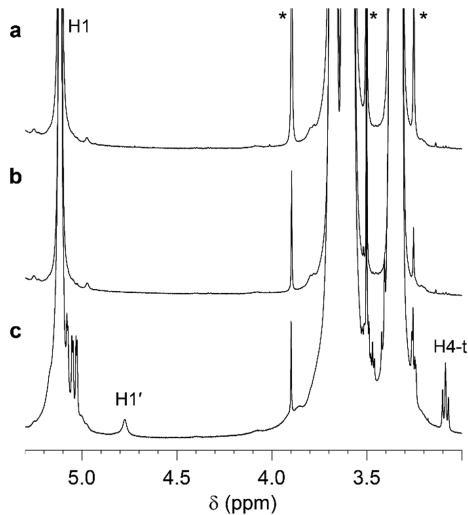


Figure 4. ^1H NMR spectra of starch from the Group 3 lines (a) 104010 and (b) 104023, and from (c) the parental variety Desiree. Glucose H1 at the $\alpha(1 \rightarrow 4)$ -linkage (H1) and at the $\alpha(1 \rightarrow 6)$ -linkage (H1') are assigned as well as H4 of non-reducing end terminal residues (H4-t). Traces of EDTA and Tris are highlighted with asterisks.

tern and the diffraction intensities of the Group 3 lines differed from the other lines. A decrease in the diffraction intensity for most of the peaks was observed in the Group 3 lines when compared to the other lines. However, it was still possible to observe all the major diffraction peaks that correspond to B type starches (Fig. 5a). Moreover, the starch from Group 3 did not show Maltese crosses in the starch granules under polarised light, as was found in starch from the parental variety Desiree or 104016 (Fig. 5b).

Starch granule phenotype. Starch stained with iodine and studied with light microscopy revealed that the granular phenotype was affected in all lines but at different levels. Starch from lines in Group 1 were most similar to starch granules from the parental variety, oval in shape but with a minor truncation in the core (Fig. 6a). The truncated core became even more pronounced in starch from the lines in Group 2 and had more irregularly shaped granules (Fig. 6c), where several of the granules had a similar phenotype as the RNAi line (Fig. 6g). Granules from the lines in Group 3 were most affected as compared to the parental line and found to have a spherical multi-lobed phenotype (Fig. 6e,i).

Greenhouse study of green biomass and transitory starch. The green biomass was measured at three time points: four, ten and fifteen weeks after planting. Five mutated lines and the RNAi line were measured relatively the parental variety: 82079 (Group 1), 104006 and 104018 (Group 2), 104010 and 104023 (Group 3) and T-2012 (RNAi) (Fig. 7a, Supplementary Fig. S8). After four weeks, the parental variety had the highest biomass, lines from Group 1 and 2 the second highest and lines from Group 3 the lowest. After ten weeks, all plants had a similar biomass, while after fifteen weeks, the lines from Group 3 had the highest biomass and had passed all other lines in growth. The parental variety plants had started to wither at time point three, which affected the biomass, most likely due to a heavy aphid infection and pest control treatment. Therefore, the values of the mutated lines as compared to the parental variety at time point three are overestimated, but still useful for comparison between the mutated lines.

Leaf tissue from the top shoots harvested at ten weeks after planting was stained with iodine after a light and dark period. As can be seen in Fig. 7b, the lines from Group 3 had no staining, showing a deficiency in transitory starch synthesis during the light period, while lines from Group 1 and 2 were similar to T-2012 and the parental variety (Fig. 7b). The lines from Group 1, 2 and 3 had the expected lack of transitory starch after the dark period. An exception was T-2012, which still stained after the dark period. It can be speculated that the granular structure of the leaf starch affects accessibility of the starch degrading enzymes, however, further studies are needed to elucidate the cause.

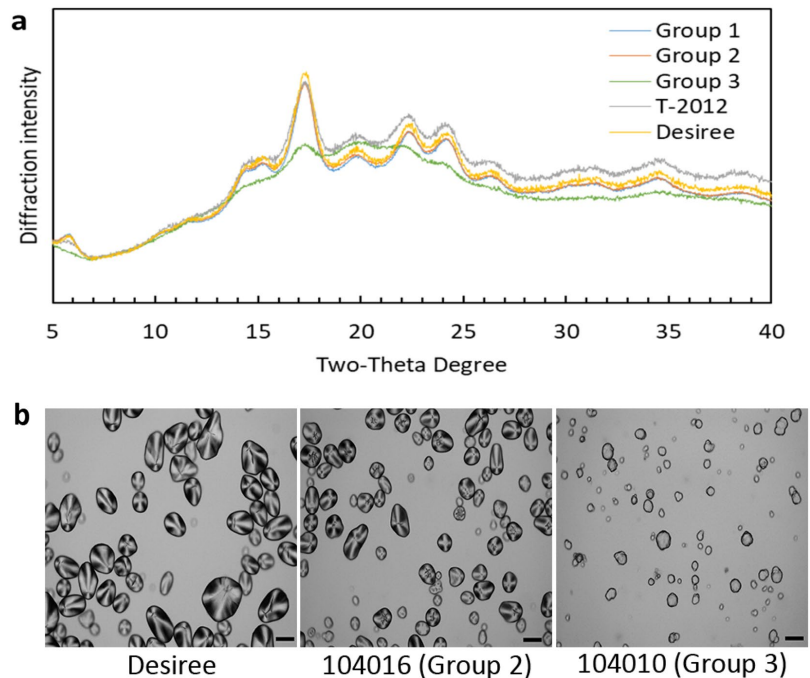


Figure 5. X-ray diffraction patterns and polarised light microscopy of potato lines from Groups 1, 2, and 3. (a) Average diffraction intensity for each group. The parental variety Desiree and the high-amylose line T-2012 were included for comparison. (b) Images of selected potato starches using polarised light microscopy. Scale bar = 40 μm .

Discussion

The number of alleles mutated, and the genomic structure of mutations induced in *Sbe1* and *Sbe2* of potato had a major impact on the starch quality. To develop a starch with a significant increase in chain lengths corresponding to the amylose fraction, mutations in all alleles of both genes were needed (Group 3). The lines from Group 3 were found to have starch with a reduced degree of branching from 3.0% in the control to below the detection limit of 0.1% and no amylopectin could be detected when analysed by HPAEC. Notably, the lines from Group 3 had at least one allele with an in-frame mutation in one or both of *Sbe1* and *Sbe2*. In a study by Tuncel et al.¹⁴, the quantity of the SBEs was reduced but not absent in lines with in-frame deletions in the *Sbe* genes. These proteins could, even with a potential loss of activity, be of importance for starch synthesis to occur. The situation has not been thoroughly investigated in potato, but several studies in cereals have shown that enzymes involved in the synthesis of starch molecules and organisation into granules are active as complexes^{21–23}. The remaining fraction of SBEI and SBEII in our lines from Group 3 might be crucial to maintaining protein–protein interactions and keeping other enzymes, such as soluble starch synthases, active.

Using the applied genome-editing method, we were not able to mimic the starch qualities of high-amylose potatoes that were previously developed by transgenic gene inhibition^{7,12,15}. In our study, lines with full knockout of SBEI together with two to three mutated *Sbe2* alleles (Group 2) only had a minor effect on the amylose content. None of the Group 2 lines were found to have the same increased amylose content or the very large fraction of intermediate sized chains like the starch structure found in the RNAi line T-2012 included in this study, which seem to be common among high-amylose potato starches achieved by reduced transcript levels. In a previous study, using antisense to inhibit both SBEs, a reduction of branching enzyme activity to less than 1% was found in tubers with starch containing more than 50% amylose¹². Hence, the presence of one or two *Sbe2* wild type alleles is enough for the tubers to produce starch close to wild type levels of amylopectin. The chain length distribution of debranched starches suggests that the targeted mutagenesis of *Sbe1* with or without *Sbe2* had different effects on starch structure, which has also been shown in other studies^{14,24–28}. This is believed to be due to different activities of the potato SBE isoforms²⁵ affecting the amylopectin structure²⁹. Simultaneous suppression of SBEs in potato has been shown to induce drastic effects on starch structure^{12,14,15}. Consistent with these findings, our HPSEC results for debranched starch from Groups 2 and 3 showed a loss of the short-chain amylopectin fraction

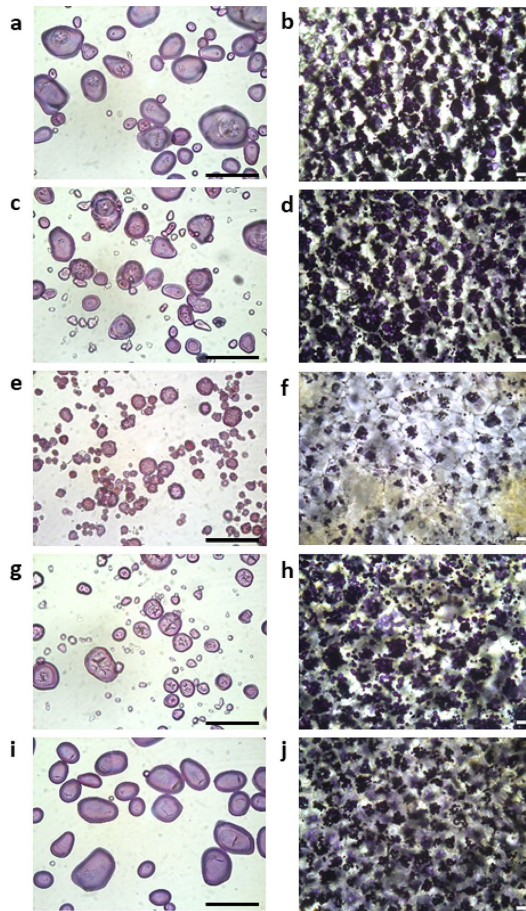


Figure 6. Starch granules (left images) and thin sliced tuber tissue (right images) stained with iodine and visualised under light microscope. (a,b) 82079 (Group 1) (c,d) 104018 (Group 2) (e,f) 104010 (Group 3). (g,h) RNAi line T-2012. (i,j) parental variety Desiree. Scale bar = 100 μm .

and elevated fractions of amylose. Accordingly, a decreased number of short chains of $\text{DP} \leq 13$ and an increased proportion of intermediate-sized chains ($\text{DP}14\text{--}33$) were observed for starch from Group 2 by HPAEC analysis.

Many studies on cereals have reported that suppression of SBEI alone has either no detectable effect or only a minor effect on starch structure³⁰. Also previous studies in potato, antisense suppression of SBEI did not affect the amylose content or the chain length distribution of the amylopectin³⁰. This is in line with our HPSEC results for Group 1 starches, which showed a similar chain length distribution of amylopectin fraction in relation to the parental variety. One exception is line 104032, which can be found similar in structure to the Group 2 starches. It can be speculated that this line might be a chimera or having one *Sbe2* allele with a very large deletion that was not amplified during the genomic analyses. Even though several attempts were made to elucidate that, only wild type alleles were found using HRFA and Sanger sequencing. When studying the starches from lines in Group 1 with higher resolution using HPAEC, an altered chain-length distribution was found, indicating that a complete knockout of SBEI alone influenced the starch structure somewhat. Moreover, light microscopy of stained starch granules from Group 1 lines revealed a minor truncation in the core of the granules.

X-ray diffraction of starch correlates with crystalline organisation of double helices in a starch granule, while the crystallinity of granular starches is mostly attributed to the amylopectin fraction³⁰. Thus, the significant loss of the amylopectin fraction in the Group 3 starches might be the reason for the considerably decreased X-ray diffraction pattern of the starches from Group 3. Moreover, the level of crystallinity has an inverse relationship

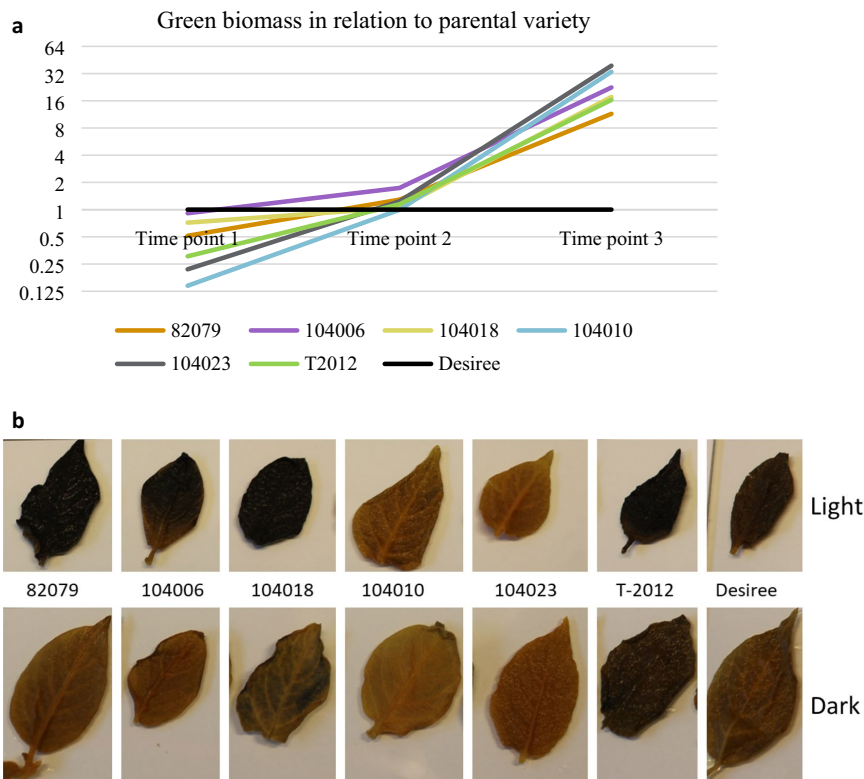


Figure 7. Transitory starch and green biomass of plants grown in greenhouse. Lines analysed are; 82079 (Group 1), 104006 (Group 2), 104018 (Group 2), 104010 (Group 3), 104023 (Group 3), T-2012 and parental variety Desiree. **(a)** Green biomass measured with low-cost RGB imaging phenotyping lab using digiCamControl (digiCamControl v2,1,2, <http://www.digicamcontrol.com>) and Easy Leaf Area. All lines are normalised to the parental variety Desiree, which is set to 1. The results are a mean of three biological replicates. Note that the vertical axis has a logarithmic scale. **(b)** Leaf tissue of top shoots harvested after a light (top row) and dark period (bottom row) stained with iodine.

to the amylose content³¹. Hence, the high-amylose feature of the potatoes from Group 3 might also contribute to the lower degree of crystallinity in the potato lines. However, the high-amylose potato starch in line T-2012, produced by RNAi, did not show a difference in the X-ray diffraction pattern compared to the parental variety.

Maltose crosses in starch granules generally indicate a higher degree of ordered structure in granules with molecules arranged in a radial pattern³². It is known that the apparent intensity of the birefringence is not only affected by the degree of crystallinity and granule thickness but also by the orientation of the crystallites³³. Therefore, the complete loss of Maltose crosses in the starch from Group 3 could be attributed to a deviation in the orientation of the crystallites from its radial arrangement. The results from X-ray diffraction, polarised light microscopy and NMR spectroscopy revealed a type of starch that has the ability to organise into granules with a poorly ordered amylose crystalline arrangement, even with the considerable loss of the amylopectin fraction. These results are also in agreement with the study of amylose-only barley starch¹⁶.

Lines from Group 3 had a significantly decreased tuber yield, tuber size and tuber dry matter content. In a previous study of high-amylose potato lines grown in the field for several years, plants were found to be stunted in growth¹⁵. It was speculated that the gene inhibitions could also have an effect on diurnal starch, which might have led to a depletion in the energy turnover, or that an increase in sugars in the plant might disturb other metabolic processes. In this study, the development of the Group 3 lines was suppressed during the first period after planting but those lines developed a higher green biomass than lines from Groups 1 and 2 up until senescence; despite that, the transitory starch was clearly decreased after a light period. One hypothesis could be that once tuber initiation occurs and throughout the tuber development phase, the low efficiency of channelling sugars into long-term storage as tuber starch is instead redistributed to produce green biomass.

To our knowledge, this is the first time potato starch with no detectable branching has been developed and studied. It highlights the expanded knowledge we can gain from using genome editing to study enzymatic functions and consequences of the loss of enzymatic activities on biosynthesis and plant products. This study has also raised new questions, for example, how can the self-organisation of starch into granules occur even with complete absence of branching, or are they simple molecular aggregates?

Material and methods

Design of targets. Genomic DNA was extracted from Desiree leaf tissue using the Gene Jet Plant Genomic DNA purification Mini Kit (Thermo Fisher Scientific, Waltham, MA) and sequenced through the Illumina TruSeq PCR-free library preparation (average fragment size 350 bp) and Illumina HiSeqX (PE 2 × 150 bp) (National Genomics Infrastructure, Stockholm, Sweden). Targets were selected in regions of exon 5 in *Sbe1* (GenBank accession no. NW_006238958.1:c2098376-2090439) and in exon 3 in *Sbe2* (GenBank accession no. NW_006238947.1:c2592132-2611729) using CRISPR RGEN Tools (<http://www.rgenome.net/cas-designer>) and a previously available guide design tool (<http://crispr.mit.edu/>). Double sgRNA targets were selected for each gene and named BE1T3 and BE1T4 as well as BE2T3 and BE2T4 (Fig. S1). All sgRNAs were designed to target allelic homologous regions, except for BE2T4 which had a mismatch at the first bp prior PAM in one of the four alleles.

Mutagenesis and genotyping. Mutations were induced in *Solanum tuberosum* L. cultivar Desiree through PEG-mediated protoplast transfection of RNPs. In vitro propagation, protoplast isolation, regeneration and mutation screening and characterisation were performed as described in Andersson et al.¹¹. Transfection of RNPs to isolated protoplasts was done essentially as described in Andersson et al.³⁵ using 5 µg in vitro transcribed RNA preassembled with 5 µg Cas9 per target (Thermo Fisher Scientific, Waltham, MA) for lines named 82- or 0.1 nmol synthetically produced crRNA preassembled with 5 µg Cas9 per target (IDT, Coralville, IA, USA) for lines named 104-.

The transfection conditions were 40% PEG and 30 min incubation time. Care was taken to only pick one shoot from each calli. High-resolution fragment analysis (HRFA) was performed as previously described¹¹ by multiplexing primers SBE1f.-HEX and SBE1_r with SBE2_3f.-FAM and stbe2exonr and screening for mutations in both genes simultaneously. Sanger sequencing (Eurofins Genomics, Ebersberg, Germany) was performed using unlabelled primers of SBE1f.-HEX and SBE1_r, SBE2_3f.-FAM and stbe2exonr as well as stbe2exonr and Stbe2exonf (Supplementary Table S1).

Greenhouse cultivation. Thirteen genome edited lines, the parental variety Desiree and one RNAi line, T-2012 from the parental variety Dinamo developed in a previous study⁷, were grown in a greenhouse. *In vitro* cuttings of the lines were planted in soil (Yrkesplantjord, SW Horto, Hammenhög, Sweden) in three to five biological replicates in 7.5 L pots and cultivated under controlled greenhouse conditions: 16-h day length, 18/15 °C day/night temperature, supplementary light intensity up to approximately 200 µmol s⁻¹ m⁻² photons, 60% relative humidity. The lines were grown for 5 months between 13 December and 21 May and were regularly fertilised with SW Bouyant RikaS 7-1-5 + mikro (SWHorto, Hammenhög, Sweden).

Starch isolation, dry matter and amylose measurement. Starch was extracted from tubers harvested after senescence according to Larsson et al.³⁴ with a minor modification where the time for sedimentation after extraction and each buffer washing steps were performed overnight to secure that small granules were retained. Dry matter content was measured on freshly harvested tubers as previously described³⁵. Amylose content was measured on isolated starch using both an enzymatic assay and a colorimetric assay. The enzymatic assay was made using an amylose/amylopectin kit (Megazyme, Bray, Co, Ireland) according to the supplier's instructions. The colorimetric method was based on iodine complex formation stabilized with trichloroacetic acid. The amylose content was analyzed according to Chrastil³⁶ with minor modification. After solubilisation of starch with Urea-dimethylsulphoxide (UDMSO) according to Morrison and Laigneul³⁷, 25 µL of sample was transferred to each of two test tubes, 5 mL 0.5% trichloroacetic acid and 50 µL 0.01 N KI-I₂ solution were directly added for 30 min incubation at 25 °C before the absorbance measurement. A standard curve (R² = 0.999) was developed using waxy potato starch (Lyckeby starch AB, Kristianstad, Sweden) and potato amylose standard (type III, Sigma Chemical Co., MO, USA) with varying amylose contents of 0%, 25%, 50%, 75% and 100%. All samples were analyzed in duplicate and results are reported as average values with standard deviation (SD) based on total starch content.

Starch structural analysis. Starch samples solubilised in UDMSO (0.6 M urea in 90% DMSO) were used for chain-length distribution analysis by high-performance size exclusion chromatography (HPSEC) and high-performance anion exchange chromatography (HPAEC) as previously described^{38–40}. The starch samples were debranched with isoamylase from *Pseudomonas* sp (EC 3.2.1.68, 500 U/mL, Megazyme, Wicklow, Ireland) and pullulanase M1 from *Klebsiella planticola* (EC 3.2.1.41, 700 U/mL, Megazyme, Wicklow, Ireland) before both analyses. The enzymes were desalted and ten-fold diluted using acetate buffer (0.01 M, pH 5.0) before applied for debranching.

For HPSEC, 300 µL each enzyme and 400 µL distilled water was mixed with 500 µL solubilised starch sample for debranching overnight at 40 °C. For HPAEC, 60 µL each enzyme and 880 µL distilled water and 400 µL sodium-acetate buffer (0.01 M, pH 5.0) was mixed with 100 µL solubilised starch sample for debranching overnight at 40 °C. For both HPSEC and HPAEC, the samples were boiled for 10 min after debranching to terminate the enzyme reaction and then filtered through a 0.45 µm nylon filter before analysis.

The HPSEC was performed as described in Andersson et al.⁴¹ with minor modifications. The HPSEC system has two serially connected OHPak SB-802.5 HQ columns with a guard column (Shodex, Showa Denko KK, Minato, Japan) kept at 35 °C. The eluent was 0.1 M NaNO₃, containing 0.02% NaN₃ with a flow rate of 0.5 mL/min. The HPSEC is equipped with refractive index (RI) detector (Wyatt Technology Corp., Santa Barbara, CA) and multiple-angle laser light scattering detector (MALLS; Dawn DSP equipped with a He-Ne laser at 632.8 nm, Wyatt Technology Corp., Santa Barbara, CA). Data for molecular-weight determinations were analysed using ASTRA software version 4.70.07 (wyatt.com/products/software/astra.html, Wyatt Technology Corp., Santa Barbara, CA) based on a dn/dc of 0.147⁴¹. The angular fit was based on the Debye procedure⁴¹. The HPSEC columns were calibrated with Dextran T2000, Dextran T500, maltoheptaose, maltopentaose, maltotriose, and glucose (Supplementary Fig. S9). Results are given as the average of two replicates and the total area of HPSEC chromatograms were normalized between elution volume 10 mL and 17 mL, after which maltopentaose, maltotriose, and glucose were eluted (Supplementary Fig. S9).

The HPAEC (Series 4500i, Dionex Corp., Sunnyvale, CA, USA) coupled with a BioLC gradient pump and a pulsed amperometric detector (PAD) was used in this study. Separation was performed on a CarboPac PA-100 (4 × 250 mm) analytical column (Dionex, Sunnyvale USA) equipped with a guard column. The elution was performed at 25 °C with a flow rate of 1 mL/min and injection volume of 25 µL using 0.15 M NaOH (A) and 0.50 M NaOAc + 0.15 M NaOH (B) with the following gradient: 0–15 min, 15–28% eluent B; 15–45 min, 28–55% B; 45–75 min, 55–70% B; and 75–80 min 70–15% B (return to the start mixture). The column was equilibrated with 15% eluent B for 15 min between runs. The PAD response was converted to molar percentage and normalised³⁸. All results are given as the average of two replicates.

NMR spectroscopy. Starch from the parental variety and the Group 3 lines were analysed by NMR for degree of branching according to Tizzotti, et al.⁴². Starch samples (10 mg) were dissolved by heating in deuterated dimethyl sulfoxide (DMSO-*d*₆; 600 µL) with the addition of deuterated trifluoroacetic acid (TFA-*d*₃; 10 µL) prior to NMR analysis to avoid spectral interference with hydroxyl protons. ¹H NMR spectra were recorded on a Bruker Avance III 600 MHz spectrometer using a 5 mm broadband observe detection SmartProbe. Spectra were acquired at 50 °C using 128 scans and a relaxation delay of 12 s and were processed with TopSpin 3.6. The degree of branching was measured as the ratio $I_{1-6}/(I_{1-6} + I_{1-4})$, where I_{1-6} is the integrated signal at 4.77 ppm and I_{1-4} is the integrated signal at 5.12 ppm, corresponding to H1 of glucose at the α(1 → 6) and α(1 → 4)-linkages, respectively.

X-ray diffraction patterns. The method for X-ray diffraction analysis has been previously described⁴⁵. Starch X-ray patterns were identified using a PANalytical X'Pert alpha powder X-ray diffractometer in Theta-2Theta geometry, and coupled with a focusing Johansson Ge monochromator producing pure Cu-Kα1 radiation (λ = 1.54060 Å). The starches were spread onto 1.5 × 2 cm² Si wafers. The scanning region of the diffraction angle (2θ) was from 5° to 40°.

Polarised light microscopic analysis of starch granules. Starch dispersions (0.5 mL, 50 mg/mL) in distilled water were freshly prepared. One drop (25 µL) of each starch dispersion was taken for microstructural analysis⁵ using a light microscope (Leica DMLB, Wetzlar, Germany) equipped with an infinity X-32 digital camera (DeltaPix, Samour, Denmark). The images of starch granules were captured at a 20 × objective under polarised light to compare the birefringence of starch granules from lines from Group 3, 104016 (from Group 2) and the parental variety.

Starch granule phenotyping. Starch granule distribution and phenotype was studied by staining thin tuber discs and purified starch granules with Lugol's solution. The results were visualised with a light microscope (Leica DMLB, Leica Microsystems, Wetzlar, Germany) and documented with an assembled camera (Leica DFC450C, Leica Microsystems, Wetzlar, Germany).

Green biomass phenotyping. Green biomass of five of the mutated lines, 82079, 104006, 104018, 104010, 104023 as well as Desiree and T-2012, were studied in a greenhouse. The plants were grown between 7 October and 22 January under the same growth conditions as described above.

Green biomass was measured at four, ten and fifteen weeks after planting using a low-cost RGB imaging phenotyping lab published by Armoniene et al.³⁵. The plants were placed on a rotating disc and images were taken as side views with a standard camera (Canon 1300D, Canon, USA) tethered to the software digiCamControl v2.1.2 (<http://www.digicamcontrol.com>)⁴³. Four photos were taken of each plant and three biological replicates covering 360° of the plants. The images were processed using Easy Leaf Area⁴⁴.

Top leaves were harvested at week 10, decoloured by boiling in 80% EtOH and stained with 50% Lugol's solution.

Sprouting. Harvested greenhouse grown potatoes were stored in the dark at 6 °C for five months before being incubated at 22 °C for 3 months. Sprout development was studied through naked eye observation once a week.

Received: 20 May 2020; Accepted: 29 January 2021

Published online: 22 February 2021

References

- Nadakuduti, S. S., Starker, C. G., Voytas, D. F., Buell, C. R. & Douches, D. S. Genome Editing in Potato with CRISPR/Cas9. In *Plant Genome Editing with CRISPR Systems. Methods in Molecular Biology* Vol. 1917 (ed. Qi, Y.) (Humana Press, New York, 2019).
- Nadakuduti, S. S., Buell, C. R., Voytas, D. F., Starker, C. G. & Douches, D. S. Genome editing for crop improvement: applications in clonally propagated polyploids with a focus on potato (*Solanum tuberosum* L.). *Front. Plant Sci.* <https://doi.org/10.3389/fpls.2018.01607> (2018).
- Birch, P. R. J. *et al.* Crops that feed the world 8: potato—are the trends of increased global production sustainable?. *Food Secur.* **4**, 477–508. <https://doi.org/10.1007/s12571-012-0220-1> (2012).
- Zeeman, S. C., Kossmann, J. & Smith, A. M. Starch: its metabolism, evolution, and biotechnological modification in plants. *Annu. Rev. Plant Biol.* **61**, 209–234. <https://doi.org/10.1146/annurev-arplant-042809-112301> (2010).
- Zhao, X., Andersson, M. & Andersson, R. Resistant starch and other dietary fiber components in tubers from a high-amylose potato. *Food Chem.* **251**, 58–63. <https://doi.org/10.1016/j.foodchem.2018.01.028> (2018).
- Lehmann, U. & Robin, F. Slowly digestible starch: its structure and health implications—a review. *Trends Food Sci. Technol.* **18**, 346–355. <https://doi.org/10.1016/j.tifs.2007.02.009> (2007).
- Menzel, C. *et al.* Improved material properties of solution-cast starch films: effect of varying amylopectin structure and amylose content of starch from genetically modified potatoes. *Carbohydr. Polym.* **130**, 388–397. <https://doi.org/10.1016/j.carbpol.2015.05.024> (2015).
- Jacobsen, E., Ramanna, M. S., Huigen, D. J. & Sawor, Z. Introduction of an amylose-free (amf) mutant into breeding of cultivated potato, *Solanum tuberosum* L. *Euphytica* **53**, 247–253. <https://doi.org/10.1007/bf00023276> (1991).
- Visser, R. G. F. *et al.* Inhibition of the expression of the gene for granule-bound starch synthase in potato by antisense constructs. *Mol. Gen. Genet.* **225**, 289–296. <https://doi.org/10.1007/bf00269861> (1991).
- Andersson, M. *et al.* A novel selection system for potato transformation using a mutated AHAS gene. *Plant Cell Rep.* **22**, 261–267. <https://doi.org/10.1007/s00299-003-0684-8> (2003).
- Andersson, M. *et al.* Efficient targeted multiallelic mutagenesis in tetraploid potato (*Solanum tuberosum*) by transient CRISPR-Cas9 expression in protoplasts. *Plant Cell Rep.* **36**, 117–128. <https://doi.org/10.1007/s00299-016-2062-3> (2017).
- Schwall, G. P. *et al.* Production of very-high-amylose potato starch by inhibition of SBE A and B. *Nat. Biotechnol.* **18**, 551–554 (2000).
- Andersson, M. *et al.* Targeted gene suppression by RNA interference: an efficient method for production of high-amylose potato lines. *J. Biotechnol.* **123**, 137–148. <https://doi.org/10.1016/j.jbiotec.2005.11.001> (2006).
- Tuncel, A. *et al.* Cas9-mediated mutagenesis of potato starch-branching enzymes generates a range of tuber starch phenotypes. *Plant Biotechnol. J.* **17**, 2259–2271. <https://doi.org/10.1111/pbi.13137> (2019).
- Hofvander, P., Andersson, M., Larsson, C. T. & Larsson, H. Field performance and starch characteristics of high-amylose potatoes obtained by antisense gene targeting of two branching enzymes. *Plant Biotechnol. J.* **2**, 311–320. <https://doi.org/10.1111/1/j.1467-7652.2004.00073.x> (2004).
- Carciño, M. *et al.* Concerted suppression of all starch branching enzyme genes in barley produces amylose-only starch granules. *BMC Plant Biol.* <https://doi.org/10.1186/1471-2229-12-223> (2012).
- Sun, Y. W. *et al.* Generation of high-amylose rice through CRISPR/Cas9-mediated targeted mutagenesis of starch branching enzymes. *Front. Plant Sci.* <https://doi.org/10.3389/fpls.2017.00298> (2017).
- Wang, H. X. *et al.* CRISPR/Cas9-based mutagenesis of starch biosynthetic genes in sweet potato (*Ipomoea batatas*) for the improvement of starch quality. *Int. J. Mol. Sci.* <https://doi.org/10.3390/ijms20194702> (2019).
- Delcour, J. A. H. *Chapter 2 Starch in (3rd ed.) Principles of Cereal Science and Technology* 33–55 (AACCI International Press, Minnesota, 2010).
- 20Hizukuri, S., Abe, I.-i. & Hanashiro, I. In A-C. Eliasson (Eds.), *Carbohydrates in food, 2nd edition* 363–365 (CRC Press, Boca Raton, FL, USA, 2006).
- Tetlow, I. J. *et al.* Analysis of protein complexes in wheat amyloplasts reveals functional interactions among starch biosynthetic enzymes. *Plant Physiol.* **146**, 1878–1891. <https://doi.org/10.1104/pp.108.116244> (2008).
- Tetlow, I. J. *et al.* Protein phosphorylation in amyloplasts regulates starch branching enzyme activity and protein-protein interactions. *Plant Cell* **16**, 694–708. <https://doi.org/10.1105/tpc.017400> (2004).
- Helle, S. *et al.* Proteome analysis of potato starch reveals the presence of new starch metabolic proteins as well as multiple protease inhibitors. *Front. Plant Sci.* <https://doi.org/10.3389/fpls.2018.00746> (2018).
- Brummell, D. A. *et al.* Overexpression of STARCH BRANCHING ENZYME II increases short-chain branching of amylopectin and alters the physicochemical properties of starch from potato tuber. *BMC Biotechnol.* <https://doi.org/10.1186/s12896-015-0143-y> (2015).
- Rydberg, U., Andersson, L., Andersson, R., Aman, P. & Larsson, H. Comparison of starch branching enzyme I and II from potato. *Eur. J. Biochem.* **268**, 6140–6145. <https://doi.org/10.1046/j.0014-2956.2001.02568.x> (2001).
- Andersson, L. *et al.* Characterisation of the in vitro products of potato starch branching enzymes I and II. *Carbohydr. Polym.* **50**, 249–257. [https://doi.org/10.1016/S0144-8617\(02\)00059-0](https://doi.org/10.1016/S0144-8617(02)00059-0) (2002).
- Andersson, L., Rydberg, U., Larsson, H., Andersson, R. & Aman, P. Preparation and characterisation of linear dextrans and their use as substrates in in vitro studies of starch branching enzymes. *Carbohydr. Polym.* **47**, 53–58. [https://doi.org/10.1016/S0144-8617\(01\)00162-X](https://doi.org/10.1016/S0144-8617(01)00162-X) (2002).
- Blennow, A. *et al.* Structure function relationships of transgenic starches with engineered phosphate substitution and starch branching. *Int. J. Biol. Macromol.* **36**, 159–168. <https://doi.org/10.1016/j.ijbiomac.2005.05.006> (2005).
- Kossmann, J. & Lloyd, J. Understanding and influencing starch biochemistry. *Crit. Rev. Plant Sci.* **19**, 171–226. [https://doi.org/10.1016/S0735-2689\(00\)80002-7](https://doi.org/10.1016/S0735-2689(00)80002-7) (2000).
- Safford, R. *et al.* Consequences of antisense RNA inhibition of starch branching enzyme activity on properties of potato starch. *Carbohydr. Polym.* **35**, 155–168. [https://doi.org/10.1016/S0144-8617\(97\)00249-x](https://doi.org/10.1016/S0144-8617(97)00249-x) (1998).
- Cheetham, N. W. H. & Tao, L. P. Variation in crystalline type with amylose content in maize starch granules: an X-ray powder diffraction study. *Carbohydr. Polym.* **36**, 277–284. [https://doi.org/10.1016/S0144-8617\(98\)00007-1](https://doi.org/10.1016/S0144-8617(98)00007-1) (1998).
- Bertoff, E. Understanding starch structure: recent progress. *Agronomy Basel* <https://doi.org/10.3390/agronomy7030056> (2017).
- French, D. Chapter VII—Organization of Starch Granules. In *Starch: Chemistry and Technology* 2nd edn (eds Whistler, R. L. *et al.*) 183–247 (Academic Press, London, 1984).
- Larsson, C. T. *et al.* Three isoforms of starch synthase and two isoforms of branching enzyme are present in potato tuber starch. *Plant Sci.* **117**, 9–16. [https://doi.org/10.1016/0168-9452\(96\)04408-1](https://doi.org/10.1016/0168-9452(96)04408-1) (1996).
- Andersson, M. *et al.* Inhibition of plastid PPase and NTT leads to major changes in starch and tuber formation in potato. *J. Exp. Bot.* **69**, 1913–1924. <https://doi.org/10.1093/jxb/ery051> (2018).
- Chraстил, J. Improved colorimetric determination of amylose in starches or flours. *Carbohydr. Res.* **159**, 154–158. [https://doi.org/10.1016/S0008-6215\(00\)90013-2](https://doi.org/10.1016/S0008-6215(00)90013-2) (1987).

37. Morrison, W. R. & Laignelet, B. An improved colorimetric procedure for determining apparent and total amylose in cereal and other starches. *J. Cereal Sci.* **1**, 9–20. [https://doi.org/10.1016/s0733-5210\(83\)80004-6](https://doi.org/10.1016/s0733-5210(83)80004-6) (1983).
38. Koch, K., Andersson, R. & Aman, P. Quantitative analysis of amylopectin unit chains by means of high-performance anion-exchange chromatography with pulsed amperometric detection. *J. Chromatogr. A* **800**, 199–206 (1998).
39. Zhu, F., Bertoft, E. & Seetharaman, K. Characterization of internal structure of maize starch without amylose and amylopectin separation. *Carbohydr. Polym.* **97**, 475–481. <https://doi.org/10.1016/j.carbpol.2013.04.092> (2013).
40. Kallman, A. *et al.* Starch structure in developing barley endosperm. *Int. J. Biol. Macromol.* **81**, 730–735. <https://doi.org/10.1016/j.ijbiomac.2015.09.013> (2015).
41. Andersson, R., Fransson, G., Tietjen, M. & Åman, P. Content and molecular-weight distribution of dietary fiber components in whole-grain rye flour and bread. *J. Agric. Food Chem.* **57**, 2004–2008. <https://doi.org/10.1021/jf801280f> (2009).
42. Tizzotti, M. J., Sweedman, M. C., Tang, D., Schaefer, C. & Gilbert, R. G. New ¹H NMR procedure for the characterization of native and modified food-grade starches. *J. Agric. Food Chem.* **59**, 6913–6919. <https://doi.org/10.1021/jf201209z> (2011).
43. Armoniemi, R., Odilbekov, F., Vivekanand, V. & Chawade, A. Affordable imaging lab for noninvasive analysis of biomass and early vigour in cereal crops. *Biomed. Res. Int.* <https://doi.org/10.1155/2018/5713158> (2018).
44. Easlon, H. M. & Bloom, A. J. Easy leaf area: Automated digital image analysis for rapid and accurate measurement of leaf area. *Appl. Plant Sci.* <https://doi.org/10.3732/apps.1400033> (2014).

Acknowledgements

We wish to thank Dhananjay Kumar and Aakash Chawade for their support with phenotyping of the green biomass. This work was supported by The Swedish Foundation for Strategic Environmental Research MISTRA, The Swedish Governmental Research program Trees and Crops for the Future (TC4F), Formas, a Swedish government research council for sustainable development (2018-01459) and Lyckebys Research Foundation (Stiftelsen Stärkelsen Forskning Utveckling).

Author contributions

M.A., R.A. and P.H. conceived and designed research. M.A., X.Z., S.J., H.T., A.-S.F., G.N., M.G., N.O. and M.B. designed and conducted experiments. M.A., X.Z., S.J. and G.N. wrote the manuscript. All authors read, edited and approved the manuscript.

Funding

Open Access funding provided by Swedish University of Agricultural Sciences.

Competing interests

The authors declare no competing interests.

Additional information

Supplementary Information The online version contains supplementary material available at <https://doi.org/10.1038/s41598-021-83462-z>.

Correspondence and requests for materials should be addressed to M.A.

Reprints and permissions information is available at www.nature.com/reprints.

Publisher's note Springer Nature remains neutral with regard to jurisdictional claims in published maps and institutional affiliations.



Open Access This article is licensed under a Creative Commons Attribution 4.0 International License, which permits use, sharing, adaptation, distribution and reproduction in any medium or format, as long as you give appropriate credit to the original author(s) and the source, provide a link to the Creative Commons licence, and indicate if changes were made. The images or other third party material in this article are included in the article's Creative Commons licence, unless indicated otherwise in a credit line to the material. If material is not included in the article's Creative Commons licence and your intended use is not permitted by statutory regulation or exceeds the permitted use, you will need to obtain permission directly from the copyright holder. To view a copy of this licence, visit <http://creativecommons.org/licenses/by/4.0/>.

© The Author(s) 2021



GBSS mutations in an *SBE* mutated background restore the potato starch granule morphology and produce ordered granules despite differences to native molecular structure

Shishanthei Jayarathna^{a,*}, Per Hofvander^b, Zsuzsanna Péter-Szabó^c, Mariette Andersson^b, Roger Andersson^a

^a Department of Molecular Sciences, BioCenter, Swedish University of Agricultural Sciences, P.O. Box 7015, SE-750 07 Uppsala, Sweden

^b Department of Plant Breeding, Swedish University of Agricultural Sciences, P.O. Box 190, SE-23422 Lomma, Sweden

^c Division of Glycoscience, Department of Chemistry, KTH-Royal Institute of Technology, SE-10621 Stockholm, Sweden

ARTICLE INFO

Keywords:

Potato starch
Amylose
Amylopectin
Chain length distribution
Building blocks
Gelatinization

ABSTRACT

Potato starch with mutations in starch branching enzyme genes (*SBEI*, *SBEII*) and granule-bound starch synthase gene (*GBSS*) was characterized for molecular and thermal properties. Mutations in *GBSS* were here stacked to a previously developed *SBEI* and *SBEII* mutation line. Additionally, mutations in the *GBSS* gene alone were induced in the wild-type variety for comparison. The parental line with mutations in the *SBE* genes showed a ~40% increase in amylose content compared with the wild-type. Mutations in *GBSS-SBEI-SBEII* produced non-waxy, low-amylose lines compared with the wild-type. An exception was a line with one remaining *GBSS* wild-type allele, which displayed ~80% higher amylose content than wild-type. Stacked mutations in *GBSS* in the *SBEI-SBEII* parental line caused alterations in amylopectin chain length distribution and building block size categories of whole starch. Correlations between size categories of building blocks and unit chains of amylopectin were observed. Starch in *GBSS-SBEI-SBEII* mutational lines had elevated peak temperature of gelatinization, which was positively correlated with large building blocks.

1. Introduction

The main component of potato tubers besides water is starch, which accounts for 15–20% of the weight. Potato starch is composed of two macromolecules, amylose and amylopectin. Amylose is principally a linear chain molecule with a degree of polymerization (DP) in the order of 2000–5000 residues (Hoover, 2001) and accounts for 20–30% of potato starch (Bertoft & Bleppnow, 2016). The highly branched amylopectin molecules are composed of two types of chains, defined as long (L) and short (S), which differentiate at DP 36 (Bertoft, 2017). Other than L and S chains, some starch types were reported to contain extralong amylopectin chains (Hanashiro et al., 2008). Nomenclature of different chain categories of amylopectin as A, B, and C chains was established already in 1952, where A chains are unsubstituted, B chains are substituted with A chains or other B chains, and C chains carry the sole reducing end of the starch macromolecule and otherwise features similar to B chains (Peat et al., 1952).

The latest model used to explain the distribution of chains in

amylopectin molecules is the building block backbone model, according to which the basic structural units of amylopectin are called building blocks (BB) (Bertoft, 2017; Tetlow & Bertoft, 2020). These BB spread out randomly from a backbone composed of a collective arrangement of long amylopectin chains (DP >36). Short amylopectin chains join the backbone to make branches, and also make connections with BB outside the backbone to form external BB. In some cases, these chains may remain as long branches to the backbone (Bertoft, 2017). The BB are made up of approximately 2–12 chains and, based on the number of chains, are grouped as G2 to G6. The G2 type consists of two chains (DP 5–9), G3 consists of three chains (DP 10–14), G4 has four chains (DP 15–19), G5 has on average six chains (DP 20–35), and G6 contains 9–12 chains (DP >35) (Bertoft et al., 2012; Tetlow & Bertoft, 2020).

Starch synthesis is a very complex biological process that involves many enzymes. The main enzymes involved in synthesizing amylose and amylopectin are starch synthases (SS), starch branching enzymes (SBE), and starch de-branching enzymes (DBE) (Tetlow & Bertoft, 2020). In potato, multiple isoforms of SS are present, which are differentiated

* Corresponding author.

E-mail address: shishanthei.jayarathna@slu.se (S. Jayarathna).

<https://doi.org/10.1016/j.carbpol.2024.121860>

Received 8 October 2023; Received in revised form 10 January 2024; Accepted 22 January 2024

Available online 26 January 2024

0144-8617/© 2024 The Authors. Published by Elsevier Ltd. This is an open access article under the CC BY license (<http://creativecommons.org/licenses/by/4.0/>).

based on cDNA and amino acid sequence, i.e. granule bound starch synthase (GBSS), and soluble starch synthases (SSI, SSII, and SSIII), with each isoform having a distinct function in starch synthesis (Nazarian-Firouzabadi & Visser, 2017). GBSS is primarily responsible for amylose synthesis and is also possibly involved in amylopectin synthesis, particularly in the formation of the extra-long unit chain fraction (Nazarian-Firouzabadi & Visser, 2017). In general, SSI and SSII are responsible for synthesizing short to intermediate chains of amylopectin, while SSIII is proposed to synthesize long chains of amylopectin (Tetlow & Emes, 2011; Tetlow & Bertoff, 2020). Among the soluble isoforms of SS, SSIII is the major isoform in potato tubers, accounting for almost 80 % of soluble SS activity (Nazarian-Firouzabadi & Visser, 2017). SBEs attach branches on amylose and amylopectin molecules by cleaving an α -(1,4) bond within the α -glucan chain and transferring it to an α -glucan chain as an α -(1,6)-linked branch chain. There are two isoforms of SBE in potato, SBEI and SBEII, which differ in terms of substrate specificity and length of the α -glucan chains transferred. SBEI transfers amylose and long chains, while SBEII transfers relatively short (DP 6–14) α -glucan chains of amylopectin. DBEs are involved in trimming the amylopectin molecule and determining the final molecular structure of amylopectin (Tetlow & Bertoff, 2020).

Since starch is the main dry-weight component of potato tubers, its functionality is important for subsequent commercial applications of potato starch. New gene-editing technologies such as CRISPR/Cas9 are now being used as an efficient research tool to study gene functions and alter enzymatic pathways by inducing mutations in predefined genes or genetic elements. Altering the starch synthesis pathway by affecting starch synthesis enzymes, particularly SBE and GBSS, by CRISPR/Cas9 has proven to be effective in designing potato starch with distinctive molecular composition and structures to match specific end-uses (Andersson et al., 2017; Tuncel et al., 2019; Zhao et al., 2023; Zhao, Jayarathna, et al., 2021). A previous study by our research group showed that mutations in *SBE* genes generated by the CRISPR/Cas9 technique result in starch with altered chain length distribution and amylose content (Zhao, Jayarathna, et al., 2021). To advance this research further, we hypothesized that targeted mutations by CRISPR/Cas9 in *GBSS*, in addition to in *SBE* genes, would create starch with altered molecular and thermal properties, by altering amylose synthesis by *GBSS* mutagenesis. Therefore, the present study aimed to characterize starch generated through targeted mutations in *SBE* and/or *GBSS* induced using CRISPR/Cas9 technology, and to assess the relationship between molecular properties of the starch and its thermal properties. While conventional breeding techniques have been used in maize to generate or/and characterize amylose extender waxy homozygous genotype starch (Gérard et al., 2000; Yamada et al., 1978), to our knowledge the present study is the first to evaluate molecular properties of potato starch generated through mutations in both *GBSS* and *SBE* genes using CRISPR/Cas9 technology.

2. Materials and methods

2.1. Development of potato lines, greenhouse cultivation, and starch isolation

Mutations were induced in the *GBSS* gene in both a previously generated *SBEI-SBEII* mutational line 104018 (Zhao, Jayarathna, et al., 2021) and the wild-type cultivar Desiree, using PEG-mediated ribonucleoprotein (RNP) transfection of isolated protoplast. Plant tissue culture, protoplast isolation, transfection, regeneration, and mutation screening using high-resolution fragment analysis (HRFA) are described elsewhere (Andersson et al., 2018; Nicolina et al., 2021). The target region in *GBSS* is located in exon 8 of the gene, and a sgRNA, GT2, 5'-TGTGACAAGGGTGTGAAT-3' was used to guide the Cas9 to the target site (Andersson et al., 2017). To confirm the HRFA results and analyze the distribution of mutated alleles, PCR amplification on extracted DNA from the separate event was performed using Phusion

polymerase (Thermo Fisher Scientific, Waltham, USA) with primers 5'-TCTCTGACTTCCTCTTCTCA-3' and 5'-GCAGCAACAAGAA-TATCTGAAC-3' followed by Sanger sequencing (Eurofins Genomics, Ebersberg, Germany) and online ICE analysis (<http://ice.synthego.com>). Five lines with various *GBSS* mutations in the L6 background (L1-L5) and one *GBSS* knockout line (L7) were selected for further studies, together with their parental lines L6 and L8 (Table 1). Cuttings of the lines were planted in a greenhouse and grown between October 7 and January 22 under controlled conditions described elsewhere (Zhao, Jayarathna, et al., 2021). Starch was isolated from the harvested tubers as previously described (Larsson et al., 1996).

2.2. Determination of amylose content

Amylose content was determined on isolated starch fractions, after precipitating the amylopectin fraction, using Concanavalin A according to the assay protocol for the amylose/amylopectin kit (Megazyme, Wicklow, Ireland). All analyses were performed in duplicate and results are presented as mean of duplicates.

2.3. Microscopic analysis of starch granules

Purified starch was stained with Lugol's solution (109261, Merck KGaA, Darmstadt, Germany), diluted 1:1:1 with water and glycerol, and visualized by light microscopy (LeicaDMLB, Leica Microsystems, Wetzlar, Germany) with an assembled camera (Leica DFC450C, Leica Microsystems, Wetzlar, Germany). Polarized light microscopic analysis was performed for starch dispersions as described previously (Zhao, Jayarathna, et al., 2021). Starch dispersions of 50 mg/mL were prepared in distilled water and used to capture images with a 20 \times objective lens under polarized light. A light microscope (Leica DMLB, Wetzlar, Germany) equipped with an infinity X-32 digital camera (DeltaPix, Samourn, Denmark) was used for this purpose.

2.4. Wide angle X-ray diffraction analysis

The crystalline pattern and crystallinity of starch samples were determined by wide-angle X-ray diffraction analysis with Panalytical X'pert Pro. The powder diffractometer was operated at 45 kV and 40 mA, emitting Cu-K α radiation at wavelength 1.54 Å. Diffraction patterns for duplicate samples were recorded between 5 and 40 $^{\circ}$ 2 θ . The degree of crystallinity (CI) was calculated based on the X-ray diffraction diagrams, according to a method described previously (Dome et al., 2020; Liu et al., 2009). A smooth line connecting the minimum diffraction intensities of the X-ray diffractogram was fitted, and the area under the smooth line was considered as the crystalline region. A straight line to connect the total area of 5–40 $^{\circ}$ 2 θ was also fitted. The area between the smooth line and the straight line was taken to represent the amorphous region. Then CI was calculated as the ratio between the crystalline area and the total area above the straight line (which represented both crystalline and amorphous areas).

2.5. Starch structural analysis

Chain length distribution pattern of de-branched starch and BB distribution in whole starch samples were studied. For determination of chain length distribution pattern, the starch samples were solubilized in UDMSO (0.6 M urea in 90 % DMSO), de-branched using isoamylase from *Pseudomonas* sp. (EC 3.2.1.68, 500 U/mL, Megazyme, Wicklow, Ireland) and pullulanase M1 from *Klebsiella planticola* (EC 3.2.1.41, 700 U/mL, Megazyme, Wicklow, Ireland), and studied using high-performance size exclusion chromatography (HPSEC) and high-performance anion exchange chromatography (HPAEC). The enzymes were de-salted through PD-10 desalting columns (Sephadex, Amersham Pharmacia Biotech AB, Uppsala, Sweden), and 10-fold diluted using acetate buffer (0.01 M, pH 5.0) prior to use. For HPSEC, 300 μ L of each ten-fold diluted enzyme (15

Table 1

Size of induced mutations in potato genes *GBSS*, *SBEI*, and *SBEII*. “-” represents deletion, “+” represents insert, and “0” represents wild-type allele. Lines with a “0” have one wild type allele. The lacking indel in *SBE II* means two alleles have the same size of indel.

Line	Breeder's identification	Genetic background	Descriptive sample ID	<i>GBSS</i> (size of indels)	<i>SBEI</i> (size of indels)	<i>SBEII</i> (size of indels)
L1	150172	104018	gbss-IF1	-3; -2; -2; +1	-93; -23; -17; +153	-1; 0; +104
L2	150183	104018	gbss-IF2	-37; -7; -5; -3	-93; -23; -17; +153	-1; 0; +104
L3	150154	104018	gbss-KO1	-5; -4; -2; +1	-93; -23; -17; +153	-1; 0; +104
L4	150068	104018	gbss-KO2	-5; -5; -1; -1	-93; -23; -17; +153	-1; 0; +104
L5	150207	104018	gbss-WTIF	-19; -4; -3; 0	-93; -23; -17; +153	-1; 0; +104
L6	104018	Parental line	GBSS-NA		-93; -23; -17; +153	-1; 0; +104
L7	149108	Desiree	gbss	-2; -1; +1; +1		
L8	Desiree	Wild type	WT			

Descriptive IDs were assigned based on *GBSS* mutations using the following rationale: *gbss-IF* (one in-frame allele), *gbss-KO* (four alleles with out-of-frame mutations), *gbss-WTIF* (one wild-type allele, one in-frame allele), *GBSS-NA* (no mutations for *GBSS*), *gbss* (only *GBSS* mutated), *WT* (wild-type variety). The last digits (1 and 2) of the descriptive IDs for L1-L4 indicate indel size variations between samples. Note: *SBEI* and *SBEII* mutations are consistent in samples L1-L6.

and 21 U respectively from isoamylase and pullulanase) and 400 μ L of acetate buffer (0.01 M, pH 5.0) were mixed with 500 μ L of solubilized starch sample for debranching overnight at 40 °C, followed by 10 min of boiling to terminate the enzyme reaction and filtration through a 0.45 μ m nylon filter. Final starch concentration of the de-branching mixture was 3 mg/mL. For HPAEC, a five-fold diluted sample preparation from HPSEC was used. The HPSEC was equipped with two serially connected OHPak SB-802.5 HQ columns with a guard column (Shodex, Showa Denko KK, Miniato, Japan) kept at 35 °C. The eluent was 0.1 M NaNO₃ containing 0.02 % NaN₃, with a flow rate of 0.5 mL/min. The HPSEC was equipped with a refractive index (RI) detector (Shodex RI-501, Showa Denko KK, Miniato, Japan) and a multiple-angle laser light scattering detector (Wyatt Technology Corp., Santa Barbara, CA). The HPAEC setting and the program were explained by (Zhao, Jayarathna, et al., 2021).

For BB distribution analysis, the BBs were prepared as described by (Zhao, Andersson, & Andersson, 2021) using β -amylase (*E*-BARBL, Megazyme, Wicklow, Ireland) and α -amylase (*E*-BAASS, Megazyme, Wicklow, Ireland). β -amylase was used to remove the linear external chains of amylose and amylopectin, yielding β -limit dextrins (β -LDs). The β -LDs were then hydrolyzed with α -amylase to produce α -limit dextrins (α -LDs), which were treated with β -amylase to remove any remnants of external chains in the resulting BB. The enzymes were then denatured by heating in a boiling water bath, filtered through a membrane filter (0.45 μ m) to isolate the BB, and used for further analysis as described previously (Zhao, Andersson, & Andersson, 2021). Both β -amylase and α -amylase were previously de-salted and diluted as described above.

The BB distribution was studied using HPSEC, with the same settings as described for de-branched chain length distribution pattern analysis.

ASTRA software (version 8.1.2, Wyatt Technology Corp., Santa Barbara, CA) was employed for data analysis of both the chain length distribution pattern of de-branched starch and BB distribution pattern. The presented results represent the mean of two replicates as obtained by RI detector, with the sample blank subtracted to eliminate enzyme and buffer peaks in the elution profiles. For chain length distribution of de-branched starch analysis, the chromatograms were normalized for peak area between 25 and 32 elution minutes and subsequently divided into 4 buckets for further analysis as fractions eluting between 25-26, 26-27, 27-29, and 29-32 min. The BB distribution pattern was normalized between 25 and 34 elution minutes and divided into five groups (G2-G6) as G6: 25.0-26.4, G5: 26.4-27.9, G4: 27.9-29.9, G3: 29.9-31.3, and G2: 31.3-34.3 min for further analysis.

2.6. Analysis of thermal properties

Gelatinization and retrogradation properties of starch were studied using differential scanning calorimetry (DSC) with a DSC250 device (TA Instruments, New Castle, DE, USA) calibrated with indium. Gelatinization onset, peak, and end set temperatures were studied as described

previously (Zhao et al., 2023). Retrogradation properties were studied for crystal melting onset and peak temperatures of retrograded starch. First, 25 mg of starch were cooked with 50 μ L of water at 121 °C for 15 min in sealed high-volume stainless-steel pans in an autoclave-steam sterilizer (Model 2840ELCG-D, Tuttnauer, The Netherlands), to ensure gelatinization of all starch. The gelatinized starches were then stored at 5 °C for three days prior to analysis.

2.7. Statistical analysis

Differences in measured parameters were studied by one-way analysis of variance (ANOVA). Tukey pairwise comparisons, Dunnett's test and Pearson correlation coefficient analysis were performed at confidence level 95 % ($p < 0.05$) using Minitab 21 (State College, PA, USA).

3. Results and discussion

3.1. Mutagenesis of *GBSS* for stacking mutations

Mutations in *GBSS* were induced in potato line 104018, a previously generated *SBEI* and *SBEII* mutational line of the potato cultivar Desiree that has all four alleles of *SBEI* mutated, while *SBEII* has at least one wild-type allele remaining (Zhao, Jayarathna, et al., 2021). The selected stacked lines with additionally induced mutations in *GBSS* resulted in: i) four allele mutational lines having one allele with an in-frame mutation (L1,L2); ii) all four alleles of *GBSS* having out-of-frame mutations (L3, L4); and iii) mutations in three of four alleles (L5) (Table 1). Additionally, one line (L7) with mutations induced only in *GBSS*, with four alleles with out-of-frame mutations, was generated in the Desiree (L8) background (Table 1). CRISPR/Cas9 targets were directed to coding regions of the genes, which means that it is not the expression of the genes per se that is affected but rather the structure of the resulting protein. Out-of-frame mutations will result in a disrupted protein primary structure downstream of the target site while in-frame mutations will result in the loss of one or more amino acids while the rest of the protein will remain as wild type regarding primary protein structure.

3.2. Amylose content

The amylose content, determined through the complex formation between Concanavalin A and amylopectin using an amylose/amylopectin determination kit (Megazyme, Wicklow, Co, Ireland), is depicted in Fig. 1. The highest amylose content was observed for line L5 (49%), followed by L6 (38%). The waxy potato line L7 had the lowest amylose content (3 %). The amylose content of the wild-type L8 was 27 %.

The high amylose content in L6 was attributed to the mutations in the *SBEs*. As elucidated by Zhong et al. (2022, 2023), high-amylose starches are frequently generated by inhibiting pivotal enzymes in the amylopectin biosynthesis pathway, resulting in a decrease in the amylopectin proportion and an increase in the amylose proportion. In

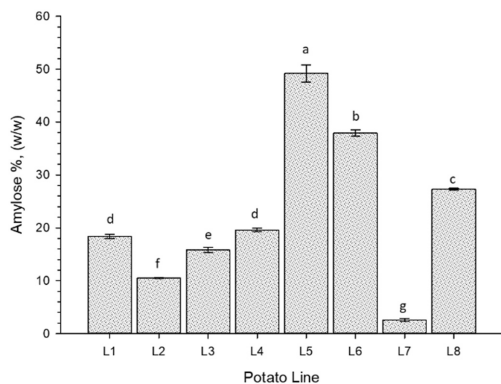


Fig. 1. Amylose content of starches from potato lines L1-L8 measured based on complex formation between Concanavalin A and amylopectin. Values shown are the mean of two technical replicates, error bars indicate standard deviation, and different letters on bars indicate statistically significant differences as analyzed by Turkey comparison ($p < 0.05$). L1: gbss -1F1, L2: gbss -1F2, L3: gbss -K01, L4: gbss -K02, L5: gbss -WT1F, L6: GBSS-NA, L7: gbss, L8: WT.

addition to the enhancement of amylose content through the inhibition of amylopectin biosynthesis, it is highly probable that these inhibitions also exert an influence on the structural composition of the amylopectin chains. High amylose or amylose-only starch in crops with down-regulated or mutated *SBEs* has been reported previously for both cereal and tuber starches (Carciofi et al., 2012; Huang et al., 2015; Li et al., 2019; Zhao et al., 2018; Zhao, Jayarathna, et al., 2021). Therefore, high amylose feature of starch in *SBE*-suppressed crops can have two explanations. First, suppressing the activity of *SBE* could reduce the amount of amylopectin, thereby increasing the relative proportion of amylose. Second, suppression of *SBE* activity could reduce the frequency of branching of amylopectin, inhibiting the introduction of α -1,6-linkages into starch and promoting formation of long amylose-like chains of amylopectin (Seung, 2020; Zhong et al., 2022, 2023).

The method of amylose determination using Concanavalin A is based on the principle described by Yun and Matheson (1990). Amylopectin was first precipitated with lectin Concanavalin A as a complex, and the supernatant containing amylose was enzymically hydrolyzed to *D*-glucose and analyzed using glucose oxidase/peroxidase reagent. As described by Matheson and Welsh (1988), Concanavalin A forms complexes with glucan polymers through interacting with the non-reducing ends of glucan polymers. These interactions and associations are less frequent with amylose, since it has much fewer non-reducing ends than amylopectin. Therefore, the molecular structure of these glucan polymers plays a crucial role in determining complex formation with Concanavalin A. Considering the method of determination, amylopectin with altered molecular structure with more long chains with fewer branches runs a risk of not complexing with Concanavalin A and ending up in the supernatant, where it can later be detected as amylose.

The high amylose content identified in line L5 may be attributed to the existence of a wild-type allele in the *GBSS* gene. Consequently, amylose production could occur nearly as normal, given the residual activity of the *GBSS* enzyme. This suggests that presence of only one wild-type allele is enough for reaching almost the same level of *GBSS* enzyme as in native potatoes. Besides the amylose produced by the *GBSS* enzyme, mutations in *SBE* genes, which inhibit the branching of amylopectin, may also contribute to the total amylose content of line L5. An interesting observation was that L5 exhibited a higher amylose content (49 %) compared to L6 (38%), even with mutations induced in three out of four *GBSS* alleles in L6. This could suggest an altered activity

of other enzymes, besides *GBSS*, building long chains in an *SBE* suppressed background. Furthermore, additional factors, such as the downregulation of amylopectin production enzymes, may impact the ratio between amylose and amylopectin. These factors could play a role in determining amylose content independently of the activity of the *GBSS* enzyme. A deeper study of L5 is needed to elucidate the mechanisms behind this effect.

All other lines (L1-L4) had a lower amylose content than L6, which can be linked to the mutations in the *GBSS* gene. However, even with complete knockout of the *GBSS* gene, L3 and L4 still had an amylose content of 20 % and 16 %, respectively. This indicates probable compensation for the role of *GBSS* by other active enzymes in starch synthesis when *GBSS* is simultaneously mutated in an *SBE*-suppressed background, or synergistic effects of different starch biosynthetic enzyme isoforms. Synergy between different isoforms of *SS* and *SBE* has been discussed previously, e.g., the substrate for a particular isoform might be the product of another (Smith, 1999). Altered expression of one isoform might then cause alteration in the substrate for another isoform, which might lead to production of structures that are abnormal (i.e., amylose-like glucan chains in a *GBSS*-knocked out *SBE* mutated background). The amylose content of *GBSS*-knocked out lines L3-L4 lines might also be attributable to the function of *SSIII* in an *SBE*-suppressed background. It is proposed that *SSIII* synthesizes long amylopectin chains (Tetlow & Emes, 2011; Tetlow & Bertoft, 2020) but in an *SBE* mutated background these chains will have lower branching frequency with fewer non-reducing ends to make complexes with Concanavalin A, and will be detected later as amylose. Further experiments are needed to confirm this.

When only *GBSS* is mutated, without suppressing the *SBEs*, the plant can no longer produce amylose and this results in waxy phenotypes such as line L7. In a previous study where mutations were induced in all four alleles of *GBSS* using the CRISPR/Cas9 technique, two different methods were used to measure the amylose content, which was found to be 0 % when determined by the perchloric acid method and 4.4 % based on the Megazyme kit method (Toinga-Villafuerte et al., 2022).

3.3. Starch granule morphology

Iodine staining of non-waxy and waxy starches showed specific blue-black and red-brown color, respectively (Seguchi et al., 2000), attributable to the presence or absence of apparent amylose. In agreement, lines L5, L6, and L8, with normal or high amylose content, stained blue, the *GBSS* knockout line (L7) stained pale red-brown, and the low-amylose lines L1 and L2 with in-frame mutations in *GBSS* stained pale purple (Fig. 2). However, starch from lines L3 and L4, with *GBSS* fully knocked out and *SBE* mutated, also stained pale purple, although some granules of L3 stained dark blue at the hilum (Fig. 2). Iodine staining of granules from *GBSS* knockouts, particularly in an *SBE* mutated background, could be attributable to the affinity of iodine to long amylopectin chains with reduced branching frequency. It could also be partly explained by starch granule formation starting from the hilum (Seung & Smith, 2019) and by *SSIII* synthesizing long amylopectin chains (Tetlow & Bertoft, 2020; Tetlow & Emes, 2011) which, with reduced branching frequency in an *SBE* mutated background, might show affinity to iodine complexation. It has been shown that *SSIII* may play a role in starch granule initiation in *Arabidopsis* (Szydlowski et al., 2009), and may also do so in potato tuber starch.

Under the light microscope, the iodine-stained starch revealed significant differences in granule morphology between the different potato lines (Fig. 2). Alterations in potato starch granule morphology as affected by Cas9-mediated mutagenesis in genes involved in starch synthesis has been observed previously (Tuncel et al., 2019; Zhao, Jayarathna, et al., 2021). The potato line L6 (parent to L1-L5), with mutations in only the *SBE* genes, had a highly altered granule phenotype compared with native potato starch, e.g., the starch granules were more irregular in shape and had rough surfaces (Fig. 2). Irregular shape of

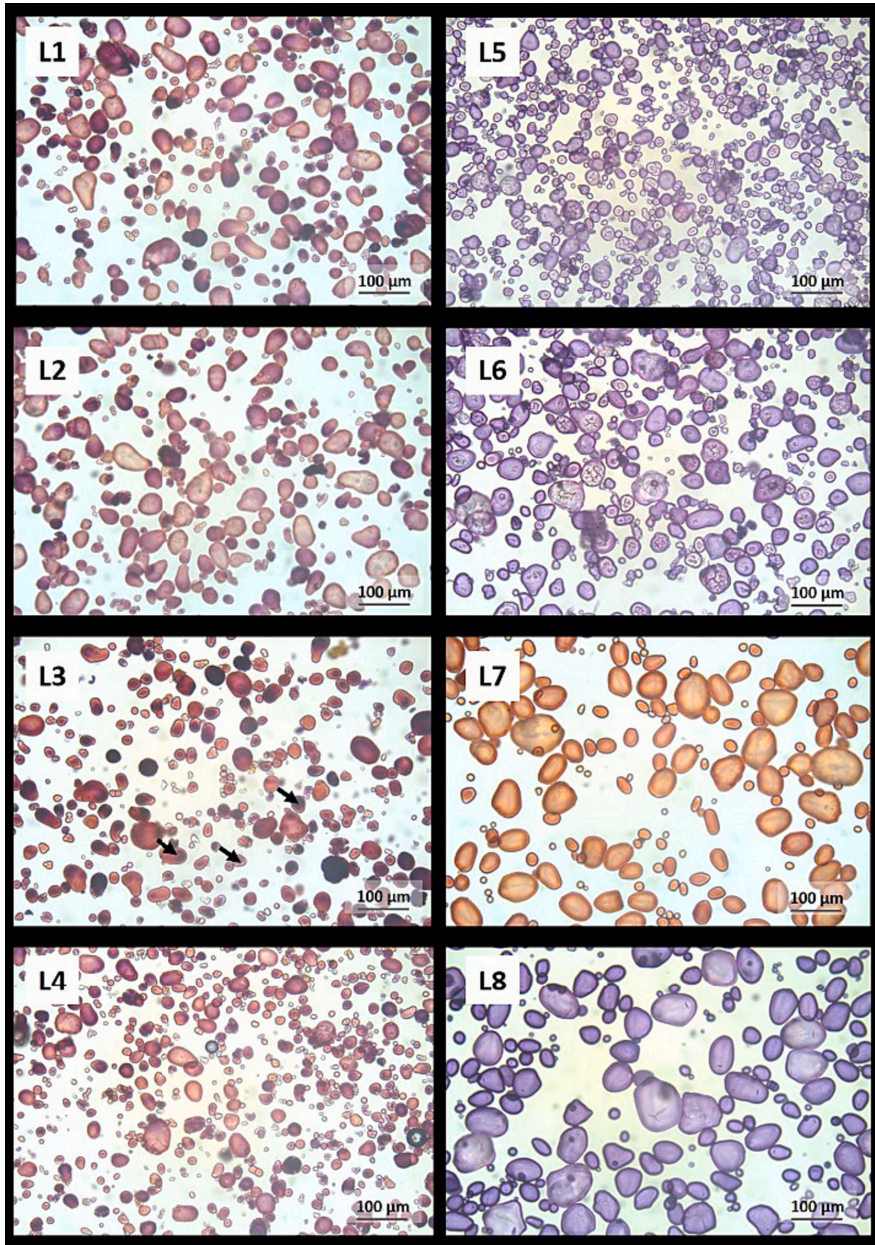


Fig. 2. Morphology of starch granules in potato lines L1-L8 stained with iodine and visualized under light microscope. Black arrows in L3 indicate the stained hilum area in dark blue. L1: gbss -IF1, L2: gbss -IF2, L3: gbss -KO1, L4: gbss -KO2, L5: gbss -WTIF, L6:GBSS-NA, L7: gbss, L8:WT.

starch granules in L6, but in a different greenhouse cultivation period, was observed in our previous study (Zhao, Jayarathna, et al., 2021). Interestingly, introducing mutations in *GBSS*, in addition to the *SBE* genes, restored the granule phenotype to a considerable extent in lines L1–L4, generating granules with nearly oval shapes and smooth surfaces (Fig. 2). However, L5 had similar granule morphology to the parental line L6, most likely owing to presence of an unmutated *GBSS* allele in L5. The *GBSS* enzyme is usually present in surplus and the presence of an unmutated allele in the *GBSS* gene might be sufficient to produce starch granules with similar morphology to those in *GBSS* unmutated potato line L6. As seen in a previous study (Zhao, Jayarathna, et al., 2021), mutations in *SBEs* alter starch granule morphology significantly. However, starch granule morphology is reported not to be affected by knocking down the *GBSS* gene (Brummell et al., 2015), as observed here for granule morphology of the *GBSS*-knocked out line L7. However, in the present study stacking mutations in *GBSS* in an *SBE*-mutated background was able to restore starch granule morphology somewhat (in L1–L4), which could be due to the individual effect of mutations of *GBSS* or a combined effect of the mutations.

3.4. Polarized light microscopy

In general, most starch granules show Maltese cross birefringence pattern when studied under polarized light microscope which indicate a radial arrangement of crystallites (Pérez et al., 2009). In agreement, all starches studied under the polarized light microscope showed Maltese crosses but with differences in appearance (Fig. 3). Starch granules from the wild-type potato (L8) showed very clear Maltese cross birefringence patterns, as reported previously for native potato starches (Tuncel et al., 2019; Zhao, Jayarathna, et al., 2021). Waxy potato starch (L7) showed similar Maltese crosses to L8, while L5 and the parental line L6 did not show clear Maltese crosses at the center of the granules (Fig. 3). As explained by French (1984), the intensity of birefringence appears to depend on the granule thickness, crystallinity and orientation of the crystallites. Hence, the reduced intensity of Maltese crosses observed in the starch from L5 and L6 may be ascribed to alteration of any of the aforementioned factors.

3.5. X-ray diffraction pattern and degree of crystallinity

As expected for tuber starch, starch from all potato lines displayed a B-type X-ray diffraction pattern (Fig. 4), with main peaks at 15° (broad), and 17° (strong), and a doublet at 22–24° for 2θ (Zhao et al., 2018; Zhao, Jayarathna, et al., 2021). Therefore, none of the targeted mutations altered the crystalline pattern of the starches. However, variations in CI were observed (Table 2). According to previous studies, the CI of native potato starch is around 20–25% (dos Santos et al., 2016), while the total crystallinity of waxy potato starch is 30.01 ± 0.11% (Jiranuntakul et al., 2011). The CI values obtained in the present study were close to previously reported values. Dunnett's multiple comparison, taking L8 as the control sample, revealed that potato starches from lines L2, L5, and L7 grouped with L8, with lower CI than starch from the other lines. Among those lines with a lower CI, line L5 displayed the lowest CI value (24.6%), which could be due to the large increase in amylose content lowering the relative content of amylopectin, the fraction responsible for the crystallinity of starch granules.

3.6. Chain length distribution of debranched starch

HPSEC and HPAEC were used to investigate the chain-length distribution pattern of de-branched starches. In the HPSEC chromatogram (Fig. 5a), the fraction eluting after 25 min is associated with chains originating from the amylopectin molecules, while the peaks eluting before 25 min are associated with chains from amylose molecules. Based on the HPSEC results, all mutant potato lines (L1–L6) showed substantially different chain length distribution pattern compared with the

wild-type L8 for both amylose and amylopectin fractions, while the amylopectin fraction in the *GBSS*-knockout L7 was similar to that in L8 (Fig. 5a). On comparing the chain length distribution patterns of lines with mutations in both *SBEs* and *GBSS* (L1–L5) with that of their parental line with mutations only in *SBEs* (L6), substantial changes to the amylose fraction were observed. Long chains eluting between 22 and 23 min were observed only for L8, L6, and L5 (Fig. 5a). This could be attributed to a certain chain category of amylose. The same lines all stained blue in color with iodine (Fig. 2), which indicates that molecules eluting at 22–23 min were responsible for the color shift in iodine from red-brownish to blue in those samples. An interesting observation was a peak of around 24 min in all the samples. Compared with the wild-type L8 and *GBSS* mutated L7, the 24-min peak was more prominent in all lines with *SBE* mutations. In a previous study, we also observed a prominent peak of such amylose component in *SBE* mutated lines compared with a wild-type line (Zhao, Jayarathna, et al., 2021). Comparing the chain length distribution to the granule phenotype and coloring from the iodine staining (Fig. 2), the molecules eluting in this region were likely responsible for the pale purple staining in *GBSS*-knocked out lines in an *SBE* mutated background. Taking into account the prominent peak observed approximately at 24 min in *SBE* mutated lines, coupled with the diminished iodine binding capacity of the constituent eluting at around 24 min, it may also be recognized as a constituent of high-amylose starch formed due to restrained *SBE* activity. This phenomenon has been denoted as amylose-like material, as explained by Zhong et al. (2022). Further, lines L4 and L3 had a similar amylose chain length distribution pattern, as did lines L1 and L2. From this observation, it can be concluded that the chain length distribution pattern of the amylose fraction in potato starch is determined systematically and may be related to the type of mutation.

However, the chain distribution pattern of the amylopectin fraction in lines L1–L5 was mostly closer to that of L6 for all lines except for L5. This suggests that activity of the intact wild-type allele of *GBSS* in L5 not only increased the proportion of amylose in starch but also had a small effect on the molecular structure of amylose and amylopectin polyglucans in an *SBE* mutated background. A contribution of *GBSS* enzyme activity in determining amylopectin molecular structure has been reported previously (Brummell et al., 2015), with authors suggesting that reduced activity of *GBSS* may have some small effects on amylopectin structure, besides enhanced amylopectin content of potato starch.

The molar proportion distribution of starch from different potato lines, analyzed by HPAEC, is shown in Fig. 5b. In agreement with previous findings (Zhao, Jayarathna, et al., 2021), starch from L8 showed a dominant broad peak of amylopectin chains spanning DP ~9–33, but with a shift in the highest molar proportion of chains to DP 13 instead of DP 11. The Waxy L7 line, with mutations only in *GBSS*, had a very similar chain length distribution pattern of the amylopectin fraction as L8. All other lines showed substantial differences in amylopectin chain length distribution pattern compared with L8.

Differences in the abundance of different categories of amylopectin unit chains in the different lines were apparent from both the HPSEC and HPAEC results (Table 3). Interestingly, high-amylose line L5 showed the highest abundance of the longest amylopectin fractions (fractions eluting between 25 and 26 min and 26–27 min in HPSEC analysis, B2 and B3 chains in HPAEC analysis) and the lowest abundance of short amylopectin fractions (fractions eluting between 27 and 29 min and 29–32 min in HPSEC analysis, A chains in HPAEC analysis). Therefore, L5 revealed a very interesting starch type with high amylose content and long amylopectin chains.

Tukey pairwise comparisons for the normalized amylopectin fraction eluted between 25 and 32 min in HPSEC analysis revealed no difference in abundance or distribution pattern of amylopectin chain fractions between L8 and waxy L7. Therefore, knocking out only the *GBSS* gene did not affect the distribution pattern or abundance of different categories of amylopectin fractions. This observation was further supported by Tukey pairwise comparisons of the different chain categories for the

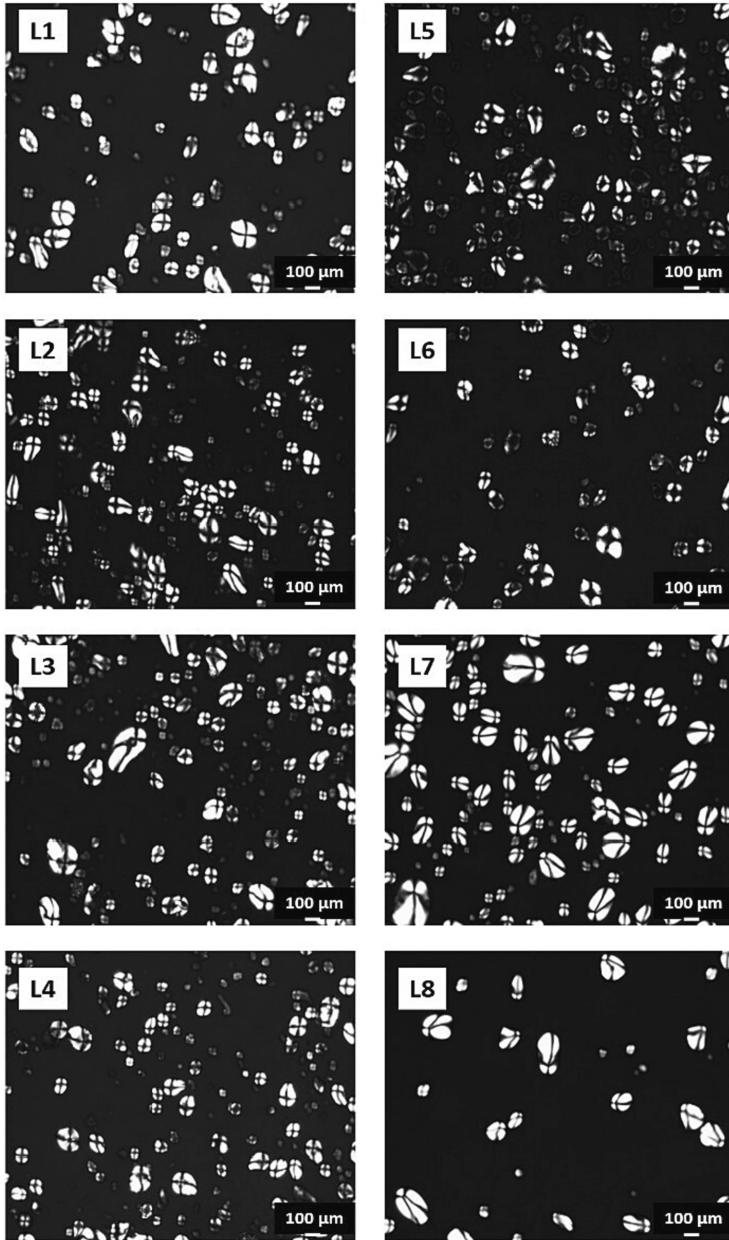


Fig. 3. Polarized light microscopy images of potato lines L1-L8. L1: gbss -IF1, L2: gbss -IF2, L3: gbss -KO1, L4: gbss -KO2, L5: gbss -WTIF, L6:GBSS-NA, L7: gbss, L8:WT.

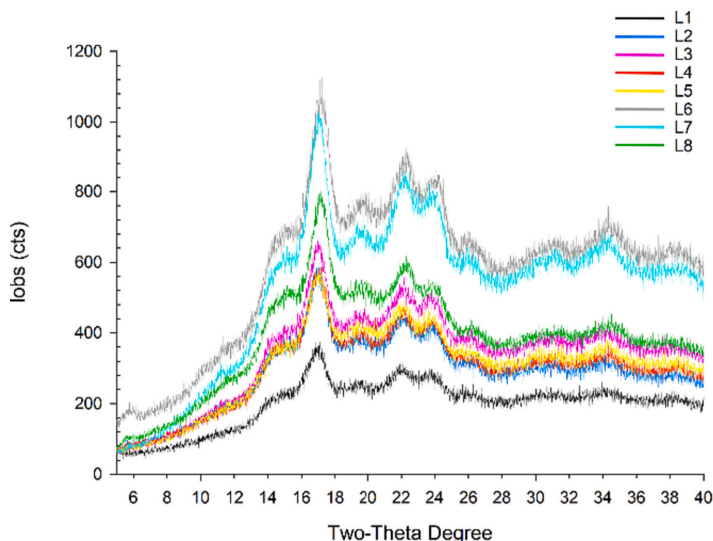


Fig. 4. X-ray diffraction patterns of starches from the experimental potato lines L1-L7 and reference variety L8. Diffraction intensity values are the mean of two replicates. L1: gbss -IF1, L2: gbss -IF2, L3: gbss -KO1, L4: gbss -KO2, L5: gbss -WTIF, L6:GBSS-NA, L7: gbss, L8:WT.

Table 2

Crystallinity degree (Cl, %) of starches from potato lines L1-L8. L1: gbss -IF1, L2: gbss -IF2, L3: gbss -KO1, L4: gbss -KO2, L5: gbss -WTIF, L6:GBSS-NA, L7: gbss, L8:WT.

Potato line	Cl %
L1	34.4 ± 0.1
L2	29.7 ± 2.3
L3	32.5 ± 2.1
L4	31.3 ± 0.3
L5	24.6 ± 0.4
L6	30.6 ± 0.7
L7	28.7 ± 0.1
L8	26.1 ± 1.7

molar proportion distributions in HPAEC analysis (Table 3). Similar chain length distribution of the short amylopectin fraction (up to DP 35) between a wild-type potato line and *GBSS* antisense lines has been reported previously (Fulton et al., 2002).

However, differences in the abundance of different amylopectin unit chain categories compared with L8 were observed in many of the lines evaluated in the present study, indicating that simultaneous mutations in *GBSS* together with *SBE* genes could result in starch with altered structure in the amylopectin fraction. It is of interest to note the influence of the *GBSS* gene in determining amylopectin molecular structure in an *SBE* mutated background.

Further, Pearson correlation analysis revealed a positive correlation between amylose content and B3 chains of amylopectin. Positive correlations between long amylopectin chains and amylose content have been reported previously for other types of starches (Lin et al., 2022; Wang et al., 2018). As reviewed by Wang et al. (2017), and as mentioned previously in this paper, crops deficient in *SBE* activity not only tend to produce more amylose, but also produce amylopectin enriched with long branches. This might be the reason for the positive correlation between amylose content and B3 chains in the present study.

Dunnnett multiple comparison of the HPSEC results for lines L1-L5,

taking parental L6 line as the control sample, revealed differences in the abundance of different amylopectin unit chains except for the peaks eluted at 27–29 min (data not shown). This could be explained by the fact that both molecular structure and relative amounts of glucan polymers are affected by the mutations. Individual variations in *GBSS* mutations in an *SBE* mutated background could have a significant impact on chain length distribution of the amylopectin fraction, where a remaining wild-type allele in *GBSS* (L5) could produce long amylopectin glucan chains in an *SBE* mutated background.

3.7. Starch internal structure at the building block level

The distribution of building blocks (BB) was studied using HPSEC. In the HPSEC chromatogram (Fig. 6), the BB distributions were divided into five groups (G6-G2) for further analysis. The chromatogram also included the linear dextrin produced during BB preparation. The BB distribution displayed two clear distribution patterns that were attributed to samples with and without mutations in the *SBE* genes. The Waxy L7 line, with only mutation in *GBSS*, had a similar BB distribution to wild-type L8. There were some individual variations in the abundance of different groups of BB, as shown in Table 4, which can be attributable to the type of mutations induced.

Mutations only in *GBSS* (potato line L7) had no influence in determining the size distribution of BB, which grouped with the wild-type L8. Mutations only in *SBEs* (line L6) caused alterations in the size distribution of BB compared with wild-type L8, proving that mutations in *SBE* play a significant role in starch fine structure at BB level (Table 4).

There was a trend for large (G6 and G5) and medium-sized (G4) BBs to be present in comparatively higher abundance in lines L1, L4, and L5, while the small BBs (G3 and G2) were least abundant in those lines. This is an interesting observation and indicates that BB size is determined in a systematic way. There were variations in some BB group categories between the lines with various *GBSS* mutations in the L6 background line (L1-L5) and the parental line L6 (Table 4). This provides the important insight that gene *GBSS* has an influence in determining the abundance of different size categories of BB in an *SBE* mutated

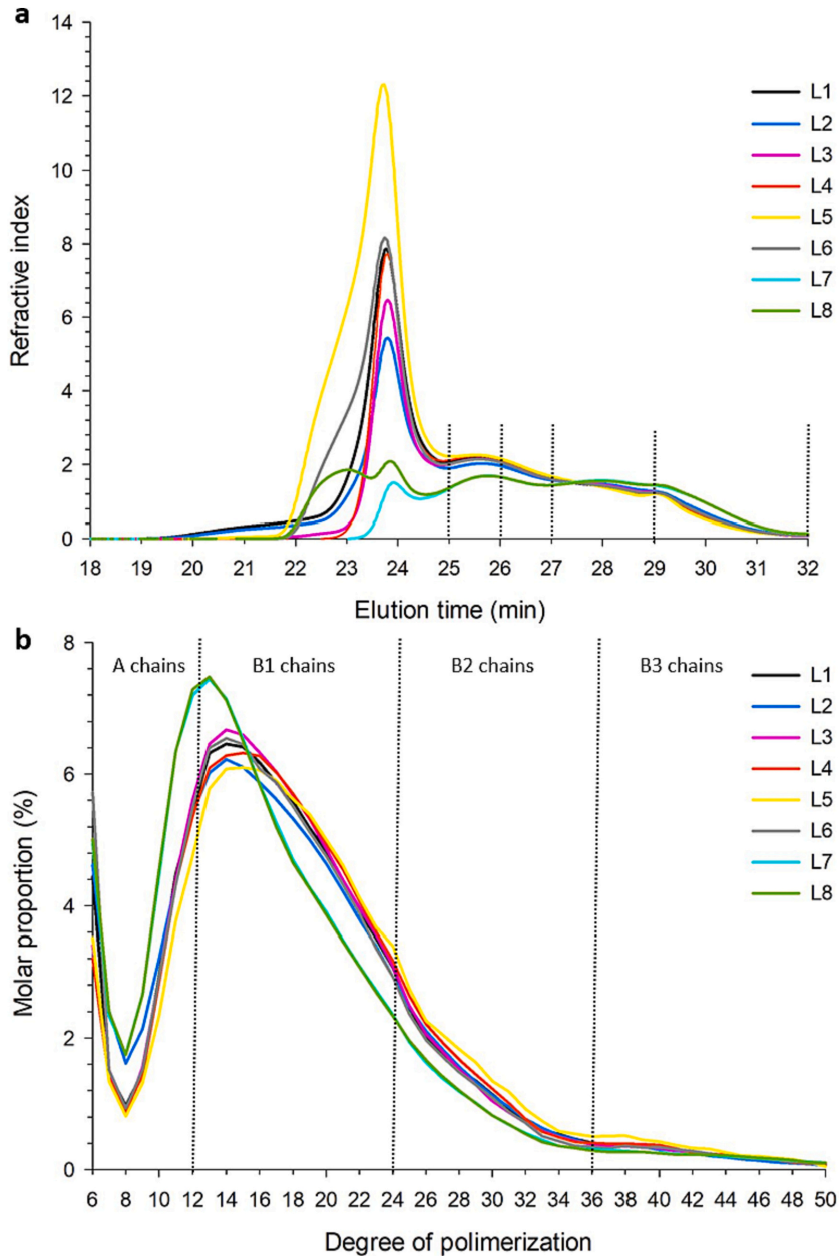


Fig. 5. Chain-length distribution of debranched starches from potato lines L1-L8, analyzed (a) by HPSEC on a relative weight basis after normalization for the amylopectin peak area (25–32 min), (b) by HPAEC on a relative molar basis with the degree of polymerization (DP) 6–50. In the HPSEC chromatogram (a), the amylopectin fraction eluted after 25 min is bucketed into several buckets marked by dash lines as fractions eluting between 25 and 26, 26–27, 27–29, and 29–32 min. In the HPAEC analysis (b), amylopectin chains were categorized according to [Hanashiro et al. \(1996\)](#) as A chains (DP 6–12), B1 chains (DP 13–24), B2 chains (DP 25–36), and B3 chains (DP ≥37). L1: gbss -IF1, L2: gbss -IF2, L3: gbss -KO1, L4: gbss -KO2, L5: gbss -WTIF, L6: GBSS-NA, L7: gbss, L8: WT.

Table 3

Abundance of amylopectin chain categories in potato lines L1-L8, analyzed by HPSEC and HPAEC. HPSEC categorization was based on elution minutes (as shown in Fig. 5a), presented as refractive index area on a relative weight basis. HPAEC analysis categorized amylopectin chains as indicated in Fig. 5 (B) and presented as molar proportions (%). Significantly different values within cells are denoted by different superscript letters (ANOVA, $\alpha = 0.05$). L1: gbss -IF1, L2: gbss -IF2, L3: gbss -KO1, L4: gbss -KO2, L5: gbss -WTIF, L6:GBSS-NA, L7: gbss, L8:WT.

	Amylopectin chain category							
	25.00–26.00 min		26.01–27.00 min		27.01–29.00 min		29.01–32.00 min	
HPSEC analysis	L5	274 ^a	L5	232 ^a	L7	367 ^a	L8	254 ^a
	L4	269 ^b	L4	226 ^b	L8	365 ^a	L7	253 ^a
	L1	261 ^c	L1	222 ^b	L2	351 ^b	L2	191 ^b
	L3	258 ^c	L6	221 ^b	L3	346 ^{bc}	L6	179 ^{bc}
	L6	258 ^c	L3	220 ^b	L6	342 ^{bc}	L1	178 ^{bc}
	L2	244 ^d	L2	214 ^c	L1	339 ^c	L3	175 ^c
	L7	196 ^e	L8	184 ^d	L4	338 ^c	L4	168 ^{cd}
	L8	196 ^e	L7	184 ^d	L5	336 ^c	L5	157 ^d
HPAEC analysis	B3 chains		B2 chains		B1 chains		A chains	
	L5	4.1 ^a	L5	16.3 ^a	L3	62.9 ^a	L8	30.0 ^a
	L4	3.4 ^b	L4	14.8 ^{ab}	L4	62.4 ^a	L7	29.7 ^a
	L6	3.2 ^b	L2	14.1 ^{ab}	L5	61.7 ^a	L2	23.7 ^b
	L1	3.2 ^b	L1	13.9 ^{ab}	L1	61.7 ^a	L6	22.4 ^b
	L3	3.2 ^b	L3	13.7 ^b	L6	61.2 ^a	L1	21.2 ^b
	L2	3.0 ^b	L6	13.2 ^b	L2	51.2 ^a	L3	20.2 ^b
	L7	2.9 ^b	L8	10.7 ^c	L7	56.8 ^a	L4	19.5 ^b
	L8	2.9 ^b	L7	10.7 ^c	L8	56.5 ^a	L5	18.8 ^b

background.

Pearson correlation analysis revealed an interesting correlation between different size categories of BB and different chain categories of amylopectin (HPAEC results) (Fig. 7). The large BB (G4, G5, and G6) showed a strong negative correlation with A chains, while the small BB (G2 and G3) showed a strong positive correlation. The large BB (G4, G5, G6) showed positive correlation with B1, B2, and B3 chains, while the smaller BB (G3, G2) showed a negative correlation.

Table 4

Variation in the normalized peak area of different size groups (G6-G2) of building block distributions in potato lines L1-L8. Values within columns with different superscript letters differ significantly (ANOVA, $\alpha = 0.05$). L1: gbss -IF1, L2: gbss -IF2, L3: gbss -KO1, L4: gbss -KO2, L5: gbss -WTIF, L6:GBSS-NA, L7: gbss, L8:WT.

Potato line	Building block group				
	G6	G5	G4	G3	G2
L1	17.3 ^{ab}	85.6 ^b	356.7 ^b	121.3 ^c	419.1 ^d
L2	12.1 ^c	70.6 ^d	320.1 ^d	141.6 ^b	455.6 ^b
L3	14.4 ^{bc}	79.3 ^c	345.8 ^c	128.5 ^c	432.1 ^c
L4	19.4 ^a	90.7 ^a	365.7 ^b	120.6 ^d	403.6 ^c
L5	14.9 ^{bc}	88.2 ^{ab}	382.2 ^a	112.2 ^e	402.5 ^c
L6	13.2 ^c	79.1 ^c	347.3 ^c	132.1 ^c	428.3 ^{cd}
L7	2.1 ^d	24.5 ^e	189.3 ^c	199.6 ^a	584.5 ^a
L8	2.9 ^d	26.9 ^e	195.5 ^c	197.0 ^a	577.7 ^a

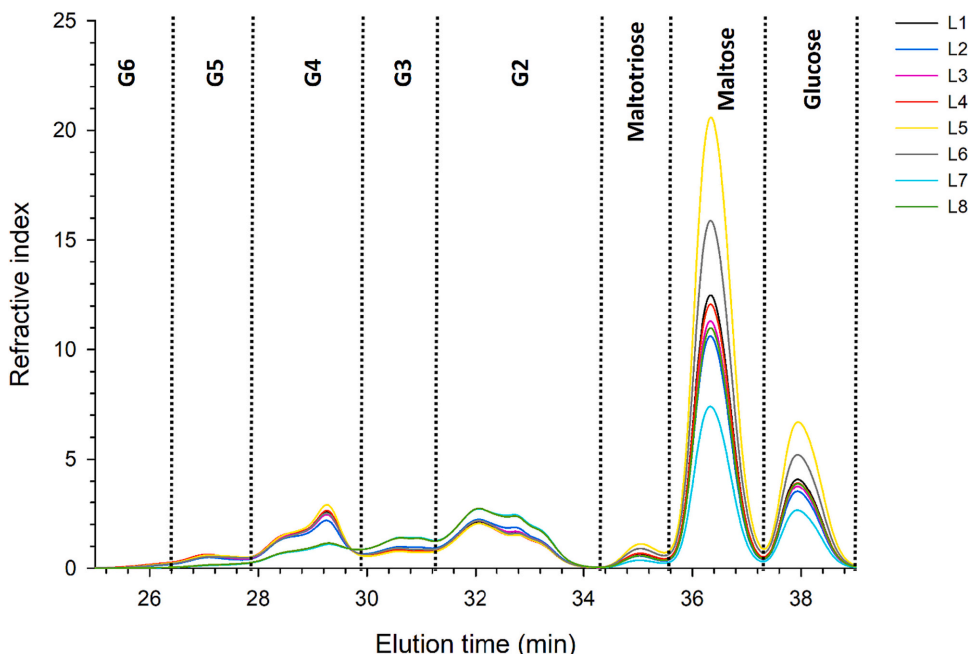


Fig. 6. Building block distribution in starch from potato lines L1-L8 after normalization for peak area, as determined by HPSEC. Normalization was performed for the area between 25 and 34 elution minutes. The distribution was bucketed in groups as G6: elution time 25.0–26.4, G5: 26.4–27.9, G4: 27.9–29.9, G3: 29.9–31.3, G2: 31.3–34.3 min. L1: gbss -IF1, L2: gbss -IF2, L3: gbss -KO1, L4: gbss -KO2, L5: gbss -WTIF, L6:GBSS-NA, L7: gbss, L8:WT.

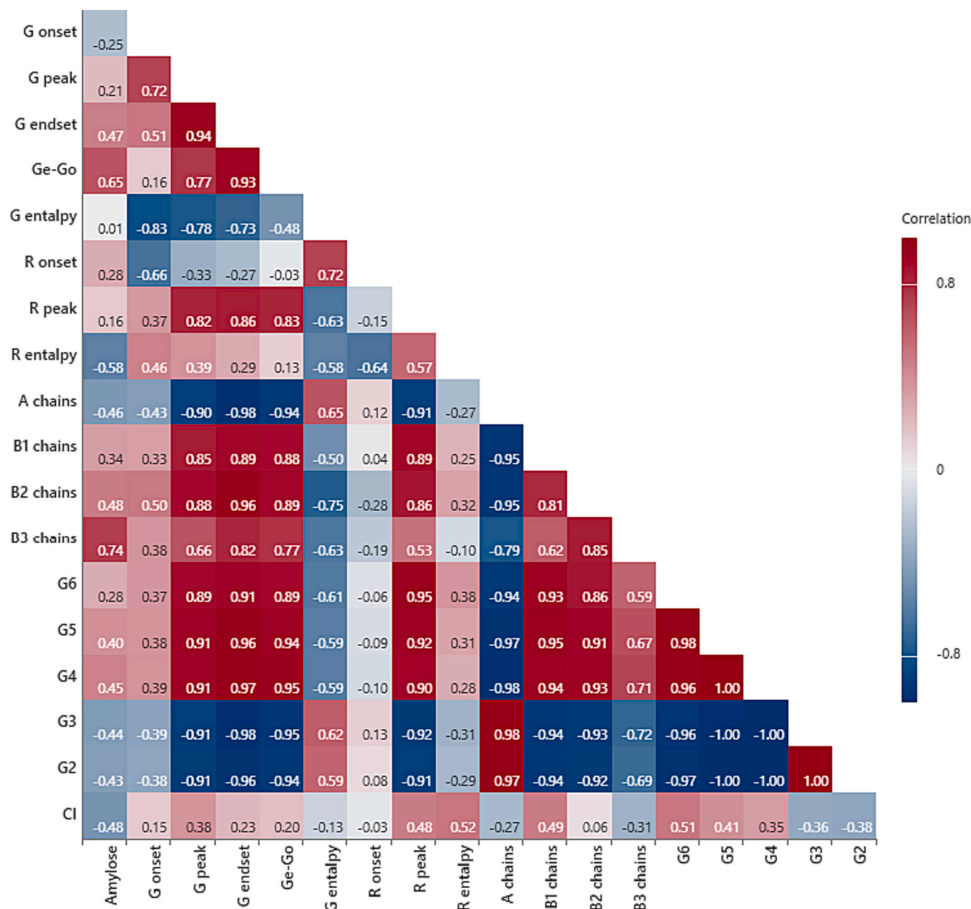


Fig. 7. Heat map of Pearson correlation results. G onset - gelatinization onset temperature, G peak - gelatinization peak temperature, G endset - gelatinization end set temperature, Ge-Go - gelatinization temperature range, R onset - retrogradation onset temperature, R peak - retrogradation peak temperature, R enthalpy - retrogradation enthalpy, A, B1, B2, B3 - amylopectin unit chains, G6-G2 - different size categories of building blocks, Cl degree of crystallinity (%).

3.8. Thermal properties

3.8.1. Gelatinization properties

The gelatinization onset temperature (T_o) of starch from the different lines varied from 67.0 to 68.8 °C (Table 5). Line L8, with a higher proportion of shorter amylopectin chains (i.e., A chains from HPAEC analysis) showed the lowest T_o , peak temperature (T_p), and end set temperature (T_e). Line L5, with the highest proportion of long chains (i.e., B2 and B3 chains from HPAEC analysis) showed the highest T_o , T_p , and T_e values. This is in agreement with previous findings of low gelatinization temperature for samples with a high proportion of short amylopectin chains, and vice versa (Gomand et al., 2010). However, it is of interest to note that waxy line L7 also had high T_o , in agreement with previous findings of increases in potato starch T_o of around 4 °C when GBSS is silenced (Brummell et al., 2015). All the potato starches with mutations in SBEs, with or without mutation in GBSS, showed higher gelatinization temperatures than wild-type L8. This agrees with previous

Table 5

Gelatinization properties of starches from potato lines L1-L8. L1: gbss -IF1, L2: gbss -IF2, L3: gbss -KO1, L4: gbss -KO2, L5: gbss -WTIF, L6:GBSS-NA, L7: gbss, L8:WT.

Sample	T_o (°C)	T_p (°C)	T_e (°C)	$T_e - T_o$ (°C)	ΔH J/g (amylopectin)
L1	67.5 ^c	75.8 ^b	85.3 ^b	17.7 ^{ab}	16.0 ^{cd}
L2	68.4 ^b	75.4 ^b	83.4 ^b	15.0 ^c	16.7 ^{cd}
L3	67.7 ^c	75.3 ^b	84.1 ^b	16.4 ^{bc}	17.8 ^{bc}
L4	68.4 ^b	76.9 ^a	85.2 ^b	16.8 ^{bc}	16.0 ^{cd}
L5	68.5 ^{ab}	76.8 ^a	87.8 ^a	19.2 ^a	15.1 ^d
L6	67.0 ^d	75.3 ^b	84.0 ^b	17.0 ^{bc}	19.5 ^{ab}
L7	68.8 ^a	72.8 ^c	78.7 ^c	9.9 ^e	17.4 ^{bcd}
L8	64.8 ^e	69.3 ^d	77.4 ^c	12.6 ^d	20.7 ^a

T_o - onset temperature, T_p - peak temperature, T_e - end set temperature, ΔH - gelatinization enthalpy (calculated as J/g amylopectin). Values within columns with different superscript letters differ significantly (ANOVA, $\alpha = 0.05$).

reports of a $\sim 5^\circ\text{C}$ increment in T_p of starch from potato tubers with low SBE activity (Safford et al., 1998). From Pearson correlation analysis (Fig. 7), it was apparent that T_o , T_p , and T_e and the gelatinization temperature range (T_e - T_o) had strong negative correlations with A chains and positive correlations with B1, B2, and B3 chains of the amylopectin fraction. As reviewed by Zhong et al. (2023), amylopectin with DP 6–12 (referred as A chains in the present study) may introduce defects to the crystals, leading to the formation of starch granules with reduced gelatinization temperatures. This could potentially explain the observed negative correlation between A chains and gelatinization temperatures. Further, these gelatinization parameters were strongly positively correlated with large BB of G4, G5, and G6, and negatively correlated with small BB of G2 and G3, in agreement with (Zhao et al., 2023). A negative correlation between T_e and A chains has been reported previously for maize starch (Lin et al., 2022). The gelatinization temperature range (T_e - T_o) of waxy L7 was significantly lower ($p < 0.05$) than that of all other samples, possibly due to the fact that this line produced more uniform starch granules than the other samples. The fact that T_e - T_o was highest for L5 may be due to the huge variation in granule morphology seen in the light microscopy images (Fig. 2).

Gelatinization enthalpy (ΔH) (corrected for amylopectin) was highest for wild-type L8, but with no significant difference compared with L6, which had the second highest ΔH value. In general, ΔH is an indicator of loss of molecular order within the granule, and gives an overall measure of quality and quantity of granule crystallinity. Introducing mutations might have negatively affected the molecular organization of starch granules, as represented by lower ΔH in all mutant lines than in L8. Pearson correlation analysis (Fig. 7) revealed a positive relationship of ΔH to A chains and a negative relationship to B chains. Even though both CI and crystal melting ΔH of starch are associated with the crystalline arrangement inside the starch granules, the trend in CI of starch samples from all lines except L5 did not follow the trend observed for ΔH of the starch samples. As discussed by Lourdin et al. (2015), it is not possible to use starch melting enthalpy to determine crystallinity, since numerous other processes such as plasticization, swelling in water, competition between melting, dissolution in water etc., are involved in melting. According to those authors, residual melting enthalpy should be used for relevant interpretations, but quantitative correlations with crystallinity cannot be made (Lourdin et al., 2015).

3.8.2. Retrogradation properties

Gelatinized starch undergoes a disorder-to-order transition defined as retrogradation. Starch retrogradation in lines L1-L8 was characterized by determining the Onset (T_o) and peak (T_p) temperatures of crystal melting and enthalpy change of retrograded starch gels (ΔH) after storage at 4°C . However, an endothermic transition of retrograded starch reflects both melting of residual crystallites after gelatinization and recrystallized starch formed during retrogradation (Wang et al., 2016).

Table 6

Retrogradation properties of starches from potato lines L1-L8. L1: gbss -IF1, L2: gbss -IF2, L3: gbss -KO1, L4: gbss -KO2, L5: gbss -WTIF, L6:GBSS-NA, L7: gbss, L8:WT.

Sample	T_o ($^\circ\text{C}$)	T_p ($^\circ\text{C}$)	ΔH J/g (amylopectin)
L1	40.0 ^e	74.0 ^{ab}	10.6 ^{ab}
L2	40.0 ^e	73.0 ^{ab}	11.0 ^a
L3	42.5 ^{ab}	74.2 ^{ab}	10.2 ^{abc}
L4	43.3 ^a	75.0 ^a	9.8 ^{abc}
L5	40.3 ^{bc}	73.2 ^{ab}	9.3 ^{abc}
L6	44.0 ^f	70.8 ^{bc}	8.4 ^c
L7	40.3 ^{bc}	67.3 ^d	9.5 ^{abc}
L8	44.0 ^f	68.3 ^{cd}	8.8 ^{bc}

T_o - retrogradation onset temperature, T_p - retrogradation peak temperature, ΔH - retrogradation enthalpy. Values within columns with different superscript letters differ significantly (ANOVA, $\alpha = 0.05$).

The highest T_p values were obtained for line L4, with no significant differences to lines L1, L2, L3 and L5 (Table 6). This is an interesting relationship of T_p to type of mutation where T_p raised by at least 5°C in both GBSS and SBE mutated lines compared with L8. In Pearson correlation analysis (Fig. 7), a strong positive correlation of T_p with large BB (G4, G5, and G6) and a strong negative correlation with small BB (G2, G3) was observed. Correlations between BB size categories and retrogradation parameters have been reported previously (Zhao et al., 2023).

Retrogradation enthalpy (ΔH) was measured as enthalpy of the endotherm, and essentially reflected melting of ordered amylopectin. The highest ΔH value was obtained for L2, but it differed only from L8 and L6. There was an interesting trend for mutation in the GBSS gene to raise ΔH in the GBSS mutated lines (L1-L5, L7) compared with L8 and L6.

4. Conclusions

Mutations in SBE genes altered starch granule morphology from mostly oval-shaped, smooth granules to uneven granules with rough surfaces. However, stacking mutations in all four alleles of GBSS restored the granule phenotype to a considerable extent. Knocking out GBSS in an SBE mutated background decreased the measured amylose content (w/w) in starch from 38 % to around 20 %, while a waxy starch phenotype generated by individual knock-out of GBSS contained 3 % amylose. In addition to affecting amylose content, the enzyme GBSS played a role in determining the molecular structure of amylose in an SBE mutated background. Mutations only in GBSS had no significant impact in determining chain length and building block distribution pattern. However, mutations in GBSS influenced the abundance of different amylopectin unit chain categories and size distribution of whole starch building blocks in an SBE mutated background. The whole starch building block size categories were correlated with the abundance of different unit chains of amylopectin and with the thermal properties of the starch. The novel starch types, distinguished by their unique molecular and thermal properties, offer significant opportunities for application in both food and non-food domains. For example, L5, with its notable high amylose content and long amylopectin chains likely facilitate retrogradation and, shows promise as a potential resistant starch for healthier food components. Moreover, the increased gelatinization temperatures of SBE mutated lines could prove valuable in contexts favouring delayed gelatinization, while the increased retrogradation temperatures of SBE + GBSS mutated lines might be preferable in both food and non-food applications, enhancing sensory qualities and material properties, respectively. However, further studies are recommended to comprehensively explore the potential applications of these novel starch types.

CRedit authorship contribution statement

Shishanthi Jayarathna: Writing – review & editing, Writing – original draft, Visualization, Validation, Software, Methodology, Investigation, Formal analysis, Data curation, Conceptualization. **Per Hofvander**: Writing – review & editing, Methodology, Investigation, Funding acquisition, Data curation. **Zsuzsanna Péter-Szabó**: Writing – review & editing, Methodology, Investigation, Data curation. **Mariette Andersson**: Writing – review & editing, Supervision, Project administration, Methodology, Investigation, Funding acquisition, Formal analysis, Data curation, Conceptualization. **Roger Andersson**: Writing – review & editing, Supervision, Project administration, Funding acquisition, Conceptualization.

Declaration of competing interest

The authors declare that they have no known competing financial interests or personal relationships that could have appeared to influence the work reported in this paper.

Data availability statement

The original contributions presented in the study are included in the article, further inquiries can be directed to the corresponding author.

Acknowledgements

Henrik Hansson and Janicka Nilsson are acknowledged for technical support with HPAEC and HPSEC analysis, respectively. Ann-Sofie Fält, Niklas Ollson, and Helle Turesson are acknowledged for support with genome editing and genetic analyses. Graphical abstract was created using BioRender.com. This study was (partially) funded by Trees and Crops for the Future (TC4F), a Strategic Research Area at the Swedish University of Agricultural Sciences (SLU) supported by the Swedish Government and Formas-Swedish Research Council for Sustainable Development (grant number 2018-01459).

References

- Andersson, M., Turesson, H., Nicolai, A., Fält, A.-S., Samuelsson, M., & Hofvander, P. (2017). Efficient targeted multiallelic mutagenesis in tetraploid potato (*Solanum tuberosum*) by transient CRISPR-Cas9 expression in protoplasts. *Plant Cell Reports*, *36*, 117–128.
- Andersson, M., Turesson, H., Ollson, N., Fält, A.-S., Ohlsson, P., Gonzalez, M. N., ... Hofvander, P. (2018). Genome editing in potato via CRISPR-Cas9 ribonucleoprotein delivery. *Physiologia Plantarum*, *164*, 378–384.
- Bertoff, E. (2017). *Understanding starch Structure: Recent progress*. *Agronomy*, *7*, 56.
- Bertoff, E., & Blennow, A. (2016). Chapter 3—Structure of potato starch. In J. Singh, & L. Kaur (Eds.), *Advances in potato chemistry and technology* (2nd ed., pp. 57–73). San Diego: Academic Press.
- Bertoff, E., Koch, K., & Åman, P. (2012). Structure of building blocks in amylopectins. *Carbohydrate Research*, *361*, 105–113.
- Brummel, D. A., Watson, L. M., Zhou, J., McKenzie, M. J., Hallett, I. C., Simmons, L., ... Timmerman-Vaughan, G. M. (2015). Overexpression of starch branching enzyme II increases short-chain branching of amylopectin and alters the physicochemical properties of starch from potato tuber. *BMC Biotechnology*, *15*, 28.
- Carciofi, M., Blennow, A., Jensen, S. L., Shaik, S. S., Henriksen, A., Buléon, A., ... Hebelstrup, K. H. (2012). Concerted suppression of all starch branching enzyme genes in barley produces amylose-only starch granules. *BMC Plant Biology*, *12*, 223.
- Dome, K., Podgorbunskikh, E., Bychkov, A., & Lomovsky, O. (2020). Changes in the crystallinity degree of starch having different types of crystal structure after mechanical pretreatment. *Polymers*, *12*, 641.
- dos Santos, T. P. R., Leonel, M., Garcia, E. L., do Carmo, E. L., & Franco, C. M. L. (2016). Crystallinity, thermal and pasting properties of starches from different potato cultivars grown in Brazil. *International Journal of Biological Macromolecules*, *82*, 144–149.
- French, D. (1984). Chapter VII - organization of starch granules. In R. L. Whistler, J. N. Bemiller, & E. F. Paschall (Eds.), *Starch: Chemistry and technology* (2nd ed., pp. 183–247). San Diego: Academic Press.
- Fulton, D. C., Edwards, A., Pilling, E., Robinson, H. L., Fahy, B., Seale, R., ... Smith, A. M. (2002). Role of granule-bound starch synthase in determination of amylopectin structure and starch granule morphology in potato. *Journal of Biological Chemistry*, *277*, 10834–10841.
- Gérard, C., Planchot, V., Colonna, P., & Bertoff, E. (2000). Relationship between branching density and crystalline structure of A- and B-type maize mutant starches. *Carbohydrate Research*, *326*, 130.
- Gomand, S. V., Lamberts, L., Derde, L. J., Goesaert, H., Vandeputte, G. E., Goderis, B., ... Delcour, J. A. (2010). Structural properties and gelatinisation characteristics of potato and cassava starches and mutants thereof. *Food Hydrocolloids*, *24*, 307–317.
- Hanashiro, I., Abe, J., & Hizukuri, S. (1996). A periodic distribution of the chain length of amylopectin as revealed by high-performance anion-exchange chromatography. *Carbohydrate Research*, *283*, 151–159.
- Hanashiro, I., Itoh, K., Kuratomi, Y., Yamazaki, M., Igarashi, T., Matsugasako, J., & Takeda, Y. (2008). Granule-bound starch synthase I is responsible for biosynthesis of extra-long unit chains of amylopectin in Rice. *Plant and Cell Physiology*, *49*, 925–933.
- Hoover, R. (2001). Composition, molecular structure, and physicochemical properties of tuber and root starches: A review. *Carbohydrate Polymers*, *45*, 253–267.
- Huang, J., Shang, Z., Man, J., Liu, Q., Zhu, C., & Wei, C. (2015). Comparison of molecular structures and functional properties of high-amylose starches from rice transgenic line and commercial maize. *Food Hydrocolloids*, *46*, 172–179.
- Jiranuntakul, W., Puttanlek, C., Rungsardthong, V., Pancha-arnon, S., & Uttapap, D. (2011). Microstructural and physicochemical properties of heat-moisture treated waxy and normal starches. *Journal of Food Engineering*, *104*, 246–258.
- Larsson, C.-T., Hofvander, P., Khoshnoodi, J., Ek, B., Rask, L., & Larsson, H. (1996). Three isoforms of starch synthase and two isoforms of branching enzyme are present in potato tuber starch. *Plant Science*, *117*, 9–16.
- Li, H., Dhital, S., Slade, A. J., Yu, W., Gilbert, R. G., & Gidley, M. J. (2019). Altering starch branching enzymes in wheat generates high-amylose starch with novel molecular structure and functional properties. *Food Hydrocolloids*, *92*, 51–59.
- Lin, L., Zhao, S., Li, E., Guo, D., & Wei, C. (2022). Structural properties of starch from single kernel of high-amylose maize. *Food Hydrocolloids*, *124*, Article 107349.
- Liu, Q., Donner, E., Tarn, R., Singh, J., & Chung, H.-J. (2009). Chapter 8—Advanced analytical techniques to evaluate the quality of potato and potato starch. In J. Singh, & L. Kaur (Eds.), *Advances in potato chemistry and technology* (pp. 221–248). San Diego: Academic Press.
- Lourdin, D., Putaux, J.-L., Potocki-Véronèse, G., Chevigny, C., Rolland-Sabaté, A., & Buléon, A. (2015). Crystalline structure in starch. In Y. Nakamura (Ed.), *Starch: Metabolism and structure* (pp. 61–90). Tokyo: Springer Japan.
- Matheson, N. K., & Welsh, L. A. (1988). Estimation and fractionation of the essentially unbranched (amylose) and branched (amylopectin) components of starches with concanavalin A. *Carbohydrate Research*, *180*, 301–313.
- Nazarian-Firouzabadi, F., & Visser, R. G. F. (2017). Potato starch synthases: Functions and relationships. *Biochemistry and Biophysics Reports*, *10*, 7–16.
- Nicolai, A., Fält, A.-S., Hofvander, P., & Andersson, M. (2021). Protoplast-based method for genome editing in tetraploid potato. In P. Tripodi (Ed.), *Crop breeding: Genetic improvement methods* (pp. 177–186). New York, NY: Springer US.
- Peat, S., Whelan, W., & Thomas, G. J. (1952). Evidence of multiple branching in waxy maize starch. *Journal of The Chemical Society (Resumed)*, 4546–4548. Retrieved from <https://www.semanticscholar.org/paper/Evidence-of-multiple-branching-in-waxy-maize-starch-Peat-Whelan/47d3c5d5f521cddc06a92856fde6dc1122e59e1>.
- Pérez, S., Baldwin, P. M., & Gallant, D. J. (2009). Chapter 5—Structural features of starch granules I. In J. BeMiller, & R. Whistler (Eds.), *Starch* (3rd ed., pp. 149–192). San Diego, USA: Academic Press.
- Safford, R., Jobling, S. A., Sidebottom, C. M., Westcott, R. J., Cooke, D., Tober, K. J., ... Gidley, M. J. (1998). Consequences of antisense RNA inhibition of starch branching enzyme activity on properties of potato starch. *Carbohydrate Polymers*, *35*, 155–168.
- Seguchi, M., Yasui, T., Hosomi, K., & Imai, T. (2000). Study of internal structure of waxy wheat starch granules by KI/2 solution. *Cereal Chemistry*, *77*, 339–342.
- Seung, D. (2020). Amylose in starch: Towards an understanding of biosynthesis, structure and function. *New Phytologist*, *228*, 1490–1504.
- Seung, D., & Smith, A. M. (2019). Starch granule initiation and morphogenesis—Progress in Arabidopsis and cereals. *Journal of Experimental Botany*, *70*, 771–784.
- Smith, A. M. (1999). Making starch. *Current Opinion in Plant Biology*, *2*, 223–229.
- Szydłowski, N., Ragel, P., Raynaud, S., Lucas, M. M., Roldán, I., Montero, M., ... Mérida, Á. (2009). Starch granule initiation in Arabidopsis requires the presence of either class IV or class III starch synthases. *The Plant Cell*, *21*, 2443–2457.
- Tetlow, I. J., & Emes, M. J. (2011). 4-05 - starch biosynthesis in higher plants: The enzymes of starch synthesis. In M. Moo-Yung (Ed.), *Comprehensive biotechnology* (2nd ed., pp. 47–65). Burlington: Academic Press.
- Tetlow, I. J., & Bertoff, E. (2020). A review of starch biosynthesis in relation to the building block-backbone model. *International Journal of Molecular Sciences*, *21*, 7011.
- Toinga-Villafuerte, S., Vales, M. I., Awika, J. M., & Rathore, K. S. (2022). CRISPR/Cas9-mediated mutagenesis of the granule-bound starch synthase gene in the potato variety Yukon gold to obtain amylose-free starch in tubers. *International Journal of Molecular Sciences*, *23*, 4640.
- Tunçel, A., Corbin, K. R., Ahn-Jarvis, J., Harris, S., Hawkins, E., Smedley, M. A., ... Smith, A. M. (2019). Cas9-mediated mutagenesis of potato starch-branching enzymes generates a range of tuber starch phenotypes. *Plant Biotechnology Journal*, *17*, 2259–2271.
- Wang, J., Hu, P., Chen, Z., Liu, Q., & Wei, C. (2017). Progress in high-amylose cereal crops through inactivation of starch branching enzymes. *Frontiers in Plant Science*, *8*. Retrieved from <https://www.frontiersin.org/articles/10.3389/fpls.2017.00469>.
- Wang, J., Hu, P., Lin, L., Chen, Z., Liu, Q., & Wei, C. (2018). Gradually decreasing starch branching enzyme expression is responsible for the formation of heterogeneous starch granules. *Plant Physiology*, *176*, 582–595.
- Wang, S., Li, C., Zhang, X., Copeland, L., & Wang, S. (2016). Retrogradation enthalpy does not always reflect the retrogradation behavior of gelatinized starch. *Scientific Reports*, *6*, 20965.
- Yamada, T., Komiya, T., Akaki, M., & Taki, M. (1978). A novel type of corn starch from a strain of maize. Part 3. The properties of the starch from Amylo-waxy maize and its hybrids with waxy maize. *Starch - Stärke*, *30*, 145–148.
- Yun, S.-H., & Matheson, N. K. (1990). Estimation of amylose content of starches after precipitation of amylopectin by Concanavalin-A. *Starch - Stärke*, *42*, 302–305.
- Zhao, X., Andersson, M., & Andersson, R. (2018). Resistant starch and other dietary fiber components in tubers from a high-amylose potato. *Food Chemistry*, *251*, 58–63.
- Zhao, X., Andersson, M., & Andersson, R. (2021). A simplified method of determining the internal structure of amylopectin from barley starch without amylopectin isolation. *Carbohydrate Polymers*, *255*, Article 117503.
- Zhao, X., Hofvander, P., Andersson, M., & Andersson, R. (2023). Internal structure and thermal properties of potato starches varying widely in amylose content. *Food Hydrocolloids*, *135*, Article 108148.
- Zhao, X., Jayarathna, S., Turesson, H., Fält, A.-S., Nestor, G., González, M. N., ... Andersson, M. (2021). Amylose starch with no detectable branching developed through DNA-free CRISPR-Cas9 mediated mutagenesis of two starch branching enzymes in potato. *Scientific Reports*, *11*, 4311.
- Zhong, Y., Qu, J. Z., Liu, X., Ding, L., Liu, Y., Bertoff, E., ... Blennow, A. (2022). Different genetic strategies to generate high amylose starch mutants by engineering the starch biosynthetic pathways. *Carbohydrate Polymers*, *287*, Article 119327.
- Zhong, Y., Tai, L., Blennow, A., Ding, L., Herburger, K., Qu, J., ... Liu, X. (2023). High-amylose starch: Structure, functionality and applications. *Critical Reviews in Food Science and Nutrition*, *63*, 8568–8590.



High fructan barley lines produced by selective breeding may alter β -glucan and amylopectin molecular structure

Shishanthi Jayarathna^{a,*}, Yunkai Jin^b, Gleb Dotsenko^{a,1}, Mingliang Fei^{b,c,d},
Mariette Andersson^e, Annica A.M. Andersson^a, Chuanxin Sun^b, Roger Andersson^a

^a Department of Molecular Sciences, BioCenter, Swedish University of Agricultural Sciences, P.O. Box 7015, SE-750 07 Uppsala, Sweden

^b Department of Plant Biology, BioCenter, Swedish University of Agricultural Sciences, P.O. Box 7080, SE-750 07 Uppsala, Sweden

^c Key Laboratory of Crop Epigenetic Regulation and Development in Hunan Province, Hunan Agricultural University, Changsha 410128, China

^d Key Laboratory of Education Department of Hunan Province on Plant Genetics and Molecular Biology, College of Bioscience and Biotechnology, Hunan Agricultural University, Changsha 410128, China

^e Department of Plant Breeding, Swedish University of Agricultural Sciences, P.O. Box 190, SE-234 22 Lomma, Sweden

ARTICLE INFO

Keywords:

Fructan
Starch
 β -Glucan
Amylopectin
Building block structure

ABSTRACT

Six cross-bred barley lines developed by a breeding strategy with the target to enhance the fructan synthesis activity and reduce the fructan hydrolysis activity were analyzed together with their parental lines, and a reference line (Gustav) to determine whether the breeding strategy also affected the content and molecular structure of amylopectin and β -glucan. The highest fructan and β -glucan content achieved in the novel barley lines was 8.6 % and 12 %, respectively (12.3-fold and 3.2-fold higher than in Gustav). The lines with low fructan synthesis activity had higher starch content, smaller building blocks in amylopectin, and smaller structural units of β -glucan than the lines with high-fructan synthesis activity. Correlation analysis confirmed that low starch content was associated with high amylose, fructan, and β -glucan content, and larger building blocks in amylopectin.

1. Introduction

Barley (*Hordeum vulgare*) was one of the first domesticated crops, and the main component of barley grain is starch. It is also rich in dietary fiber and attracting growing interest as a healthy food (Baik & Ullrich, 2008; Sullivan, Arendt, & Gallagher, 2013). There are two major components in barley dietary fiber, mixed linkage (1 \rightarrow 3, 1 \rightarrow 4)- β -D-glucan (β -glucan) and arabinoxylan. The β -glucan content typically ranges from 3 % to 7 % (Oscarsson, Andersson, Salomonsson, & Åman, 1996) and the molecular structure of the β -glucan plays a vital role in determining its functionality (Du, Meenu, Liu, & Xu, 2019). The arabinoxylan content in barley typically varies from 4 % to 11 % (Oscarsson et al., 1996). Cellulose, fructan, and lignin are among the minor components of barley dietary fiber.

Since the main component of barley endosperm is starch, the quality of barley-based foods could be affected by the quality of the starch (Zhu, 2017). The molecular structure, composition, and amylose:amylopectin

ratio in starch play a vital role in determining the quality of the starch for food and non-food applications. In general, barley starch contains 20–25 % amylose and 70–75 % amylopectin (Morrison, Milligan, & Azudin, 1984), although the amylose content depends on the method of determination. Barley amylose is a linear molecule with molecular weight 1.03×10^5 g/mol, compared with 1.15×10^6 g/mol for highly branched amylopectin (Bello-Pérez, Rodríguez-Ambríz, Agama-Acevedo, & Sanchez-Rivera, 2009). The properties of starch have been shown to be affected by amylopectin molecular structure and amylose:amylopectin ratio (e.g., Källman et al., 2015; Vamadevan & Bertoft, 2015; Vamadevan & Bertoft, 2018; Zhao, Hofvander, Andersson, & Andersson, 2023; Zhu, 2018; Zhu & Liu, 2020).

A building block (BB) backbone model is currently used to describe the distribution of chains in amylopectin molecules (Bertoft, 2017; Tetlow & Bertoft, 2020). BBs, which are the basic structural units of amylopectin, are tightly branched and distributed along the long chains of amylopectin. The BBs are made up of approximately 2–11 chains,

* Corresponding author.

E-mail addresses: shishanthi.jayarathna@slu.se (S. Jayarathna), yunkai.jin@slu.se (Y. Jin), mariette.andersson@slu.se (M. Andersson), annica.andersson@slu.se (A.A.M. Andersson), chuanxin.sun@slu.se (C. Sun), roger.andersson@slu.se (R. Andersson).

¹ Present address: Laboratory of Evolutionary Genomics, Vavilov Institute of General Genetics, Russian Academy of Sciences, Moscow, Russia.

<https://doi.org/10.1016/j.carbpol.2023.121030>

Received 17 February 2023; Received in revised form 8 May 2023; Accepted 14 May 2023

Available online 16 May 2023

0144-8617/© 2023 The Authors. Published by Elsevier Ltd. This is an open access article under the CC BY license (<http://creativecommons.org/licenses/by/4.0/>).

with the number of chains increasing proportionally with increasing BB size (Bertoft, Koch, & Åman, 2012). BBs contribute directly in determining the physical properties of starch such as gelatinisation and retrogradation properties (Källman et al., 2015; Zhao et al., 2023). Therefore, information regarding BBs contributes to determining the end uses of particular starch types and the knowledge can be utilized by plant breeders to tailor starches that are, for example, more stable for freeze-thaw cycles.

Barley is one of the most genetically diverse cereals, which provides ample opportunities for breeders to identify and produce novel varieties for specific end uses (Baik & Ullrich, 2008). For example, when barley is bred for human consumption, high β -glucan content in grain is preferred since high β -glucan is favorable to reduce blood cholesterol and risk of colorectal cancer (Kerckhoffs, Hornstra, & Mensink, 2003). Therefore, improving grain β -glucan content has become one of the foci in barley breeding programs (e.g., Ehrenbergerová et al., 2008; Steele et al., 2013). High fructan content is an advantage in edible dietary fiber, since fructan and fructooligosaccharides are standard prebiotics with beneficial health effects and considered as a low calorie healthy food and feed ingredient (Bosscher, 2009; Ritsema & Smeekens, 2003; Roberfroid, 2007; Roberfroid et al., 2010). Fructans also play a role in protecting plants against stress factors such as drought and freezing (Benkeblia, 2022; Livingston, Hinch, & Heyer, 2009).

In barley carbon allocation between starch and fructan is regulated via sugar signaling in barley (SUSIBA) transcription system where SUSIBA2 is a transcription factor which induces starch synthesis, and SUSIBA1 is a negative transcription factor which inhibits fructan synthesis. The presence of SUSIBA2 and SUSIBA1 forms a carbon competing system in barley that could be employed for the barley breeding (Jin et al., 2017). In a recent study, a cross-breeding strategy was applied to produce barley lines with enhanced fructan content by upregulating fructan synthesis activity and downregulating fructan hydrolysis activity (Fei et al., 2022). During breeding, the SUSIBA transcription system (Jin et al., 2017) was used as a molecular marker for progeny screening as described by Fei et al. (2022). In parallel with artificial screening for high-fructan lines, starch content was modified based on the function of the SUSIBA system in regulating carbon allocation (Fei et al., 2022; Jin et al., 2017; Sun et al., 2003). Moreover, an interesting correlation between fructan and β -glucan in high fructan barley lines was already revealed by Fei et al. (2022) (with Pearson correlation coefficient (r) of 0.9121), showing the possibility of producing barley lines with simultaneous high fructan and β -glucan.

In the present study, starch and β -glucan from the high-fructan barley lines and their parents were chemically characterized, to test the hypothesis that the function of the SUSIBA system in regulating carbon allocation affects the content, composition, and molecular structure of starch and β -glucan, in addition to the fructan content.

2. Materials and methods

2.1. Development of cross-bred barley lines

Barley plants were cultivated in phytotrons, with conditions of 9 h light ($300 \mu\text{mol m}^{-2} \text{s}^{-1}$) at 12°C , 15 h darkness at 8°C , 60 % relative humidity for the first 4 weeks, and then to 16 h light ($400 \mu\text{mol m}^{-2} \text{s}^{-1}$) at 20°C , 8 h darkness at 12°C , and 70 % relative humidity until maturation. Barley crossing was performed according to Pöhlman and Slexer (2013) and as explained by Fei et al. (2022). In brief, SW 28708 (line 224, Lantmännen, Sweden) was used as the maternal to cross with KVL 1113 (line 199, Royal Veterinary and Agricultural University, Denmark) and SLU 7 (line 155, Swedish University of Agricultural Sciences), and KVL 1113 was used as the maternal to cross with SW 49368 (line 235, Lantmännen, Sweden). All the parental lines were genetically homozygous. The flat seed phenotype was correlated with high fructan content, so in the selection process flat seed phenotype was used as a screening marker of high-fructan grain to increase the speed of screening

high fructan lines (Fei et al., 2022). After three-generations of inbreeding the F₄ progeny of barley lines with unique flat seeds (Fig. S1) were screened and used in further analyses unless otherwise stated.

The selection of parental lines was based on the fructan content of the developing barley grains at 9 day after flowering (daf), 22 daf and at maturity respectively and the fructan level reduction between 22 daf and maturity (Table 1 and Fei et al. (2022)). As measured by Fei et al. (2022), lines 155 and 199 accumulated high amount of fructan during the developmental stages of 9 daf to maturity and reach >3 % at mature stage, while lines 224 and 235 accumulated low level of fructan than 155 and 199 at mature stage. The fructan level decrease between 22 daf and maturity were highest in 199 (decreased by 12.0 %), followed by 155 (decreased by 7.8 %). Lines 224 and 235 reported the lowest fructan level (decreased by <2.0 %) between 22 daf and maturity (Fei et al., 2022). Based on the fructan accumulation and fructan level reduction between 22 daf and maturity, different combinations of parental lines were crossed with each other to combine the properties of a high rate of fructan synthesis and a low rate of fructan hydrolysis as explained by (Fei et al., 2022).

Fructan synthesis and hydrolysis activity were defined based on fructan content analysis using the F3 progenies, as described by Fei et al. (2022). Five grains from middle positions of each spike were collected from ten individual plants of each line where three plants were randomly selected to present the fructan levels. Grain samples from the same plants were collected at 15:00 h at developmental stages 9 daf, 22 daf, and maturity. As fructan synthesis in barley generally occurs at an early stage of development, the fructan content at 9 daf in experimental barley lines compared with a reference line (Gustav) was used to represent fructan synthesis activity. Lines with significantly higher fructan content than Gustav (20.7 ± 0.8 %) were classified as having high fructan synthesis activity, while all the other lines, together with Gustav, were classified as lines with low fructan synthesis activity (Table 1).

Fructan hydrolysis generally occurs at the later stage of barley grain development, and therefore the hydrolysis rate between 22 daf and maturity was used to define hydrolysis activity. Lines with hydrolysis rate higher than 50 % were defined as having high hydrolysis activity, while all other lines were defined as having low hydrolysis activity (Table 1).

The samples obtained were categorized into two main groups based on fructan synthesis activity as (1): samples with high fructan synthesis activity (group A) and (2): samples with low fructan synthesis activity (group B) (Table 1).

2.2. Starch extraction

A laboratory-scale barley starch extraction procedure was developed based on the method described by Källman et al. (2015) with the following three modifications: i) Barley grains were milled using an ultra-centrifugal mill of type ZM 200 (Retsch GmbH, Germany) at a speed of 1800 min^{-1} ; ii) barley whole flour (3 g) was steeped in 15 mL 0.02 M HCl, the pH was adjusted to between 2.5 and 3.0, and the mixture stirred overnight before neutralizing and mixing with an Ultra-Turrax; and iii) 0.05 M Tris-HCl buffer (pH 7.8, containing 0.25 % NaHSO₃ and 0.02 % sodium azide) and proteinase K (from *Paronydium album* (*Triticium album*); E-PRKMB, EC 3.4.21.62, specific activity >40 U/mg protein (on urea-denatured hemoglobin) at pH 7.5 and 37°C) were used.

2.3. β -Glucan and fructan content

β -Glucan content was determined using the mixed-linkage β -glucan kit (K-BGLU, Megazyme, Bray, Ireland) according to McCleary and Codd (1991). Fructan content was determined using the fructan kit (K-FRUC, Megazyme, Bray, Ireland) according to McCleary, Murphy, and Mugford (1997).

Table 1

Grain fructan content (% DM basis) of barley lines of F₃ progenies at different development stages, their fructan hydrolysis rate between 22 daf and maturity and the groups based on fructan synthesis activity (A = high, B = low) together with the grain fructan and β-glucan content (% DM basis) of 10 experimental barley lines (samples 1–10) and a reference barley variety (Gustav, sample 11) of F₄ progenies (mean ± standard deviation). Values within columns with different superscript letters differ significantly (ANOVA, α = 0.05). Some of the data presented in the table has previously reported by Fei et al. (2022)*. Standard deviations are modified for sample standard deviation.

Sample	Genealogy	Fructan content at 9 daf (% DM basis) of F ₃ progenies	Fructan synthesis activity	Fructan synthesis activity group	Fructan content at 22 daf (% DM basis) of F ₃ progenies	Fructan content at maturity (% DM basis) of F ₃ progenies	Fructan hydrolysis rate (%)	Fructan hydrolysis activity	Fructan content of at maturity (% DM basis) of F ₄ progenies	β-Glucan content at maturity (% DM basis) of F ₄ progenies
1	#155	30.3* ± 2.2 ^a	High	A	12.0*	4.2*	65.2	High	3.8 ± 0.2 ^c	9.6 ± 0.2 ^c
2	#199	32.2* ± 1.3 ^a	High	A	15.6*	3.9*	74.9	High	3.4 ± 0.1 ^d	9.3 ± 0.3 ^c
3	#224	21.3* ± 0.9 ^b	Low	B	3.9*	2.5*	35.2	Low	2.2 ± 0.1 ^e	7.5 ± 0.1 ^d
4	#235	21.2* ± 0.8 ^b	Low	B	3.7*	1.9*	47.7	Low	1.0 ± 0.1 ^f	6.6 ± 0.2 ^e
5	♀#224 × ♂#155, flat	36.0* ± 3.4 ^a	High	A	14.3*	11.8*	17.7	Low	8.6 ± 0.1 ^a	11.5 ± 0.1 ^a
6	♀#224 × ♂#199	31.5* ± 2.0 ^a	High	A	14.3*	11.1*	22.7	Low	8.1 ± 0.2 ^b	12.0 ± 0.0 ^a
7	♀#199 × ♂#155	34.4 ± 1.0 ^a	High	A	12.9	5.3	58.5	High	2.1 ± 0.1 ^e	10.6 ± 0.1 ^b
8	♀#155 × ♂#199	30.9 ± 0.9 ^a	High	A	18.2	6.0	66.9	High	2.0 ± 0.1 ^e	10.9 ± 0.0 ^b
9	♀#224 × ♂#155, round	21.5 ± 1.0 ^b	Low	B	7.7	2.5	67.0	High	0.8 ± 0.0 ^f	7.1 ± 0.1 ^{d,e}
10	♀#199 × ♂#235	25.5 ± 2.8 ^{a,b}	High	A	11.6*	6.1*	47.5	Low	3.3 ± 0.1 ^d	10.8 ± 0.1 ^b
11	249 (Gustav)	20.7 ± 0.8 ^b	Low	B	8.9	1.8	80.2	High	0.7 ± 0.1 ^f	3.8 ± 0.0 ^f

(Link to the Creative Commons license- <http://creativecommons.org/licenses/by/4.0/>.)

2.4. β-Glucan structural composition

β-Glucan structural composition was determined by lichenase digestion followed by high performance anion-exchange chromatograph/pulsed amperometric detection (HPAEC-PAD) analysis, as described by Andersson et al. (2004). HPAEC-PAD was performed with a CarboPac PA-100 column eluted at 1 mL/min with eluent A (0.15 M NaOH) and eluent B (0.15 M NaOH and 0.5 M NaOAc) according to the following program: 0–20 min: 15–28% eluent B; 20–35 min: 28–50% B; 35–45 min: 50% B; 45–50 min: 50–15% B (return to the start mixture); and 50–65 min: 15% B. Electrode pulse potential and duration were as follows: E1 = 0.1 V, 0.4 s; E2 = -2.0 V, 0.02 s; E3 = 0.6 V, 0.01 s; E4 = -0.1 V, 0.06 s. Signals were integrated over 0.2 s (0.2 to 0.4 s).

2.5. Starch content and amylose content

The starch content in barley whole flour was determined according to an existing method (Åman, Westerlund, & Theander, 1994) with the slight modifications that barley whole flour (20 mg), 50 μL thermostable α-amylase from *Bacillus licheniformis* (EC 3.2.1.1, 3000 U/mL, Megazyme, Wicklow, Ireland), 100 μL of 10-fold diluted amyloglucosidase from *Aspergillus niger* (EC 3.2.1.3, 3260 U/mL soluble starch, Megazyme, Wicklow, Ireland) in acetate buffer, and 3 mL of GOPOD reagent (Megazyme, Wicklow, Ireland) were used. The absorbance was measured at 510 nm against a reagent blank. A two-point calibration curve was developed using 1 mg/mL and 0.5 mg/mL glucose standards incubated with a 3 mL GOPOD reagent, to calculate the glucose concentration of the samples.

The amylose content in barley whole flour was analyzed by a colorimetric method according to Chrastil (1987) with the following slight modifications: Barley whole flour (30 mg) was solubilized according to Morrison and Laignelet (1983) in 3 mL UDMSO (0.6 M urea in 90% DMSO) added on two occasions, and incubated in a 100 °C water bath for 30 min with occasional mixing. Then 100 μL of sample were transferred to each of two Eppendorf tubes and 200 μL and 700 μL of 99.5% ethanol were added and mixed on two occasions. The tubes were left to stand in an ice bath for 30 min, centrifuged at 10500 ×g for 15 min and the pellet was washed with 1.8 mL 95% ethanol and redissolved in 100 μL UDMSO at 100 °C for 15 min. The samples were transferred to new tubes by washing with 3 × 1 mL of 0.5% Trichloroacetic acid (TCA) and an additional 2 mL of 0.5% TCA were added. Two reaction blanks containing 5 mL of TCA were included from this step onwards. Then 50

μL 0.01 N I₂-KI solution (1.27 g I₂ and 3 g KI per L) were added, the tube contents were mixed, and the tubes were placed in a 25 °C water bath for 30 min. The absorbance was read against water at 620 nm. The amylose content was determined using a standard curve with defined amylose content and values are reported as average of two replicates based on total starch content (DM basis).

2.6. Production of BBs

Production and characterization of BBs were performed according to the method developed and described by Zhao, Andersson, and Andersson (2021). For BB block distribution analysis, the BBs were prepared by hydrolyzing whole starch using β-amylase (E-BARBL, Megazyme, Wicklow, Ireland) and α-amylase (E-BAASS, Megazyme, Wicklow, Ireland).

First, whole starch samples were subjected to β-amylolysis by β-amylase to remove the linear chains of amylose and amylopectin external chains and to produce β-limit dextrins (β-LD) s. The β-amylase was twice de-salted through PD-10 desalting columns (Sephadex, Amersham Pharmacia Biotech AB, Uppsala, Sweden) using sodium acetate (NaOAc) buffer before using.

The β-LDs produced were then hydrolyzed with α-amylase. Extensive α-amylosis yielded α-limit dextrins (α-LD) s. The isolated α-LDs were again treated with β-amylase to ensure no external chains remained in the resulting BBs. The enzymes were then denatured by heating in a boiling water bath and the BBs were isolated by, filtering through a membrane filter (0.45 μm) (Zhao et al., 2021).

2.7. High performance size exclusion chromatography (HPSEC) for BB analysis

The BBs were analyzed using HPSEC and the HPSEC setting was as described by Zhao et al. (2021). In brief, the HPSEC system was equipped with a refractive index (RI) detector (Wyatt Technology Corp., Santa Barbara, CA) which measures the concentration of the elutes, and two serially connected OHpak SB-802.5 HQ columns with a guard column (Shodex, Showa Denko KK, Miniato, Japan) which have been kept at 35 °C. The fragments were eluted using 0.1 M NaNO₃, containing 0.02% NaN₃ with a flow rate of 0.5 mL/min. Data were analyzed using ASTRA software (version 4.70.07, Wyatt Technology Corp., Santa Barbara, CA).

The results were presented as the mean of two replicates, and the sample blank was subtracted to eliminate the enzyme and buffer peaks

in the elution profiles. The chromatograms were normalized for the peak area between 13 and 17.5 mL elution volume and divided into 9 buckets for further analysis.

2.8. HPAEC-PAD for BB analysis

An HPAEC instrumentation (Series 4500i, Dionex Corp., Sunnyvale, CA, USA) equipped with a BioLC gradient pump and a pulsed amperometric detector (PAD) was used in this study. The HPAEC-PAD setting was as described by Zhao et al. (2021). In brief, a CarboPac PA-100 (4 × 250 mm) analytical column (Dionex, Sunnyvale USA) equipped with a guard column was used for separation. Elution was performed at 25 °C, at a flow rate of 1 mL/min, with an injection volume of 25 µL, using 0.15 M NaOH (eluent A) and 0.50 M NaOAc + 0.15 M NaOH (eluent B) with the following gradient: 0–15 min: 15–28 % eluent B; 15–45 min: 28–55 % B; 45–55 min: 55 % B; and 55–60 min: 55–15 % B (return to the start mixture). The PAD response of BBs was calculated as relative peak area.

2.9. Statistical analyses

Differences in measured parameters were studied by One-way analysis of variance (ANOVA). Tukey pairwise comparisons and Dunnett's test were performed using Minitab 18 (State College, PA, USA). Principal component analysis (PCA) was carried out using Simca 14.0 (Umetrics, Umeå, Sweden). Spearman's rank correlation coefficient analysis was performed using Minitab 18 (State College, PA, USA).

3. Results and discussion

3.1. Fructan synthesis activity of the barley lines

Based on the fructan synthesis activity of the F₃ progenies, the barley lines were divided into two groups, defined as having high fructan synthesis activity with an average fructan content of 31.5 ± 3.6 % at 9 daf (group A) and low fructan synthesis activity, with an average fructan content of 21.2 ± 0.8 % at 9 daf (group B) (Table 1).

3.2. Fructan and β-glucan content of mature grain

Fructan and β-glucan content in mature grain of F₄ progenies differed ($p < 0.05$) between the two groups. Group A lines had a higher grain fructan content (4.5 ± 2.6 % on average) than group B lines (1.2 ± 0.6 % on average). The average grain β-glucan content of group A lines was 10.7 ± 0.9 % and that of group B lines was 6.3 ± 1.6 %. Individual values of fructan and β-glucan content in grains of F₄ generation are presented in Table 1 and used for further analysis and interpretation of the data. The maximum fructan content was 8.6 % (sample 5), which was 12-fold higher than in Gustav. All experimental barley lines (samples 1–10) demonstrated at least 1.5-fold higher β-glucan content than Gustav. In general, the β-glucan content in barley varies between 3 and 11 % (Loskutov & Khlestkina, 2021) and the maximum β-glucan content obtained in the current study was 12.0 % (sample 6), closer to upper limit reported by Loskutov and Khlestkina (2021), which was nearly 3-fold higher than in Gustav.

An interesting correlation between β-glucan and fructan content was observed. Higher β-glucan content was accompanied by higher fructan content, which demonstrated an exponential increase (Fig. 1). One possible explanation for this is that processes of β-glucan and fructan biosynthesis are orchestrated (or at least upregulated) by the same mechanism.

3.3. β-Glucan structural composition

Molecular features of β-glucan affect its solubility and rheological properties (Skendi, Biliaderis, Lazaridou, & Izydorczyk, 2003). The molecular structure of β-glucan was investigated using lichenase

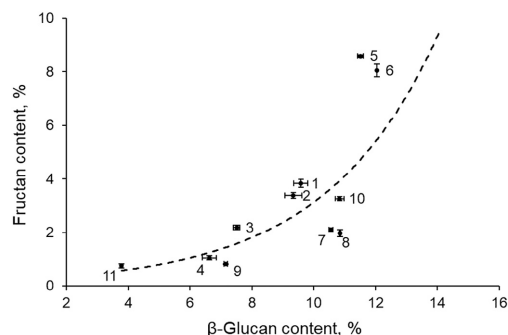


Fig. 1. Relationship between β-glucan content and fructan content in grain from the experimental barley lines (1–10) and the reference variety (11). Mean ($n = 2$), bars indicate standard deviation. For sample descriptions, see Table 1.

analysis. Lichenase (*endo*-β-1,3,1,4-glucanase; EC 3.2.1.73) specifically cleaves the β-(1 → 4)-linkage of the 3G1 → 4G1 units of β-glucan, yielding oligosaccharides containing a single β-(1 → 3)-linkage adjacent to the reducing end (Izydorzcyk & Dexter, 2008). As β-glucan consists mainly of cellotriosyl and cellotetraosyl units, trisaccharide (Degree of polymerization (DP)3), and tetrasaccharide (DP4) are the main products of β-glucan hydrolysis by lichenase (Izydorzcyk & Dexter, 2008; Skendi et al., 2003; Stevenson & Inglett, 2009).

Based on the data obtained the samples were divided into two groups (the same groupings as for fructan synthesis activity) according to their pattern of β-glucan molecular structure. The sample group A (samples 1, 2, 5, 6, 7, 8, 10) displayed a higher proportion of longer structural units, with a normalized average relative peak area of 24.0 ± 1.5 %, compared to barley lines belonging to group B (samples 3, 4, 9, and 11), which had a normalized average relative peak area of 14.0 ± 1.2 % ($p < 0.05$). However, the sample group B (samples 3, 4, 9, and 11), displayed a higher proportion of DP3 and DP4 structural units, with a normalized average relative peak area of 85.9 ± 1.2 %, compared to barley lines belonging to group A (samples 1, 2, 5, 6, 7, 8, 10), which had a normalized average relative peak area of 76 ± 1.5 % ($p < 0.05$). It should be noted that barley lines of group A had high fructan synthesis activity, while barley lines of group B had low fructan synthesis activity.

The ratio of cellotriosyl to cellotetraosyl units (DP3/DP4) was found to be similar in all samples (DP3 / DP4 = 1.65) (Supplementary Table S1), which is common for barley cultivars sharing the same genotypic and environmental background (Izydorzcyk & Dexter, 2008). The DP3/DP4 ratio obtained was slightly lower than reported previously for barley grain, e.g., 1.8–2.2 (Izydorzcyk, Macri, & MacGregor, 1998) and 1.8–2.4 (Lazaridou, Chornick, Biliaderis, & Izydorzcyk, 2008).

There was an interesting correlation between β-glucan molecular structure and β-glucan content. As the proportion of β-glucan increased, proportions of DP3 and DP4 structural units decreased, while the proportions of longer structural units increased (Figs. 2, Fig. S2). Therefore, as it follows from the data obtained, upregulation of β-glucan biosynthesis resulted in production of β-glucan with lower ratios of DP3 and DP4 structural units, but with higher ratios of longer structural units. Although the genes associated with β-glucan synthesis have been identified, the method by which genetic regulation of β-glucan accumulation in barley grains occurs, is not yet known (Geng et al., 2021).

3.4. Starch and amylose content

A low starch content (mean 38.7 ± 3.5 %) was found to be associated with group A samples with high fructan synthesis activity ($p < 0.05$). A high starch content (mean 49.9 ± 3.9 %) was associated with group B

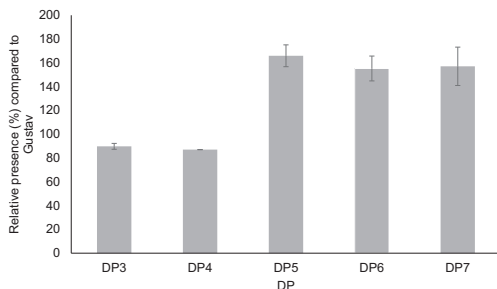


Fig. 2. Relative presence (%) of β -glucan structural units of barley grain samples of experimental line 6 ($\varphi\#224 \times \sigma\#199$) with high β -glucan content (12 %) compared to Gustav (100 %) with low β -glucan content (3.8 %, reference variety 11). Bars indicate standard deviation of two replicates.

samples with low fructan synthesis activity ($p < 0.05$). As reported in subsection 3.2, Group B samples with high starch content of 49.9 % had low fructan and β -glucan content than group A samples ($p < 0.05$). The negative relationship between starch and β -glucan content is in agreement with findings by Munck, Møller, Jacobsen, and Søndergaard (2004) who reported lower starch content in high-lysine barley mutants with elevated β -glucan content. Shimabata et al. (2011) reported high fructan content in sweet wheat lacking two enzymes involved in starch synthesis (GBSS1 and SSIIa). According to Shimabata et al. (2011), decreased starch synthesis and high abundance of sucrose may be the reason for higher fructan content, since sucrose is the substrate for fructan.

Amylose content, as analyzed by colorimetric assay, varied between the samples, with the highest (39.5 %) and lowest (1.8 %) in samples 2 and 3, respectively (Fig. 3). The amylose content was <10 % in samples 3, 4, 6, and 9, which were therefore considered to be waxy lines.

In the present study, we speculated that because of the constant carbon source, a low level of β -glucan and fructan apparently led to allocation of more carbon to starch synthesis.

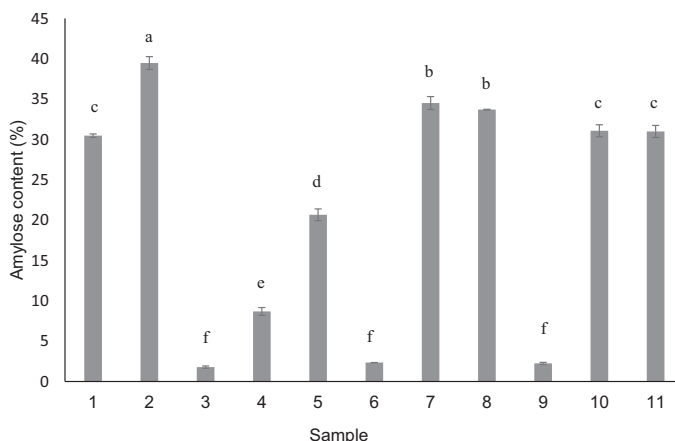


Fig. 3. Amylose content (% of starch content) in the experimental barley lines (samples 1–10) and the reference barley variety Gustav (sample 11). Different letters on bars indicate statistically significant differences. For sample descriptions, see Table 1.

3.5. BB distribution

The distribution of BBs was studied using HPSEC and HPAEC. In the HPSEC chromatogram (Fig. 4), the BB distributions were divided into nine buckets (B1–B9) for further analysis. Buckets B1–B6 contained branched BBs from hydrolysis of the amylopectin β -LD, while buckets B7, B8, and B9 contained linear dextrans produced during BB preparation. PCA identified two major clusters associated with the BB distribution (Fig. 5). These were group A, with high fructan synthesis activity (dashed ellipse in Fig. 5a), and group B, with low fructan synthesis activity (solid ellipse in Fig. 5a). From the data derived from peak area of different buckets (B1–B9) of HPSEC BB distribution, variations in the BB distribution between these groups are shown in Table 2. Group A was associated with a higher proportion of larger BBs ($B1 = 20.0 \pm 1.8$, $B2 = 107.7 \pm 4.2$, $B3 = 107.6 \pm 2.1$) and lower proportion of smaller BBs ($B5 = 256.8 \pm 4.7$, $B6 = 301.0 \pm 7.2$), while group B lines had a lower proportion of B1–B3 ($B1 = 10.6 \pm 2.4$, $B2 = 83.4 \pm 4.2$, $B3 = 98.1 \pm 1.7$) and higher proportion of B5 and B6 ($B5 = 268.1 \pm 3.8$, $B6 = 323.0 \pm 7.9$) ($p < 0.05$). There was no difference in abundance of medium-size BBs (B4) between the groups (Table 2). Hence for BBs derived from the amylopectin fraction (B1–B6), there was a good balance between distribution as affected by fructan synthesis activity or suppression of starch synthesis, with high fructan synthesis (suppressed starch synthesis) being associated with larger BBs and vice versa. For the buckets that contained the linear dextrans (B7–B9), higher proportions, based on refractive index (Fig. 4) were found for samples belonging to group A.

The results of HPAEC analysis complemented those of HPSEC analysis of BB distribution, with higher resolution. Categorization of BBs into groups (G2–6) was performed according to Bertoft, Källman, Koch, Andersson, and Åman (2011) and Zhao et al. (2021), but with slight modifications (Fig. S3). However, resolving the peaks separately for G5 and G6 was not possible and therefore BBs belonging to G5 and G6 were treated together as G5 + G6. Group G1 was not considered, since it mostly contained linear dextrans (glucose, maltose, maltotriose) produced during BB preparation.

In agreement with the HPSEC results, PCA revealed two categories based on the groups of BBs (Fig. S4). One cluster consisted of samples in group A and the other of samples in group B.

Analysis of the abundance of each group of BB revealed that small BBs from G2 were present in high abundance in samples in group B, while medium (G3) and larger (G4, G5 + 6) BBs were more abundant in

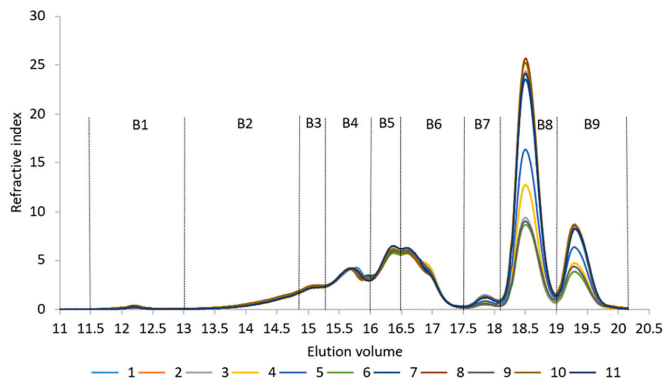


Fig. 4. Building block distribution in starch from the experimental barley lines (samples 1–10) after normalization for the peak area between 13 and 17.5 mL, as determined by HPSEC. The variety Gustav (sample 11) is included for reference. The distribution was bucketed as: B1: elution volume 11.49–12.99 mL, B2: 13.00–14.79 mL, B3: 14.80–15.27 mL, B4: 15.28–15.94 mL, B5: 15.95–16.49 mL, B6: 16.50–17.46 mL, B7: 17.50–18.08 mL, B8: 18.09–18.99 mL, B9: 19.00–20.15 mL. Refractive index signal is proportional to the concentration (weight/volume). 1–11 refer to different genotypes used in the study and for descriptions, see Table 1.

samples in group A ($p < 0.05$) (Supplementary Table S2). These observations are in agreement to results from HPSEC analysis.

3.6. Correlations of BB to other parameters

Correlations between BB size and other parameters (content of amylose, starch, β -Glucan, fructan) were investigated using PCA (Fig. 6) and Spearman's rank correlation coefficient analysis (Table 3). A clear grouping of samples based on the different parameters was determined, where samples in group B (cluster within solid ellipse in Fig. 6) were associated with small BBs and high starch content, while samples belonging to group A (within dashed ellipse) were associated with medium and large BBs and a high content β glucan, and fructan. These associations with each bucket of BBs (as determined by HPSEC analysis) were further analyzed based on Spearman's rank correlation coefficients (Table 3).

Interestingly, starch synthesis showed a prominent relationship to BB size, with low starch content associated with a higher proportion of larger BBs, and vice versa. It is known that regulation of starch synthesis is mediated to a large extent by sugar signaling in plants and numerous studies have found that genes related to starch synthesis, i.e., ADP-glucose pyrophosphorylase, granule-bound starch synthase (GBSS1), and branching enzymes (SBEs), are regulated by sugars (Nakata & Okita, 1995; Wang, Yeh, & Tsai, 2001). According to a recent review by Tetlow and Bertoft (2020), BBs are the major structural components of amylopectin. The main enzymes involved in determining the structure of the BBs are soluble starch synthases (SSSI and/or SSSII) and SBEII isoforms (Tetlow & Bertoft, 2020). Hence, SUSIBA transcription factor-based selective breeding could affect one or all of those enzymes or their combined complex, thereby affecting the structure and/or size of the BBs. These results suggest that SUSIBA transcription factor-based cross-breeding can allow breeding programs to achieve novel types of starch with tailored structure at the BB level. It has been reported previously that genetic background has a direct link to BB size in barley starch (Källman et al., 2015; Zhao et al., 2021). However, to the best of our knowledge, this study is the first to report an effect on starch structure at BB level as affected by SUSIBA-based sugar regulation for fructan synthesis.

Interestingly, there was a strong association between amylose content and B7, B8, and B9 buckets considered to represent maltotriose, maltose, and glucose, respectively (Table 3). In the method used for isolating BBs, β -LDs are produced from branched amylose during the first β -amylyolysis, and continuing α -amylyolysis converts β -LD to α -LD. This α -LD is converted into glucose, maltose, and maltotriose during the second β -amylyolysis (Zhao et al., 2021). As reviewed by Bertoft (2017),

the linear part of amylose is completely hydrolyzed into maltose during the first β -amylyolysis and the branched component of amylose partly forms maltose and β -LD. During α -amylyolysis, further linear dextrans are produced by cleaving the internal chain segments between the BBs (Zhao et al., 2021). Considering the steps associated with production of BBs from amylose, the origin of B7 and B8 can be linked to both the linear and branched fraction of the amylose component. Although branches from the amylose fraction account for only 1–2 % of total branches in normal starch (Zhu, Bertoft, & Seetharaman, 2013), around 10–70 % of amylose molecules (depending on the botanical source) are branched and contain 5–20 chains (Kong, 2020). The strong positive association of B7, B8, and B9 with amylose in the present study reveals the connection between the selective breeding technique applied and the amylose component in barley starch. Studies focused in understanding amylose fine structure by approaches such as model fitting of chain length distributions has become a recent research interest to better understand the starch biosynthesis-structure-property relations (e.g., Li, Yu, Dhital, Gidley, & Gilbert, 2019; Yu et al., 2019). Hence, future work to study the fine structure of amylose as affected by SUSIBA activity would be advantageous for the knowledge platform which connects starch biosynthesis-structure-property relations, since our results indicate a possible correlation of amylose fine structure as affected by SUSIBA activity.

The correlations between β -glucan content and different categories of BBs opposed to the correlations observed for starch content and different categories of BBs. This observation is supported by the fact that β -glucan content and starch content had a negative relationship. Correlations between the different categories of BBs and fructan content were observed for B1, B2 and B5 of the BB distribution groups as determined by HPSEC analysis.

4. Conclusions

A recent study adopted a new strategy for cross-breeding of barley based on SUSIBA transcription factor to generate barley lines with high fructan content. The present study revealed that these high fructan lines also had elevated content of β -glucan with decreased proportions of DP3 and DP4 structural units and increased proportions of longer structural units. Starch content and the molecular structure of amylopectin were also altered in the high-fructan lines. Upregulation of fructan synthesis is likely to suppress starch synthesis and is furthermore associated with larger building blocks in amylopectin. These results provide insights to plant breeders regarding *in planta* modification of starch and glucan to fit with the intended end use. Further detailed characterization of amylose fine structure would improve understanding of the effect of

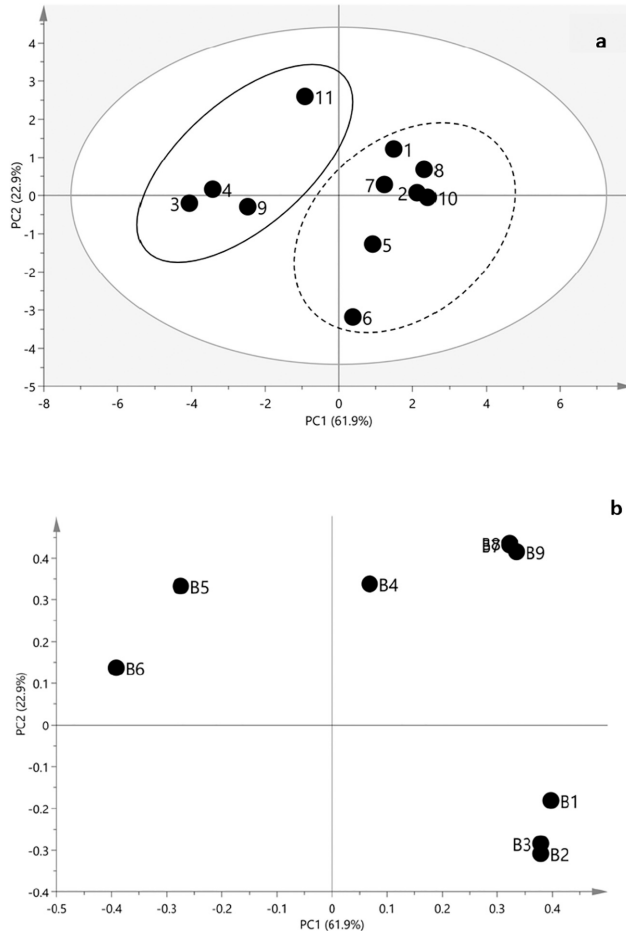


Fig. 5. Principal component analysis (a) score plot and (b) loading plot of building block distribution in starch based on HPSEC results. Each dot represents a sample. The buckets of building block distribution (B1–B9) are as shown in Fig. 5. Clusters within the dashed ellipse belong to group A (lines with high fructan synthesis activity) and those within the solid ellipse to group B (lines with low fructan synthesis activity). For sample descriptions, see Table 1.

Table 2

Variation in peak area for the different buckets (B1–B9) from the HPSEC data, this estimate building block distribution for barley lines in sample group A (high fructan synthesis activity) and group B (low fructan synthesis activity). Values within columns with different superscript letters differ significantly (ANOVA, $\alpha = 0.05$). Buckets are as described in Fig. 4. For sample descriptions, see Table 1.

Sample group	Bucket								
	B1	B2	B3	B4	B5	B6	B7	B8	B9
A	20.0 ^a ± 1.8	107.7 ^a ± 4.2	107.6 ^a ± 2.1	226.2 ^a ± 3.5	256.8 ^b ± 4.7	301.0 ^b ± 7.2	45.5 ^a ± 12.6	863.9 ^b ± 250.6	324.3 ^a ± 74.3
B	10.6 ^b ± 2.4	83.4 ^b ± 4.2	98.1 ^b ± 1.7	226.8 ^a ± 3.1	268.1 ^a ± 3.8	323.0 ^a ± 7.9	30.2 ^b ± 11.1	575.3 ^b ± 263.4	231.9 ^b ± 79.3

upregulating fructan synthesis on starch synthesis.

Supplementary data to this article can be found online at <https://doi.org/10.1016/j.carbpol.2023.121030>.

CRedit authorship contribution statement

Shishanthi Jayarathna: Conceptualization, Methodology, Formal analysis, Investigation, Data curation, Visualization, Writing – original draft, Writing – review & editing. **Yunkai Jin:** Methodology, Formal analysis, Writing – original draft, Writing – review & editing. **Gleb**

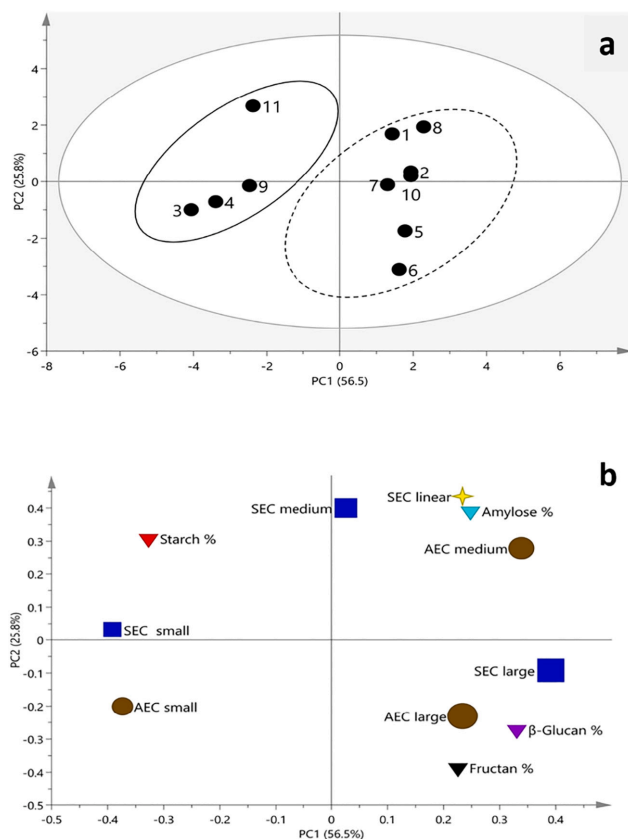


Fig. 6. Principal component analysis (a) score plot and (b) loading plot for bucket distribution of building blocks (BBs) as determined by HPSEC and HPAEC, amylose content, starch content, β glucan content, and fructan content. The BB distribution buckets based on HPSEC analysis are as described in Fig. 5, while those based on HPAEC are as follows: building blocks of group G2 (AEC small), building blocks of G2 and G3 (AEC medium), and building blocks of G5 + G6 (AEC large). Clusters within the dashed ellipse belong to group A (barley lines with high fructan synthesis activity) and those with the solid ellipse to group B (lines with low fructan synthesis activity). For sample descriptions, see Table 1.

Table 3

Spearman's rank correlation coefficient for relationships between buckets B1–B9 of building block distribution (see Fig. 5) and starch, amylose, β -glucan, and fructan content.

Bucket	Starch	Amylose	β -glucan	Fructan
B1	-0.79**	0.52	0.64*	0.62*
B2	-0.90***	0.37	0.85**	0.66*
B3	-0.84**	0.57	0.72*	0.54
B4	0.10	0.04	0.10	-0.04
B5	0.80**	-0.15	-0.88***	-0.71*
B6	0.75**	-0.73*	-0.64*	-0.48
B7	-0.17	0.8**	0.05	0.13
B8	-0.08	0.78**	0.11	-0.05
B9	-0.21	0.79**	0.19	0.1

* Indicates statistical significance at $p < 0.05$.

** Indicates statistical significance at $p < 0.01$.

*** Indicates statistical significance at $p < 0.001$.

Dotsenko: Methodology, Formal analysis, Investigation, Data curation, Visualization, Writing – original draft, Writing – review & editing. **Mingliang Fei:** Methodology, Formal analysis, Investigation, Data curation, Writing – review & editing. **Mariette Andersson:** Writing – review & editing. **Annica A.M. Andersson:** Methodology, Investigation, Data curation, Writing – review & editing. **Chuanxin Sun:**

Conceptualization, Supervision, Project administration, Funding acquisition. **Roger Andersson:** Conceptualization, Supervision, Project administration, Funding acquisition, Writing – review & editing.

Declaration of competing interest

The authors declare that they have no known competing financial interests or personal relationships that could have appeared to influence the work reported in this paper.

Data availability

Data will be made available on request.

Acknowledgements

We wish to thank Xue Zhao for technical and intellectual support. Henrik Hansson and Laura Okmane are acknowledged for technical support with the HPAEC analysis, and Silvana Moreno for capturing the C grain images. This study was (partially) financed by Trees and Crops for the Future (TC4F), a Strategic Research Area at the Swedish University of Agricultural Sciences (SLU) supported by the Swedish Government and the Lantmännen Research Foundation (projects 2015H024

and 2016F003), and the SLU program Grogrund (SLU Center for Plant Breeding of Food Crops), supported by the Faculty of Natural Resources and Agricultural Sciences, SLU.

References

- Åman, P., Westerlund, E., & Theander, O. (1994). Determination of starch using a thermostable α -amylase. In *Methods in carbohydrate chemistry* (10th ed., pp. 111–115). New York: Wiley.
- Andersson, A. A. M., Armö, E., Grangeon, E., Fredriksson, H., Andersson, R., & Åman, P. (2004). Molecular weight and structure units of (1 \rightarrow 3, 1 \rightarrow 4)- β -glucans in dough and bread made from hull-less barley milling fractions. *Journal of Cereal Science*, *40*, 195–204.
- Baik, B.-K., & Ullrich, S. E. (2008). Barley for food: Characteristics, improvement, and renewed interest. *Journal of Cereal Science*, *48*, 233–242.
- Bello-Pérez, L. A., Rodríguez-Ambríz, S. L., Agama-Acevedo, E., & Sánchez-Rivera, M. M. (2009). Solubilization effects on molecular weights of amylose and amylopectins of normal maize and barley starches. *Cereal Chemistry*, *86*, 701–705.
- Benkella, N. (2022). Insights on fructans and resistance of plants to drought stress. *Frontiers in Sustainable Food Systems*, *6*. <https://doi.org/10.3389/fsufs.2022.827758>. Retrieved from.
- Bertoft, E. (2017). Understanding starch structure: Recent progress. *Agronomy*, *7*, 56.
- Bertoft, E., Källman, A., Koch, K., Andersson, R., & Åman, P. (2011). The building block structure of barley amylopectin. *International Journal of Biological Macromolecules*, *49*, 900–909.
- Bertoft, E., Koch, K., & Åman, P. (2012). Structure of building blocks in amylopectins. *Carbohydrate Research*, *361*, 105–113.
- Boscher, D. (2009). Fructan prebiotics derived from inulin. In D. Charalampopoulos, & R. A. Rastall (Eds.), *Vol. 1. Prebiotics and probiotics science and technology* (pp. 163–205). New York, NY: Springer.
- Chrastil, J. (1987). Improved colorimetric determination of amylose in starches or flours. *Carbohydrate Research*, *159*, 154–158.
- Du, B., Meenu, M., Liu, H., & Xu, B. (2019). A concise review on the molecular structure and function relationship of β -glucan. *International Journal of Molecular Sciences*, *20*, 4032.
- Ehrenbergerová, J., Brezínová Belcredi, N., Psota, V., Hrstková, P., Cerkal, R., & Newman, C. W. (2008). Changes caused by genotype and environmental conditions in beta-glucan content of spring barley for dietetically beneficial human nutrition. *Plant Foods for Human Nutrition (Dordrecht, Netherlands)*, *63*, 111–117.
- Fei, M., Jin, Y., Hu, J., Dotsenko, G., Ruan, Y., Liu, C., ... Sun, C. (2022). Achieving of high-diet-fiber barley via managing fructan hydrolysis. *Scientific Reports*, *12*, 19151.
- Geng, L., Li, M., Xie, S., Wu, D., Ye, L., & Zhang, G. (2021). Identification of genetic loci and candidate genes related to β -glucan content in barley grain by genome-wide association study in international barley core selected collection. *Molecular Breeding*, *41*, 6.
- Izydorczyk, M. S., & Dexter, J. E. (2008). Barley β -glucans and arabinoxylans: Molecular structure, physicochemical properties, and uses in food products—a review. *Food Research International*, *41*, 850–868.
- Izydorczyk, M. S., Macri, L. J., & MacGregor, A. W. (1998). Structure and physicochemical properties of barley non-starch polysaccharides—I. Water-extractable β -glucans and arabinoxylans. *Carbohydrate Polymers*, *35*, 249–258.
- Jin, Y., Fei, M., Rosequist, S., Jin, L., Gohli, S., Sandström, C., ... Sun, C. (2017). A dual-promoter gene orchestrates the sucrose-coordinated synthesis of starch and fructan in barley. *Molecular Plant*, *10*, 1556–1570.
- Källman, A., Vamadevan, V., Bertoft, E., Koch, K., Seetharaman, K., Åman, P., & Andersson, R. (2015). Thermal properties of barley starch and its relation to starch characteristics. *International Journal of Biological Macromolecules*, *81*, 692–700.
- Kerckhoffs, D. A. J. M., Hornstra, G., & Mensink, R. P. (2003). Cholesterol-lowering effect of beta-glucan from oat bran in mildly hypercholesterolemic subjects may decrease when beta-glucan is incorporated into bread and cookies. *The American Journal of Clinical Nutrition*, *78*, 221–227.
- Kong, X. (2020). Fine structure of amylose and amylopectin. In S. Wang (Ed.), *Starch structure, functionality and application in foods* (pp. 29–39). Singapore: Springer.
- Lazaridou, A., Chornick, T., Billaderis, C. G., & Izydorczyk, M. S. (2008). Sequential solvent extraction and structural characterization of polysaccharides from the endosperm cell walls of barley grown in different environments. *Carbohydrate Polymers*, *73*, 621–639.
- Li, H., Yu, W., Dhital, S., Gidley, M. J., & Gilbert, R. G. (2019). Starch branching enzymes contributing to amylose and amylopectin fine structure in wheat. *Carbohydrate Polymers*, *224*, Article 115185.
- Livingston, D. P., Hincha, D. K., & Heyer, A. G. (2009). Fructan and its relationship to abiotic stress tolerance in plants. *Cellular and Molecular Life Sciences*, *66*, 2007–2023.
- Loskutov, I. G., & Khlestkina, E. K. (2021). Wheat, barley, and oat breeding for health benefit components in grain. *Plants*, *10*, 86.
- McCleary, B. V., Murphy, A., & Muford, D. C. (1997). Determination of oligofructans and fructan polysaccharides in foodstuffs by an enzymatic/spectrophotometric method: Collaborative study. *Journal of AOAC International*, *80*, 356–364.
- McCleary, B. V., & Codd, R. (1991). Measurement of (1 \rightarrow 3),(1 \rightarrow 4)- β -D-glucan in barley and oats: A streamlined enzymic procedure. *Journal of the Science of Food and Agriculture*, *55*, 303–312.
- Morrison, W. R., Milligan, T. P., & Azudin, M. N. (1984). A relationship between the amylose and lipid contents of starches from diploid cereals. *Journal of Cereal Science*, *2*, 257–271.
- Morrison, W. R., & Laignelet, B. (1983). An improved colorimetric procedure for determining apparent and total amylose in cereal and other starches. *Journal of Cereal Science*, *1*, 9–20.
- Munck, L., Møller, B., Jacobsen, S., & Sondergaard, I. (2004). Near infrared spectra indicate specific mutant endosperm genes and reveal a new mechanism for substituting starch with (1 \rightarrow 3,1 \rightarrow 4)- β -glucan in barley. *Journal of Cereal Science*, *40*, 213–222.
- Nakata, P. A., & Okita, T. W. (1995). Differential regulation of ADP-glucose pyrophosphorylase in the sink and source tissues of potato. *Plant Physiology*, *108*, 361–368.
- Oscarsson, M., Andersson, R., Salomonsson, A.-C., & Åman, P. (1996). Chemical composition of barley samples focusing on dietary fibre components. *Journal of Cereal Science*, *24*, 161–170.
- Poehlman, J. M., & Slepier, D. A. (2013). *Breeding field crops* (4th ed.). Ames, Iowa, USA: Iowa State University Press.
- Ritsema, T., & Smeekens, S. (2003). Fructans: Beneficial for plants and humans. *Current Opinion in Plant Biology*, *6*, 223–230.
- Roberfroid, M. (2007). Prebiotics: The concept revisited. *The Journal of Nutrition*, *137*, 830S–837S.
- Roberfroid, M., Gibson, G. R., Hoyle, L., McCartney, A. L., Rastall, R., Rowland, I., ... Meheust, A. (2010). Prebiotic effects: Metabolic and health benefits. *The British Journal of Nutrition*, *104*(Suppl. 2), S1–63.
- Shimbata, T., Inokuma, T., Sunohara, A., Vrinten, P., Saito, M., Takiya, T., & Nakamura, T. (2011). High levels of sugars and fructan in mature seed of sweet wheat lacking GBSII and SSIIa enzymes. *Journal of Agricultural and Food Chemistry*, *59*, 4794–4800.
- Skendi, A., Billaderis, C. G., Lazaridou, A., & Izydorczyk, M. S. (2003). Structure and rheological properties of water soluble β -glucans from oat cultivars of *Avena sativa* and *Avena byzantina*. *Journal of Cereal Science*, *38*, 15–31.
- Steele, K., Dickin, E., Keerio, M. D., Samad, S., Kamona, C., Brook, R., ... Frost, G. (2013). Breeding low-glycemic index barley for functional food. *Field Crops Research*, *154*, 31–39.
- Stevenson, D. G., & Inglett, G. E. (2009). Cereal β -glucans. In G. O. Phillips, & P. A. Williams (Eds.), *Handbook of hydrocolloids* (pp. 615–652). CRC Press, Woodhead Publishing.
- Sullivan, P., Arendt, E., & Gallagher, E. (2013). The increasing use of barley and barley by-products in the production of healthier baked goods. *Trends in Food Science & Technology*, *29*, 124–134.
- Sun, C., Palmqvist, S., Olsson, H., Borén, M., Ahlstrand, S., & Jansson, C. (2003). A novel WRKY transcription factor, SUSIBA2, participates in sugar signaling in barley by binding to the sugar-responsive elements of the iso1 promoter. *The Plant Cell*, *15*, 2076–2092.
- Tellow, L. J., & Bertoft, E. (2020). A review of starch biosynthesis in relation to the building block backbone model. *International Journal of Molecular Sciences*, *21*, 7011.
- Vamadevan, V., & Bertoft, E. (2015). Structure-function relationships of starch components. *Starch/Stärke*, *67*, 55–68.
- Vamadevan, V., & Bertoft, E. (2018). Impact of different structural types of amylopectin on retrogradation. *Food Hydrocolloids*, *80*, 88–96.
- Wang, S.-J., Yeh, K.-W., & Tsai, C.-Y. (2001). Regulation of starch granule-bound starch synthase I gene expression by circadian clock and sucrose in the source tissue of sweet potato. *Plant Science*, *161*, 635–644.
- Yu, W., Li, H., Zou, W., Tao, K., Zhu, J., & Gilbert, R. G. (2019). Using starch molecular fine structure to understand biosynthesis-structure-property relations. *Trends in Food Science & Technology*, *86*, 530–536.
- Zhao, X., Andersson, M., & Andersson, R. (2021). A simplified method of determining the internal structure of amylopectin from barley starch without amylopectin isolation. *Carbohydrate Polymers*, *255*, Article 117503.
- Zhao, X., Hofvander, P., Andersson, M., & Andersson, R. (2023). Internal structure and thermal properties of potato starches varying widely in amylose content. *Food Hydrocolloids*, *135*, Article 108148.
- Zhu, F. (2017). Barley starch: Composition, structure, properties, and modifications. *Comprehensive Reviews in Food Science and Food Safety*, *16*, 558–579.
- Zhu, F. (2018). Relationships between amylopectin internal molecular structure and physicochemical properties of starch. *Trends in Food Science & Technology*, *78*, 234–242.
- Zhu, F., Bertoft, E., & Seetharaman, K. (2013). Characterization of internal structure of maize starch without amylose and amylopectin separation. *Carbohydrate Polymers*, *97*, 475–481.
- Zhu, F., & Liu, P. (2020). Starch gelatinization, retrogradation, and enzyme susceptibility of retrograded starch: Effect of amylopectin internal molecular structure. *Food Chemistry*, *316*, Article 126036.

ACTA UNIVERSITATIS AGRICULTURAE SUECIAE

DOCTORAL THESIS NO. 2024:42

This thesis examined the composition, molecular structure and functional properties of potato starch produced by CRISPR/Cas9 gene editing. The aim was to evaluate how genetic mutations affecting enzymes within the starch synthesis pathway modify the resulting starch. Compositional and molecular structure properties of cross-bred high-fructan barley starch were also characterised. The valuable insights gained into these modifications and their impacts on resulting starch give plant breeders the potential to customise starch to suit specific end-uses, enabling tailored starch development.

Shishanthi Jayarathna received her graduate education at the Department of Molecular Sciences, SLU, Uppsala. She has an M.Sc. in Food Science & Technology and B.Sc. in Animal Science & Fisheries from University of Peradeniya, Sri Lanka.

Acta Universitatis Agriculturae Sueciae presents doctoral theses from the Swedish University of Agricultural Sciences (SLU).

SLU generates knowledge for the sustainable use of biological natural resources. Research, education, extension, as well as environmental monitoring and assessment are used to achieve this goal.

ISSN 1652-6880

ISBN (print version) 978-91-8046-256-3

ISBN (electronic version) 978-91-8046-257-0